Breakthroughs in Cell + Gene Therapy

NOVEMBER 12-13, 2026 | NASHVILLE, TN

Breakthroughs in Cell + Gene Therapy 2026 Abstracts

ASGCT does not permit the use of any robot, spider, scraper, data mining tool, or other automated or manual means to access, copy, harvest, or extract ASGCT Annual Meeting or any other event or research abstracts. Any reproduction, distribution, or external use of the abstracts is strictly forbidden without explicit, prior written approval from ASGCT.

No Person Left Behind: Developing a cross-disease framework for equitable gene therapy access in Africa

Dominic Kemps[1 2 3], Lauren Mathae[4]

[1]Sommartel, London, United Kingdom, *[2]Centre for Infectious Disease Research in Zambia, Lusaka, Zambia*, *[3]Georgetown University, Washington DC, United States*, *[4]Georgetown University, Washington, United States*

Abstract Text

Introduction:
While gene therapies for Sickle Cell Disease (SCD) are entering into clinical practice, hopefully to be followed by HIV in the future, access remains highly concentrated in high-income settings. In low- and middle-income countries (LMICs), particularly across Africa, the gap between scientific progress and patient access is widening despite having the highest burden of disease, growing local scientific and clinical expertise, increasing policy interest and community demand. Access cannot be treated as an afterthought; it must be designed into the innovation pathway from the outset. While SCD and HIV have traditionally advanced through separate research and policy agendas, they face many of the same implementation challenges.

Methods:
We used a qualitative, multi-stakeholder consensus building process to develop a cross-disease framework for enabling equitable gene therapy access in African health systems. Between October – November 2025, two structured regional roundtables were convened in Washington, DC and Nairobi, Kenya. The consultations engaged 54 participants, representing HIV and SCD civil society advocates, clinical researchers, national regulators, ministries of health, industry stakeholders, philanthropic funders, and other regional stakeholders. Qualitative data and meeting outputs were analyzed using thematic analysis to identify recurring themes and areas of consensus.

Results:
Stakeholders concluded that equitable access to gene therapy should be approached through a shared implementation strategy spanning HIV and SCD, rather than parallel disease-specific efforts. HIV and SCD were viewed as contributing complementary strengths. HIV programs offer decades of experience in community engagement, advocacy, regulatory reform, market shaping, and expanding access to complex therapies at scale. SCD programs contribute expertise in genetic disease management, specialized diagnostics, transfusion medicine, and the clinical delivery of emerging gene therapies. Participants agreed that aligning these capabilities could accelerate implementation, strengthen health systems, and reduce duplication of investments.

Across both meetings, the thematic analysis identified four cross-cutting systemic barriers: prohibitive cost, limited clinical and laboratory infrastructure, underdeveloped or fragmented regulatory pathways, and weak local manufacturing and delivery capacity. To address these barriers, the resulting framework establishes mutually-reinforcing priorities across six operational domains: (1) intellectual property - embedding equity-by-design in research, licensing, and pricing; (2) technology transfer - extending beyond product transfer

to include manufacturing systems, training, and long-term technical support; (3) regulatory readiness - building national and regional regulatory pathways via mechanisms, such as the Africa Medicines Authority; (4) workforce capacity - investing in human capital and institutional training; (5) financing - strengthening genomic and clinical infrastructure through pooled investment models; and (6) community engagement - supporting community-led demand creation grounded in trust, accurate information, and coordinated cross-sector advocacy. The analysis further emphasizes coordinated advocacy across governments, regional bodies, civil society, funders, and industry to shift gene therapy from an exclusive innovation available only in high-income settings to a global health equity priority.

Conclusion:
Equitable access to gene therapy in LMICs will require more than scientific breakthroughs; it will require deliberate policy action, sustainable investment, and partnerships that prioritize affordability, African leadership, and long-term health and community systems strengthening. Aligning HIV and SCD efforts through a shared implementation framework and coordinated advocacy offers a practical, scalable pathway to leverage existing care platforms and ensure the next generation of cures reaches the populations that need them most.

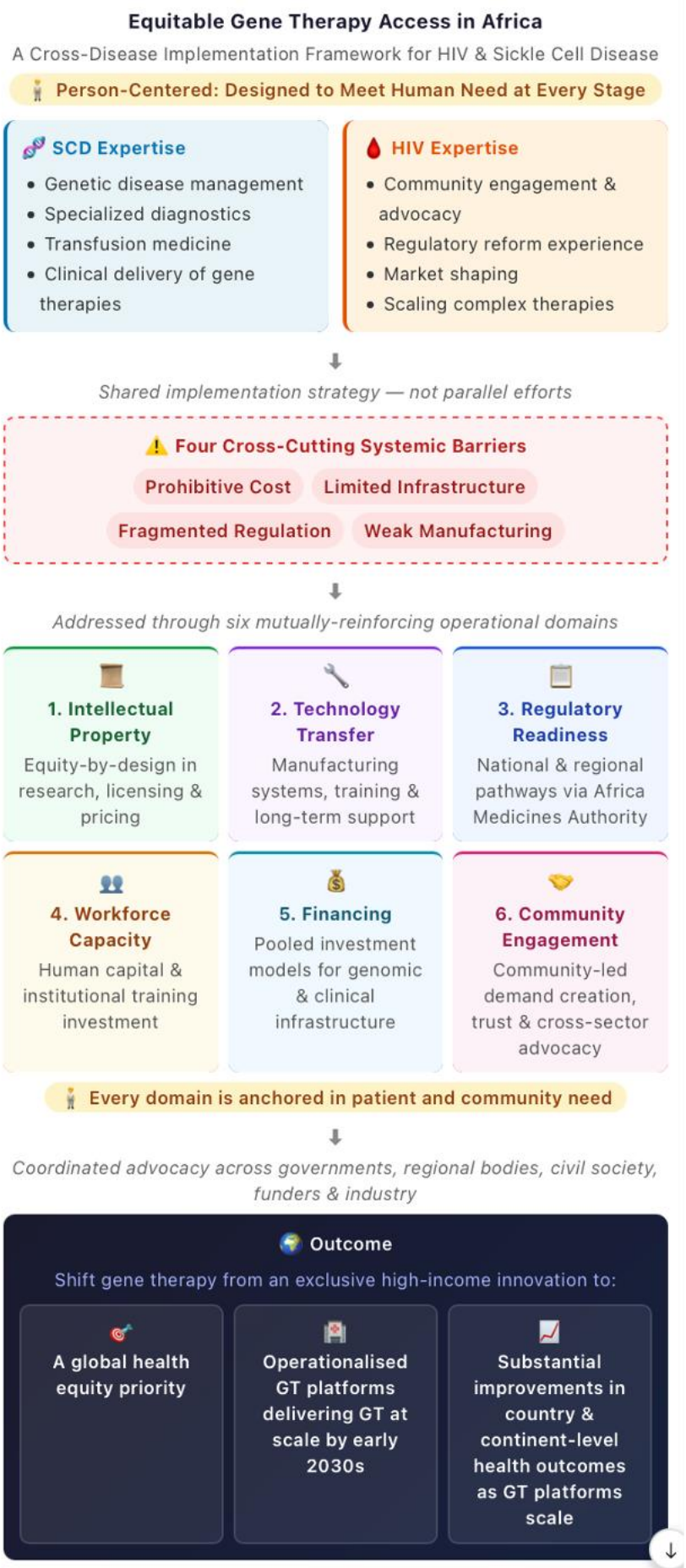
Equitable Gene Therapy Access in Africa
A Cross-Disease Implementation Framework for HIV & Sickle Cell Disease
Person-Centered: Designed to Meet Human Need at Every Stage
SCD Expertise
Genetic disease management
Specialized diagnostics
Transfusion medicine
Clinical delivery of gene therapies
HIV Expertise
Community engagement & advocacy
Regulatory reform experience
Market shaping
Scaling complex therapies
Shared implementation strategy — not parallel efforts
Four Cross-Cutting Systemic Barriers
Prohibitive Cost
Limited Infrastructure
Fragmented Regulation
Weak Manufacturing
Addressed through six mutually-reinforcing operational domains
1. Intellectual Property
Equity-by-design in research, licensing & pricing
2. Technology Transfer
Manufacturing systems, training & long-term support
3. Regulatory Readiness
National & regional pathways via Africa Medicines Authority
4. Workforce Capacity
Human capital & institutional training investment
5. Financing
Pooled investment models for genomic & clinical infrastructure
6. Community Engagement
Community-led demand creation, trust & cross-sector advocacy
Every domain is anchored in patient and community need
Coordinated advocacy across governments, regional bodies, civil society, funders & industry
Outcome
Shift gene therapy from an exclusive high-income innovation to:
A global health equity priority
Operationalised GT platforms delivering GT at scale by early 2030s
Substantial improvements in country & continent-level health outcomes as GT platforms scale

Equity by Design: Person centred framework to advance GT platform advocacy in Africa (but relevant to all Low Middle Income Countries).

Impact of the HOTAIR Variant on HOTAIR Expression and the miR-20a-5p/HMGA2 Axis in Breast and Thyroid Cancers among Pakistani Women

Ruqia Mehmood Baig[1], Nafeesa Kainat[1], Kainat Abbasi[1]

[1]*PMAS Arid Agriculture University Rawalpindi, Department of Biology/Zoology, Rawalpindi, Pakistan*

Abstract Text

Abstract:

Background: Breast and thyroid cancer are female-predominant endocrine-related malignancies that share epidemiological and molecular features. Genetic variants within long non-coding RNAs (lncRNAs) can influence transcript structure, expression, and downstream regulatory networks, thereby contributing to inter-individual variation in cancer susceptibility and progression. The lncRNA HOTAIR has been widely implicated in oncogenesis, but the functional consequences of HOTAIR polymorphisms on transcriptomic regulation remain poorly characterized.

Methods: This study investigated the impact of HOTAIR SNPs rs12826786 on the expression of the lncRNA HOTAIR and its potential downstream targets, miR-20a-5p and HMGA2, in breast and thyroid cancer. Tumors and matched adjacent normal tissues from 120 Pakistani female patients (60 BC, 60 TC) were analyzed. For expression analysis, qRT-PCR was used, and PCR-RFLP was performed for SNP genotyping. Genotype–expression associations, correlation-based regulatory relationships, diagnostic performance, and prognostic relevance were evaluated using appropriate statistical models and tests.

Results: Genotyping of rs12826786 revealed distinct genotype distributions across both cancers, with the heterozygous TC genotype most prevalent. rs12826786 genotypes were associated with HOTAIR expression, which was highest in TT carriers, intermediate in TC carriers, and lowest in CC carriers. HOTAIR and HMGA2 were significantly upregulated, while miR-20a-5p was downregulated in tumor tissues. Regression modeling revealed that expression of HOTAIR (OR = 2.04–3.18) and HMGA2 (OR = 1.30–3.06) is associated with advanced stages in both cancers. ROC analysis confirmed the strong diagnostic potential of HOTAIR and HMGA2 (AUC 0.98-1.00). Correlation analyses supported coordinated expression patterns consistent with an lncRNA–miRNA–mRNA regulatory axis. A high-risk score from the HOTAIR/miR-20a-5p/HMGA2 axis predicted worse overall survival in both breast (HR=12.86) and thyroid cancer (HR=4.33).

Conclusion: Our findings indicate that rs12826786 genotypes are associated with altered lncRNA expression and coordinated transcriptomic dysregulation in breast and thyroid cancers. This study highlights the role of lncRNA-associated genetic variation in shaping cancer-related regulatory networks and underscores the importance of population-specific genomic analyses in female-predominant malignancies.

Key Words: **rs12826786,** lncRNA HOTAIR, miR-20a-5p, HMGA2, ceRNA, Breast cancer, Thyroid cancer,

Application of Dynamic Light Scatter (DLS) for rapid optimization and understanding of transient transfection methods for AAV production.

Gabriel Conceicao[1], Stephanie Klaubert[1], Lauren Peters[1], Neil Templeton[1]

[1]*Solid Biosciences, Process Development, Charlestown, United States*

Abstract Text

Optimization of adeno-associated virus (AAV) production via transient transfection of HEK293 cells is often limited by insufficient transfection complex characterization. Cell culture-based design of experiments (DoEs) are commonly used to determine optimal static incubation times empirically, yet these approaches require extensive screening while yielding limited mechanistic insight.

In this work, dynamic light scattering (DLS) was used to determine the optimal complex size when transfecting cells with Polyethyleneimine (PEI) and pDNA complexes. Shake flask-based studies were performed where static incubation times were intentionally varied to experimentally examine the impact of transfection complex size upon yield and capsid full ratio. Driven by complex size, yield and capsid full ratio varied greater than three-fold over the course of one hour of static incubation (Figure 1). In our application, optimal complex size ranged from 800-900 nm. In practice, transfection complex protocols can be rapidly optimized for target complex size using DLS prior to cell culture experimentation.

We further evaluated the influence of key transfection parameters on complex size kinetics, including DNA concentration, incubation time, plasmid quantity (dual vs triple-plasmid systems), plasmid base pair size, and plasmid ratio. The results demonstrated that DNA mass concentration (not molar concentration) emerged as the primary driver of complex kinetics. In contrast, plasmid quantity, plasmid base pair size, and plasmid ratio had minimal impact on complex kinetics.

Collectively, this work underscores the importance of optimizing complex size to increase AAV yield and capsid full ratio. Given that complex size alone has dramatic impact upon transient transfection-based AAV production, complex size consistency offers a means to improve batch-to-batch consistency in yield or capsid full ratio. DLS can be applied to objectively quantify complex kinetics regardless of the selected conditions, mixing phenomena, or scale.

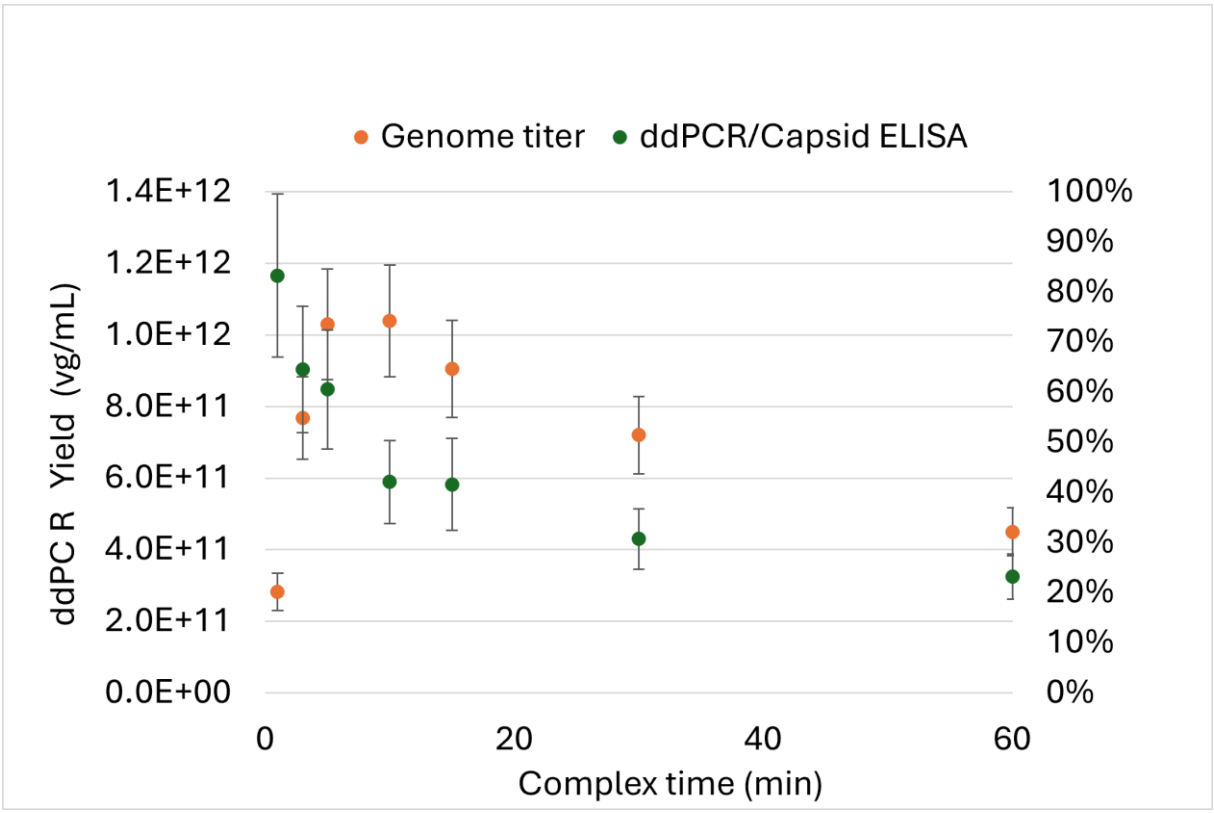

Figure 1: Impact of transfection complexation time, prior to addition to cell culture, upon yield and capsid full ratio. Complex time can be directly associated with a complex size using DLS.

NanoGalaxy hydrophilic nanoparticles enable mRNA delivery to lung endothelial cells and alveolar macrophages

Reyhane Hoshyar[1], Braden Wong[2], Niharika Sodhi[2], Yanyu Huang[2], Adam Turner[2], Sojin Shin[3], Beobsoo Kim[3], Yoonchul Shin[3], Joachim Roeise[2], Diana Voltero[2], Justin Tran[2], Derek Sloan[2], Sruthi Santhanam[2], Kevin Walsh[2], Jorge Rodrigo Mora[2], Steven Bodovitz[2]

[1]BreezeBio, Inc., Immunology & Cell Biology, Brisbane, United States, *[2]BreezeBio, Inc., Brisbane, United States*, *[3]Breezebio Korea Co., Gyeonggi-do, Korea, Rep. of South*

Abstract Text

We have developed NanoGalaxy, a platform of polymeric hydrophilic nanoparticles (HNPs) for in vivo mRNA delivery. We previously demonstrated HNP-mediated delivery or mRNA to spleen antigen-presenting cells and now identified new polymer HNP compositions that deliver mRNA to lung endothelial cells (EC) and alveolar macrophages (AM).

Lung-targeted HNPs were identified through sequential *in vivo* screening. Tissue biodistribution was evaluated by bioluminescence imaging (BLI), and cell-specific delivery was characterized by flow cytometry following a single intravenous (IV) dose (0.75–1 mg/kg) of firefly luciferase (Fluc) or GFP mRNA in C57BL/6 mice. Lead HNPs formulated with mRNA exhibited particle sizes of 100–150 nm, a polydispersity index (PDI) <0.3, and a near-neutral zeta potential.

At the tissue level, BLI demonstrated strong lung-selective delivery by NanoGalaxy HNPs. Lead formulations achieved lung:spleen signal ratios of 14 and 12 and lung:liver signal ratios of 1,080 and 1,563, confirming preferential lung targeting. At the single-cell level, flow cytometry demonstrated that tissue tropism is tunable through polymer composition. Lead HNPs efficiently transfected lung EC, reaching 58% and 39% GFP+ endothelial cells, while alveolar macrophage transfection was formulation-dependent, reaching up to ~43% GFP+ with select HNPs. All formulations were well tolerated.

These results show that NanoGalaxy HNPs can be an efficient, lung-tropic, nonviral mRNA delivery platform, extending tissue-selective delivery from the spleen to the lung. By enabling selective delivery to specific pulmonary cell types, this tunable delivery platform expands the addressable target space for *in vivo* mRNA therapeutics, with potential applications in pulmonary vascular diseases, pulmonary fibrosis, and lung-directed immunotherapies.

A Data-Driven Framework for AAV Gene Therapy Manufacturing: Upstream Process Optimization, Downstream Process Design, and Process Characterization for Late-Stage Readiness

Keerthana Subramanian[1], Sumit Dutta[1], Ganesh Krishnamoorthy[1], Steven Wesel[1], Danielle Sexton[1], Smita Menon[1], Cliff Aquino[2], Meet Patel[2], Aga Gascoyne[3], Ashley Craddick[4], Frank Agbogbo[1], David Dismuke[5]

[1]Forge Biologics, Process Development, Grove City, United States, *[2]Forge Biologics, Manufacturing Science and Technology, Grove City, United States*, *[3]Forge Biologics, GMP Manufacturing, Grove City, United States*, *[4]Forge Biologics, Operations, Grove City, United States*, *[5]Forge Biologics, Technical Leadership, Grove City, United States*

Abstract Text A data-driven framework for AAV gene therapy manufacturing: upstream process optimization, downstream process design, and process characterization for late-stage readiness

Introduction

Advancing adeno-associated virus (AAV) gene therapy programs toward late-stage development requires manufacturing strategies that combine scalable platform capabilities with the flexibility to support programs at different stages of maturity and with different technical starting points. As the gene therapy sector continues to mature, with an expanding pipeline of late-stage clinical programs and commercial launches, the manufacturing conversation is expanding beyond early process development to include the manufacturing strategies required to successfully support late-stage development and commercialization. This presentation highlights manufacturing strategies that address these evolving needs while enabling phase-appropriate development as programs progress towards commercialization.

Approach

Three manufacturing engagement models are highlighted. The first encompasses programs fully integrated into Forge's FUEL™ platform, leveraging advanced technologies, product-specific customizations, and structured process development from the outset. This group spans a range of indications and dose requirements, from programs requiring large to small vector quantities where maximizing titer reduces cost of goods, allowing clinical and commercial needs to be met from fewer or smaller-scale batches. Across these programs, end-to-end optimization including productivity improvements and downstream unit operation optimizations is paired with early process development work to position each program for an efficient path toward process performance qualification (PPQ).

The second model reflects programs that require a transition from an earlier process to an improved version utilizing client-developed technologies. These engagements demand careful bridging of comparability data, technology transfer or re-optimization of upstream and downstream operations, and close regulatory alignment to ensure process changes are executed without sacrificing program momentum. This path demonstrates how process

evolution during development can be managed systematically while preserving the data integrity needed for continued advancement.

The third model represents technology transfer engagements, where a program's existing process is fully implemented and retrofitted into Forge's facility. Rather than applying a standard platform, these programs require detailed understanding of the established methods, facility fit assessment, and careful adaptation of unit operations, preserving the integrity of processes already supported by pre-clinical data while enabling the manufacturing readiness needed for late-stage progression.

Central to all three models is a shared process characterization framework that provides every program with a consistent scientific foundation, while allowing the scope and depth of activities to evolve based on development stage and program-specific needs.

Using a structured approach that links failure modes, risk assessment, design of experiments, and attribute-to-parameter mapping, this framework is designed to be flexible, scalable to the complexity of each program and shaped by the development stage of the program. Rather than a one-size-fits-all exercise, process characterization is being approached as phased strategy, one that matures with each program and ensures the right data are in place to support control strategy development, regulatory submissions, and ultimately enable successful PPQ.

Results and conclusions

Across all three models, and across the full spectrum of patient populations, dose requirements, and development stages they represent, a shared commitment to data integrity, process robustness, and patient access drives every decision. Whether building a process from the ground up, evolving an existing one, or adopting a tech transfer process, the goal remains the same: to generate the process knowledge and manufacturing readiness needed to help every program reach the patients.

‘pA regulator’: a clinically relevant gene regulation system for gene and cell therapy

Jocelyn Jea[1], Che-Hsing Li[2], Andras Heczey[2], Laising Yen[1]

[1]Baylor College of Medicine, Pathology & Immunology, Houston, United States, *[2]Seattle Children's Research Institute, University of Washington, Seattle, United States*

Abstract Text

Controlling gene expression within the therapeutic window is crucial for safe and efficacious therapies, since overexpression could result in severe toxicity and even death. Fine-tuned expression based on disease stage or severity tailored to individual needs has become pivotal in cell and gene therapy. However, current gene transfer methods, such as Adeno-Associated Virus (AAV), are incapable of conditional and reversible gene control that require calibration after delivery. Common gene regulation tools, such as the Tet-On system, rely on foreign regulatory proteins which cause the eventual elimination of gene expression and destruction of transduced host cells. As a result, none has been approved by the FDA for clinical use.

Recently, we developed the ‘pA regulator’, an RNA-based gene regulation system that fills this critical gap by overcoming key challenges in existing systems. The pA regulator contains a polyA signal (PAS) embedded at the 5’ UTR. Efficient cleavage of the PAS at the 5’UTR destroys the mRNA, and therefore, no gene expression. To turn on gene expression, we clamp the PAS by an aptamer (an RNA ‘sensor’ sequence that recognizes a specific ligand). Binding of the ligand (tetracycline (Tc) in this case) to the aptamer inhibits cleavage, resulting in the preservation of intact mRNA and gene expression. To achieve exceptional control, the cleavage of PAS is modulated by a 'dual-mechanism': drug binding that directly inhibits PAS cleavage, and drug-induced alternative splicing that removes the PAS, both activated by drug administration to cells.

This RNA-based system achieves up to 900-fold induction with an EC_{50} of 0.5 µg/ml Tc, which is well within the FDA-approved dose range. The pA regulator can be driven by a variety of promoters in various cell lines. Unlike the Tet-On system that requires one promoter to generate the regulatory protein and another to express the transgene, the pA regulator is a compact single promoter system that can be implemented in a single plasmid or viral vector. Unlike other systems that alter transgene coding sequences thus promoting a transgene-specific immune response, the pA regulator does not change the coding sequence or require foreign regulatory proteins, thereby circumventing host immune responses. Its utilities have been demonstrated in four different contexts: transgenes in transient transfection of human cells, in stable human cell lines, in a mouse model by AAV-mediated gene transfer, and in controlling the endogenous *CD133* gene residing in the human genome, all in a dose-dependent and reversible manner with long-term stability. It is the first RNA-based, non-immunogenic gene regulation system that demonstrates an EC_{50} within the FDA-approved dose.

Lentivirus is another commonly used gene transfer vehicle. To determine the efficacy of the pA regulator by lentivirus-mediated transfer, we engineered it into the lentiviral vectors in the reverse orientation. This strategy prevents sequence loss from RNA splicing and PAS-mediated cleavage during lentivirus production. The pA regulator exhibited efficient control of eGFP in lenti-transduced 293T cells and B16 cells. Further optimizations are currently in process for applications such as CAR-T cell engineering.

The pA regulator has displayed efficient gene regulation controlled by Tc. However, like most other small-molecule ligands, Tc cannot penetrate all tissues effectively. As a result, the current pA regulator controlled by Tc would work well *in vivo* in blood cells or liver, partially in skeletal muscle, but not in the central nervous system. One key feature of the pA regulator is its strong RNA secondary structures. Ligand binding further stabilizes the RNA structure without involving complicated RNA refolding. This allows 'plug-and-play' replacement of the Tc aptamer by other aptamers with minimal modifications. To explore this feature, we engineered the AC-17 aptamer to replace the Tc aptamer in the pA regulator. This new aptamer binds ASP2905, a ligand capable of penetrating the blood–brain barrier. Our preliminary testing showed that the pA regulator with AC-17 achieved up to 156-fold induction at 2 μM of ligand in cultured cells. Further optimization of its efficiency and *in vivo* testing in the central nervous system are currently underway.

In summary, clinical applications of gene regulation require demanding features like non-immunogenicity, high dynamic ranges, low leakage expression, and low ligand concentrations for induction. The pA regulator fulfills such needs by using an FDA-approved drug within the clinically safe dose range. Furthermore, the ability of the pA regulator to accommodate various aptamers specific to ligands with different pharmacokinetic properties opens up new opportunities for *in vivo* applications targeting different tissues. As such, we envision the pA regulator to have wide-ranging applications both in biological studies as well as gene and cell therapy.

Oral Abstracts - CNS

Microglia engineered for amyloid-β-guided responses via synthetic Notch receptors for Alzheimer's therapy and modeling

Swathi Shekharan[1], Jonathan Brunger[1], Madeline Spetz[1]

[1]*Vanderbilt University, Biomedical Engineering, Nashville, United States*

Abstract Text

Alzheimer's disease (AD) is a neurodegenerative disorder characterized by chronic neuroinflammation, driven in part by the accumulation of amyloid-β (Aβ), which contributes to neuronal dysfunction and cognitive decline. Despite extensive efforts to identify disease-modifying treatments, current therapies, including FDA-approved Aβ-targeting antibodies, offer limited clinical benefits and carry significant safety concerns such as cerebral edema and hemorrhage. These gaps highlight the need for targeted, curative strategies that modulate neuroinflammation without systemic toxicity. Here, we present a potential engineered microglial cell therapy that utilizes synthetic Notch (synNotch) receptors to conditionally sense Aβ and trigger programmable responses. As the resident immune cells of the brain, microglia play critical roles in maintaining homeostasis by providing trophic support to neurons and clearing debris. However, during AD, these functions become dysregulated and can exacerbate disease, as well as cause damaging crosstalk with other cell types. These features of disease within microglia provide a unique opportunity to study and reprogram these mechanisms to be neuroprotective.

We have designed synNotch receptors to detect Aβ and activate downstream transcriptional programs (Figure 1a). Human immortalized microglia were transduced with lentiviral vectors encoding an Aβ-synNotch receptor as well as transgene payloads including firefly luciferase and mCherry reporter. Aβ-synNotch microglia elicit potent responses to treatment with synthetic Aβ42, issuing greater than 100-fold increase in reporter transgene expression (Figure 1b, c). To enable therapeutic function, microglia were further engineered to secrete anti-TNF factors by replacing reporters with transgenes derived from the TNF3e nanobody and ozoralizumab antibody. Conditioned media from Aβ-stimulated microglia significantly attenuated NFkB transcriptional activity in TNF-treated cells (Figure 2a). In addition, cells were also engineered with a payload containing secreted TREM2 and BDNF, which were measured in cell culture media at 600 and 170 pg/ml respectively when plated with Aβ (Figure 2b, c).

This study demonstrates the feasibility of reprogramming microglia with synNotch receptors to create an inducible, Aβ-responsive immunomodulatory technology with novel use in AD. By coupling disease sensing with therapeutic payload delivery, we introduce a platform for context-specific neuroimmune engineering that is local and adaptive, contrasting current treatments, which are systemic and constitutive. Beyond its therapeutic potential, this system provides a framework for interrogating neuroinflammatory signaling and multicellular interactions in an iPSC-derived AD model. These experiments provide the foundation for ongoing analyses of how programmable microglial responses influence neuroinflammatory dynamics and neuronal function in AD models. Collectively, this work bridges synthetic biology and neuro-immunology through cell engineering, demonstrating

the synNotch platform as a tool for not only cell-based therapies but also for developing novel, mechanistically informed methods of studying neurodegenerative disease.

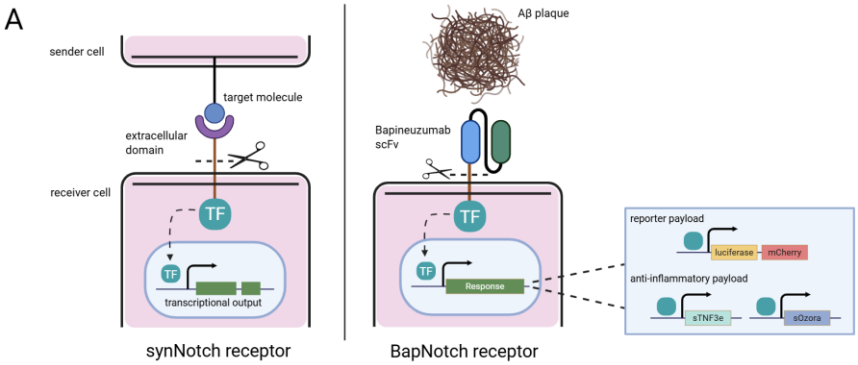

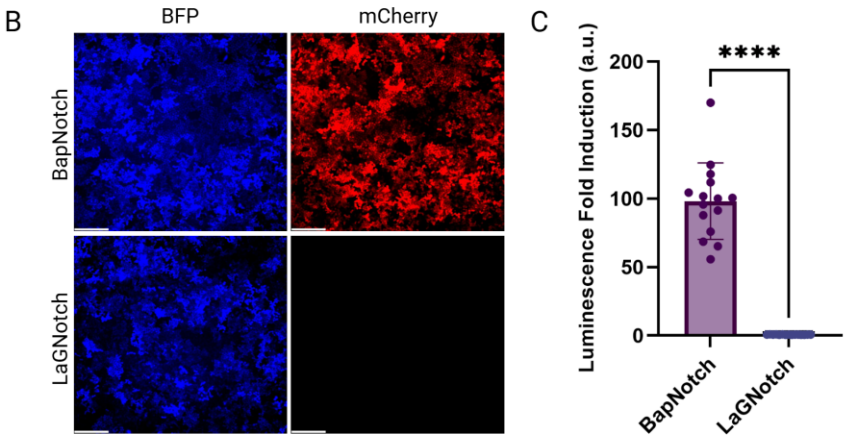

Figure 1

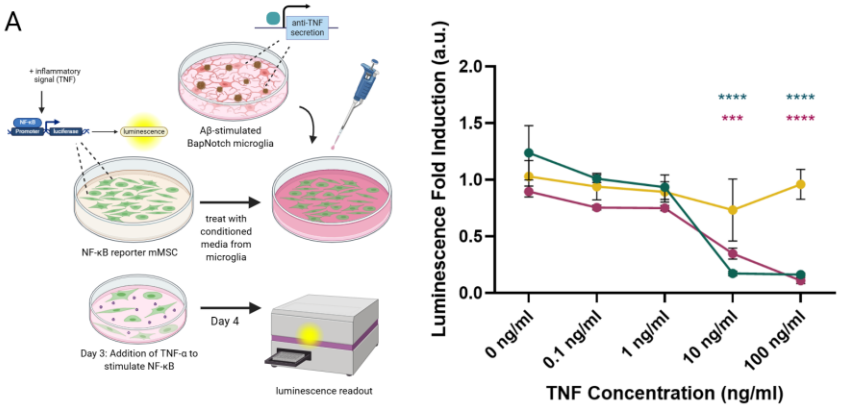

Figure 2

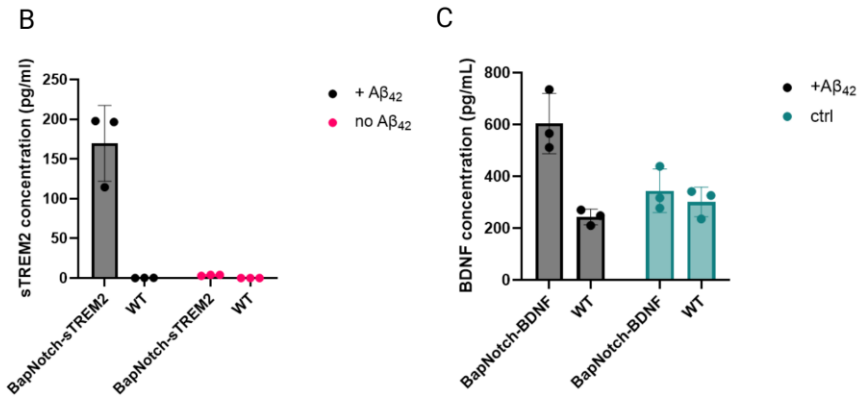

Figure 1: (A) SynNotch is based on the native Notch pathway and involves a target molecule

on a sender cell that is recognized by an extracellular domain on a receiver cell. Upon recognition, a cleavage event occurs, allowing a transcription factor to translocate to the nucleus and drive responsive transgenes. To construct the BapNotch receptor, the extracellular recognition domain is replaced with a Bapineuzumab single-chain variable fragment (scFv). The intracellular domain is replaced with a synthetic transcription factor that drives expression of a programmed transgene, such as luciferase and mCherry reporters or soluble anti-inflammatory payloads derived from TNF3e (nanobody) or ozoralizumab. (B) Fluorescent microscopy of Aβ-dependent mCherry activation in BapNotch and LaG16Notch (GFP-responsive) human microglia cells. (C) BapNotch human immortalized microglia have an average 98x luminescence fold induction of firefly luciferase in response to biotinylated Aβ. ****$p<0.0001$. Scale bar = 200µm.

Figure 2: (A) Schematic depicting NF-κB reporter assay: mMSCs were engineered to respond with luciferase upon activation of the NF-κB pathway, which occurs during inflammation. Conditioned media from BapNotch microglia plated with Aβ was plated on mMSCs for 72 hours. TNF was added after 72 hours and luminescence was measured after 24 hours. Luminescence readout for TNF3e and Ozora secreting, and WT microglia. * represents statistical significance compared to WT . (B) sTREM2 secretion measured in cell culture media of micoglia plated with β for 72 hours. (C) sTREM2 secretion measured in cell culture media of micoglia plated with β for 72 hours. ****$p<0.0001$.

Unlocking Flexibility in Viral Vector Manufacturing: High-efficiency DNA removal - Engineered to fit your process

Melissa Rangel[1]

[1]*Kerry, Beloit, United States*

Abstract Text

In viral vector manufacturing for cell and gene therapies as well as vaccine applications, the safety and efficacy of the final therapeutic product is critical. During production, lysis of genetically modified host cells releases residual host cell and plasmid DNA, which may pose immunogenic and oncogenic risks.[1,2] Regulatory agencies such as the FDA therefore defined limits for both the concentration (<10 ng/dose) and fragment size (<200 base pairs) of residual DNA in the final product.[3,4] To meet these requirements, endonucleases are routinely used to degrade nucleic acids into small, removable fragments without compromising viral particle integrity. Enzymes derived from *Serratia marcescens*, such as Denarase®, are established as the industry standard for this purpose and contribute to improved process performance by reducing DNA-related viscosity and aggregation. However, modern viral vector manufacturing processes increasingly operate across a broad range of process conditions, including variable salt and pH conditions, to optimize vector yield, stability, and overall process performance. These conditions can challenge the activity of conventional nucleases and limit overall process flexibility. Here, we present Denarase® High Salt, an engineered endonuclease specifically designed for efficient degradation of nucleic acids under a wide range of salt and pH levels. The data demonstrate consistent and efficient DNA removal across a wide range of salt concentrations, highlighting its suitability to increased process robustness, flexibility, and efficiency in viral vector purification workflows.

1 Sheng-Fowler L, Lewis AM, Peden K. Issues associated with residual cell-substrate DNA in viral vaccines. Biologicals. 2009;37(3):190-195. doi:10.1016/j.biologicals.2009.02.015

2 Singh SK. Impact of Product-Related Factors on Immunogenicity of Biotherapeutics. J Pharm Sci. 2011;100(2):354-387. doi:10.1002/jps.22276

3 US Food and Drug Administration; Rockville, MD: 2010. Guidance for industry: Characterization and Qualification of Cell Substrates and Other Biological Materials Used in the Production of Viral Vaccines for Infectious Disease Indications.

4 US Food and Drug Administration; Rockville, MD: 2020. Guidance for industry: Chemistry, Manufacturing, and Control (CMC) Information for Human Gene Therapy Investigational New Drug Applications.

Advanced DNA removal with Denarase® High Salt

#Method: Kerry Salt performance test

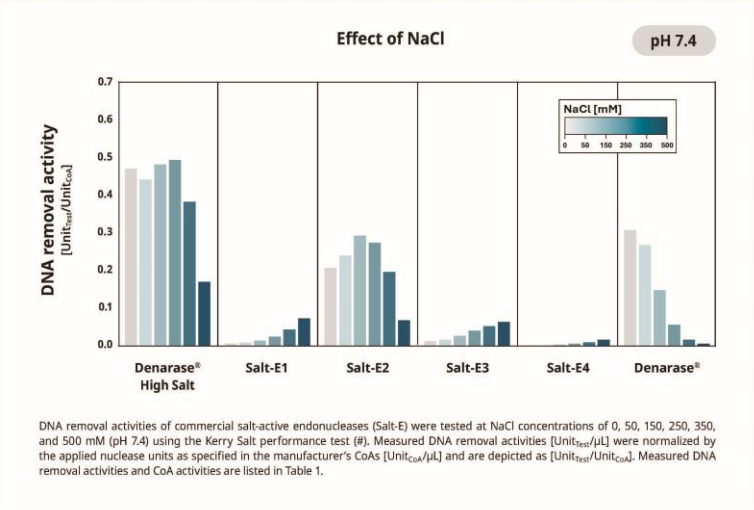

DNA removal activities of commercial salt-active endonucleases (Salt-E) were tested at NaCl concentrations of 0, 50, 150, 250, 350, and 500 mM (pH 7.4) using the Kerry Salt performance test (#). Measured DNA removal activities [$Unit_{Test}$/µL] were normalized by the applied nuclease units as specified in the manufacturer's CoAs [$Unit_{CoA}$/µL] and are depicted as [$Unit_{Test}$/$Unit_{CoA}$]. Measured DNA removal activities and CoA activities are listed in Table 1.

Denarase® High Salt

- Achieves **highest DNA removal** across 0–500 mM NaCl
- **Outcompetes other salt-active nucleases** at process-relevant pH 7.4#

DNA removal activities

Nuclease	NaCl [mM]	a) Measured with c-LEcta Test# [U_{Test}/µL] 0	50	150	250	350	500	b) CoA# [U_{CoA}/µL] acc. to CoA
Denarase® High Salt		168.8	158.1	172.5	177.0	137.3	61.4	358.0
Salt-E1		0.2	0.2	0.4	0.7	1.1	1.9	26.0
Salt-E2		5.9	6.8	8.3	7.7	5.6	1.9	28.2
Salt-E3		4.0	5.2	8.3	12.6	16.1	19.7	306.0
Salt-E4		0.4	0.6	1.0	1.5	2.4	4.1	250.0
Denarase®		107.5	93.5	51.9	19.9	5.8	2.0	349.0

Table 1: DNA removal activities of salt-active nucleases per µl sample as **a**) measured using the Kery Salt performance test# [U_{Test}/µL] and **b**) outlined in suppliers' CoAs [U_{CoA}/µL].

#Kerry Salt performance test: Nuclease products were tested at different NaCl concentrations in reactions conducted for 60 min at 30°C in 50 mM Tris-HCl (pH 7.4), 15 mM $MgCl_2$, 0.8 mg/mL salmon sperm DNA, and 0.1 mg/mL bovine serum albumin. Reactions were stopped with perchloric acid, incubated on ice for 30 min, centrifuged, and the absorbance of the supernatants was measured at 260 nm and corrected against blanks without nuclease (ΔA260). One test Unit ($Unit_{Test}$) of enzyme activity was defined as the amount of enzyme that produces a change in absorbance at 260 nm of 1.0 in the time of 30 minutes. DNA removal activities are listed as enzyme activity per 1 µL of the undiluted enzyme product ($Unit_{Test}$/µL) in Table 1.

Maximum DNA removal across all salt levels!

To test DENARASE® High Salt under actual process conditions a benchmarking study was performed in collaboration with a well-known, UK-based CDMO. DNA
removal from proprietary AAV2 lysates under different pH and salt conditions was compared to a commercially available salt-active endonuclease 1 (SALT-E1).
c-LEcta Salt Performance Test: Nuclease products were tested at different NaCl concentrations in reactions conducted for 60 min at 30°C in 50 mM Tris-HCl (pH 7.4), 15 mM MgCl2, 0.8 mg/ml salmon
sperm DNA, and 0.1 mg/ml bovine serum albumin. Reactions were stopped with perchloric acid, incubated on ice for 30 min, centrifuged, and the absorbance of the supernatants was measured at 260
nm and corrected against blanks without nuclease (A260). One test Unit (UnitTest) of enzyme activity was defined as the amount of enzyme that produces a change in absorbance at 260 nm
of 1.0 in the time of 30 minutes. DNA removal activities are listed as enzyme activity per 1 µl of the undiluted enzyme product (UnitTest/µL) in Table 1.

Advancing cell dissociation in bioprocessing with CellTrypase: A novel, high purity trypsin-like enzyme for GMP workflows

Raphael Gübeli[1]

[1]*Kerry, Leipzig, Germany*

Abstract Text

GMP-compliant manufacturing of advanced cell-based therapies, viral vaccines and vectors for gene therapies requires stringent control of raw materials to ensure safety, consistency, and regulatory compliance. Cell dissociation is a critical step in these workflows, yet conventional trypsin solutions often lack defined purity levels and only partially comply with GMP standards. Increasing regulatory and quality expectations have accelerated the adoption of recombinant alternatives[1,2,3,4]. Recombinant trypsin-like enzymes, like TrypLE™[5] have emerged as a preferred solution because they enable efficient but more gentle cell dissociation.

CellTrypase is a recombinant trypsin-like enzyme of fungal origin that combines highest purity with robust performance across diverse cell systems. Its GMP-compliant manufacturing process excludes materials of animal origin, antibiotics, Triton X-100, and TSE/BSE-risk components, ensuring consistently high purity, traceability and alignment with global regulatory standards.

Benchmarking against the current GMP-grade industry standard demonstrated that CellTrypase offers superior purity. It also delivers comparable detachment efficiency, high viability, and stable yields over multiple passages, with slightly reduced dissociation times in production cell lines and induced pluripotent stem cells (iPSCs). CellTrypase thus sets a new standard for safe, consistent, and highest quality cell dissociation in modern GMP workflows.

1 US Food and Drug Administration. (2010). Guidance for industry: Characterization and Qualification of Cell Substrates and Other Biological Materials Used in the Production of Viral Vaccines for Infectious Disease Indications. Rockville, MD.

2 European Medicines Agency. (2014). Guideline on quality, non-clinical and clinical requirements for investigational advanced therapy medicinal products in clinical trials. EMA/CHMP/BWP/814397/2011

3 European Pharmacopoeia (Ph. Eur.). Chapter 5.2.12, Raw Materials of Biological Origin for the Production of Cell-Based and Gene Therapy Medicinal Products. Strasbourg, France, Council of Europe.

4 United States Pharmacopeia. General Chapter, ⟨1043⟩ Ancillary Materials for Cell, Gene, and Tissue-Engineered Products. USP-NF. Rockville, MD.

5 TrypLE is a registered trademark of Thermo Fisher Scientific Inc.

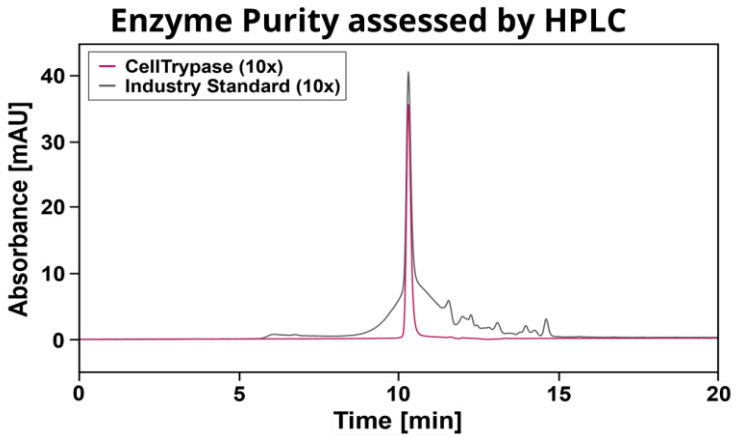

Purity Assessment: High-performance liquid chromatography (HPLC) was used to confirm and compare enzyme purity.

Performance Benchmarking: Enzyme performance of CellTrypase was compared to the current GMP-grade industry standard across:

- commonly used adherent production cell lines: CHO-K1, HEK 293, MDCK, Vero
- advanced cell systems: human iPSCs cultured as 2D colonies and 3D aggregates.

Performance metrics include microscopic and cell count-based analysis of dissociation time, cell yield, residual aggregates, post-treatment viability and growth behavior in multi-passaging experiments. Expression of pluripotency markers (Oct3/4, SSEA3 & 4, TRA-1-60, CD30, Nanog, Sox2) after dissociation was assessed by flow cytometry.

Purity: HPLC analysis confirms a purity of ≥95% and the absence of degradation products, in contrast to the common industry standard.

Performance Benchmarking: Across CHO-K1, HEK 293, MDCK and Vero cell lines, CellTrypase demonstrated effective cell detachment and equivalent performance to the current industry standard trypsin-like enzyme. It enabled comparable or slightly shorter dissociation times, high viability, stable yields, and consistent growth kinetics over five passages. In human iPSC cultures, CellTrypase reduced dissociation time from 7 min (control) to 5 min while maintaining viability (94%) and without compromising cell integrity, viability and post-dissociation morphology and growth. Pluripotency markers remained above the predefined threshold of 75%, confirming phenotype preservation. Performance in 3D aggregates was comparable to the industry standard.

Oral Abstracts - Clinical Translation

Regenerative Macrophage Therapy drives an anti-fibrotic response in lung fibrosis

Jessica Llewellyn[1], Monica Reis[1], Joanna Sweetman[1], Cecilia Rocchi[1], Celia Diaz-Nicieza[1], Mark Cant[1], Sahad Iqbal[1], Anna M. Hoy[1], Kayleigh L. Thirlwell[1], Lara Campana[1]

[1]*Resolution Therapeutics Ltd, Research and Translational Science, Edinburgh, United Kingdom*

Abstract Text

Fibro-inflammatory diseases are characterised by chronic damage, inflammation and scarring, which progressively lead to loss of function of the interested organ. In the lung, continuous damage of various aetiologies drive the development of a group of 200+ pathologies collectively referred to as ILD (Interstitial Lung Disease). The more severe pathologies in this group are charachterized by a progressive loss of breathing unit (alveoli) to fibrosis, which result in a continuous decline in lung function. Available medical therapies only slow down this decline and are marred by significant side effects. Lung transplantation is limited by availability of organs, complexity of the surgery and need for life-long post-surgery care.

Macrophages with a regenerative phenotype have been shown to have both anti-inflammatory and anti-fibrotic properties, and to be well-tolerated and effective both preclinically and clinically in liver fibrosis (cirrhosis). Moreover, we have demonstrated that engineered macrophages have improved anti-inflammatory and anti-fibrotic properties, and such macrophages are currently being tested in the EMERALD Phase 1/2 study in patients with End Stage Liver Disease.

However, to date, the effectiveness and tolerability of regenerative macrophages has not been demonstrated in other fibro-inflammatory diseases. We therefore applied our learning from the liver program to design and carry out preclinical studies to demonstrate the therapeutic potential of this modality in lung fibrosis, with the ultimate aim of utilising engineered RMT as disease-modifying therapy in the context of severe ILDs.

In these studies, we used the single-administration bleomycin model to test regenerative macrophages MoA and anti-fibrotic potential when administered intravenously. We tested non-engineered regenerative macrophages alongside regenerative macrophages engineered for increased anti-inflammatory and anti-fibrotic effects. We administered the test articles i.v. in single and double dose in a therapeutic setting, *i.e.* when fibrosis is established at day 10 or 14 post-bleomycin (Figure 1). We collected lungs, BAL (Broncho-Alveolar Lavage) and blood at one week post-administration and we utilised an independent pathologist to analyse fibrosis in the lung sections, and an independent provider to perform proteomic analysis of blood and BAL.

Preliminary histological analyses revealed an anti-fibrotic effects of engineered regenerative macrophages in the lung, with modulation of systemic inflammation. Further histological and *in vitro* analyses aiming at dissecting biodistribution and MoA further are underway to support initiation of a Phase 1/2 study.

In conclusion, RMT has a promising profile as disease-modifying approach in both liver and lung fibrosis. Our data support a role of RMT in tackling chronic fibro-inflammatory diseases thanks to their dual anti-inflammatory and anti-fibrotic effects, which modulate the local microenvironment, turning it from hostile to permissive to regeneration. Details of RMT mechanism of action are currently under investigation in patients with cirrhosis and experimental models of lung fibrosis to enable further development in the clinic.

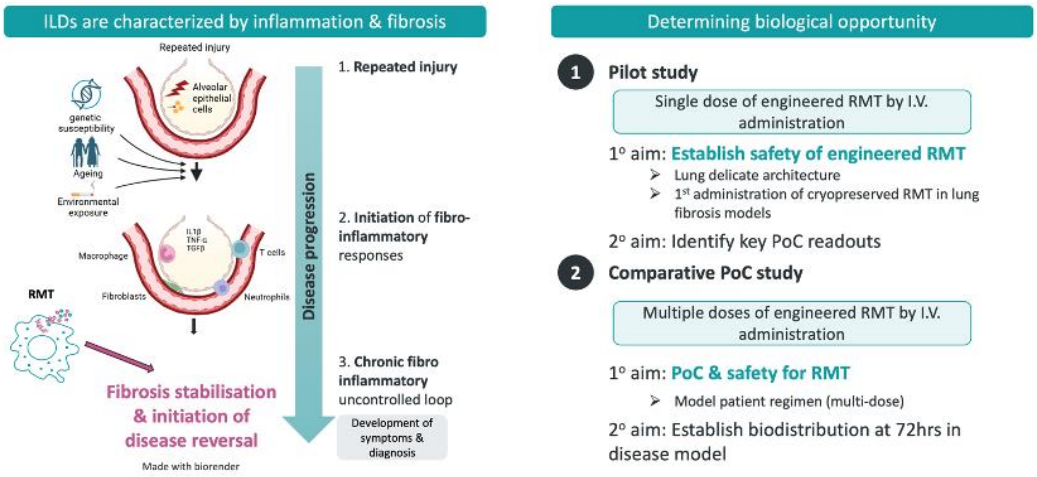

Figure 1 - Therapeutic hypothesis for RMT in ILDs (left panel); experimental design to support translation into the clinic of engineered RMT currently tested in patients with end-stage liver disease (right panel)

From Endonuclease Comparability Challenges to Harmonized Activity Testing:USP {89.3} General Chapter for Endonucleases.

Melissa Rangel[1]

[1]*Kerry, Beloit, United States*

Abstract Text In the manufacturing of viral vectors for gene and cell therapies as well as vaccines, removal of residual DNA and RNA from host cells and plasmids is critical to meet regulatory requirements1 and streamline vector purification. For this purpose, endonucleases are typically added to cleave polynucleotide chains into smaller fragments of about 3–5 base pairs. Endonucleases derived from Serratia marcescens, in particular Denarase® and Benzonase®[2], are the current industry standards due to their efficient activity on diverse DNA/RNA substrates. Both enzymes share an identical protein sequence and are generally considered interchangeable, making enzyme activity a key parameter for product comparison. However, differences in vendor-specific enzyme activity release assays and unit definitions make direct comparison of Certificates of Analysis (CoAs) challenging. Comparability of endonucleases is essential to secure supply chains, including dual sourcing strategies.

To address this long-standing comparability challenge, the USP (United States Pharmacopeia) has released the General Chapter 89.3 Endonuclease (*Serratia marcescens*), introducing a harmonized framework for endonuclease activity determination. This marks an important step toward standardization of a critical ancillary material used in cell and gene therapy (CGT) manufacturing.

Using Kerry's Denarase® activity assay, Denarase® and Benzonase® were evaluated under identical testing conditions. The study demonstrates how assay design influences reported activity values and highlights the importance of harmonized release testing methods for reliable product comparison.

1 US Food and Drug Administration. Chemistry, Manufacturing, and Control (CMC) Information for Human Gene Therapy Investigational New Drug Applications (INDs).; 2020

2 Benzonase Nuclease is a registered trademark of Merck KGaA

3 BioPhorum Operations Group Ltd; D. Blake; A. Schaefer, A. Witz, N. Preyat, R. Hodges & V. Mwanza; A proposal to align release standards for endonucleases used in nucleic acid removal; 2023. https://doi.org/10.46220/2023CGT002

Transparent product comparison starts with harmonized activity assessment

Technical performance of Denarase® & Benzonase® according to CoAs

	Denarase® GMP-grade (20804) Measured with Denarase® activity assay		**Benzonase® Emprove® Expert** (101697) Measured with Benzonase® activity assay	
	Specification[4]	**CoA** (Lot GD-a-0014)	**Specification**[5]	**CoA** (Lot K54520397)
Volumetric activity	> 250 U/µL	295 U/µL	> 250 U/µL	393 U/µL
Protein content	Not shown	0.259 mg/mL	not shown	0.187 mg/mL
Specific activity	> 0.6×10^6 U/mg	1.139×10^6 U/mg	≥ 1.1×10^6 U/mg	2.1×10^6 U/mg

Volumetric activity & protein content = measured by vendor-specific activity assay → **Specific activity** = $\frac{\text{Volumetric activity}}{\text{Protein content}}$

Why activity values differ between assays

- Nature & concentration of substrate
- Source/lot-specific variations in the DNA substrate's average fragment length and inhibitory contaminants (e.g., salts)
- Assay buffer composition
- Temperature and pH

1 Unit = amount of enzyme that causes a change in absorbance at 260 nm [A260] of 1 in 30 min.

Endonuclease activity is typically measured in vendor-specific units!

[4] Product Specification Denarase® Link

[5] Product Specification Benzonase® Link

Oral Abstracts - Clinical Translation

Impact of Immunosuppressive Agents on the Expansion and Phenotype of Antigen-Specific CAR-Tregs for Organ Transplantation

Ruoshui Hu[1], Tao Wang[1], Jean Kwun[1]

[1]*Duke University, Duke Transplant Center, Durham, United States*

Abstract Text

Introduction

Chimeric antigen receptor regulatory T cells (CAR-Tregs) are being developed as antigen-specific cellular therapies to promote immune tolerance while reducing reliance on nonspecific immunosuppression. Because CAR-Treg therapies will likely be administered alongside conventional immunosuppressive agents in organ transplantation, concomitant immunosuppression may influence CAR-Treg survival and regulatory function. In the present study, we evaluated the effects of tacrolimus, rapamycin, and methylprednisolone (Solu-Medrol) on Bw6-specific CAR-Tregs to determine how conventional immunosuppressive agents may affect CAR-Treg expansion and phenotype and their potential clinical translation in organ transplantation.

Methods

Bw6-specific CAR-Treg cells from two nonhuman primates (XJ66 and XJ67) were evaluated across drug-exposure experiments. CAR-Tregs were expanded with irradiated K562.B7.86 artificial antigen-presenting cells with IL-2 for five days to methylprednisolone (0–100 µM), tacrolimus (0–100 ng/mL), or rapamycin (0–100 ng/mL). Each drug condition was cultured in technical triplicate. Absolute CD4+ cell recovery was quantified by bead-based flow cytometry and normalized to matched no-drug controls. Transcription factors FoxP3 and Helios expressions were assessed by flow cytometry as markers of regulatory phenotype.

Results

Supplementation of immunosuppressive agents produced reproducible, drug-specific effects on CAR-Treg recovery. All drugs negatively impacted IL-2-mediated CAR-Treg expansion. At approximate clinically relevant concentrations, mean recovery was 88% of control with tacrolimus (10 ng/mL; range, 79–96%), 76% with methylprednisolone (20 µM; range, 66–88%), and 34% with rapamycin (10 ng/mL; range, 23–53%). Across the broader dose range, rapamycin consistently produced the greatest reduction in recovery, tacrolimus largely preserved recovery, and methylprednisolone showed an intermediate, dose-dependent effect. FoxP3 expression was broadly retained among surviving cells across drug conditions. However, tacrolimus at 10 ng/mL was associated with Helios frequencies of 58.7% and 42.6%, respectively, compared with

79.6% and 75.1% with methylprednisolone and 73.5% and 74.3% with rapamycin.

Conclusions

Conventional immunosuppressive agents had different effects on CAR-Treg expansion and regulatory genes, suggesting that drug choice may influence CAR-Treg performance. Rapamycin substantially impaired CAR-Treg expansion despite broad preservation of regulatory markers, whereas tacrolimus better preserved recovery but was associated with lower Helios frequency in two line-specific datasets. The impact of tacrolimus on the functional transcript of Treg varied in magnitude and warrants confirmation with additional biological replicates. These findings suggest that immunosuppressive agents considered favorable for Tregs may not necessarily be optimal for in vivo CAR-Treg expansion. Therefore, concomitant immunosuppressive regimen should be selected based on their compatibility with CAR-Tregs and their ability to preserve CAR-Treg phenotype and function during clinical translation.

Figure 1

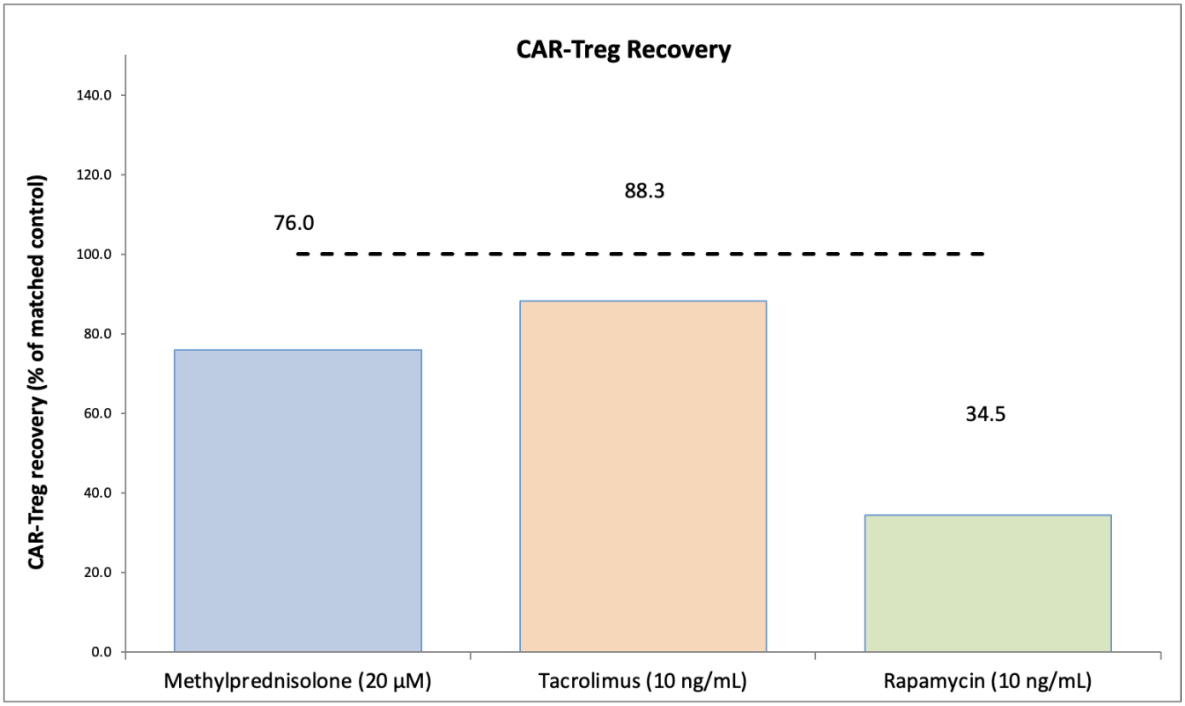

Figure 2

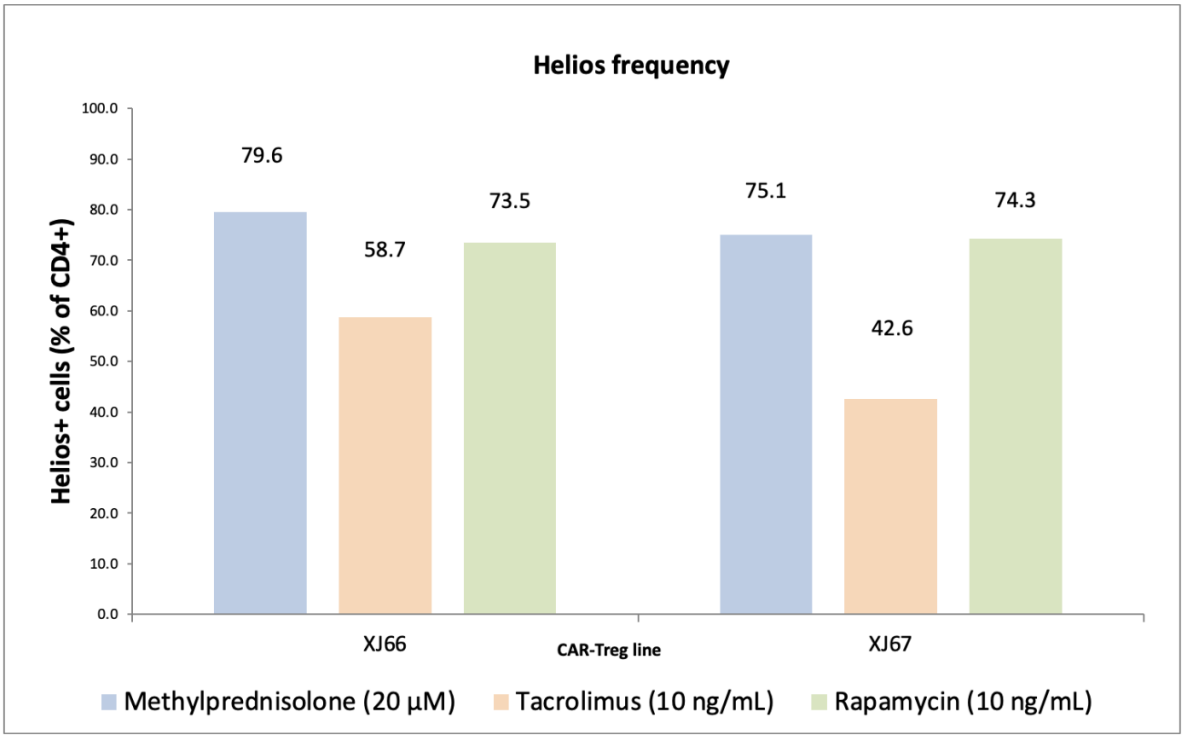

Figure 1. CAR-Treg recovery at clinically relevant immunosuppressive drug concentrations. Bars show mean CAR-Treg recovery across three line-specific datasets (XJ67 from Test 1 and XJ66 and XJ67 from Test 2) following exposure to methylprednisolone (20 µM), tacrolimus (10 ng/mL), or rapamycin (10 ng/mL). Recovery was normalized to the matched drug-specific 0-dose control. The dashed line indicates 100% recovery relative to matched control.

Figure 2. Helios frequency following clinically relevant immunosuppressive drug exposure.

Helios frequency is shown as the percentage of Helios-positive cells within the CD4+ population for XJ66 and XJ67 in Test 2 following exposure to methylprednisolone (20 µM), tacrolimus (10 ng/mL), or rapamycin (10 ng/mL). Tacrolimus was associated with lower Helios frequency in both CAR-Treg lines compared with methylprednisolone and rapamycin.

Oral Abstracts - Delivery and Targeting

An RNA-based dual AAV vector system to deliver large dystrophins with high efficiency to muscle for the treatment of Duchenne muscular dystrophy

Jason West[1], Aakanksha Nandagave[1], Zachary Kennedy[1], Jennifer Martin[2], Natania Kurien[2], Ramzi Khairallah[2], Keith Alkek[3], Doug Anderson[3 4], Gerald Cox[1]

[1]CANbridge Pharmaceuticals, Inc., Boston, United States, *[2]Myologica, LLC., Baltimore, United States*, *[3]ScriptR Global, Inc., Rochester, United States*, *[4]University of Rochester School of Medicine and Dentistry, Rochester, United States*

Abstract Text

Duchenne muscular dystrophy (DMD) is caused by loss-of-function mutations in the *DMD* gene encoding dystrophin, a large (427 kDa) cytoskeletal protein. The small packaging capacity of current adeno-associated-virus (AAV)-based gene therapies for DMD limit their delivery to partial-sized dystrophins, commonly called micro-dystrophins, which are between 30-40% of the full-length coding sequence (3.5 to 4 kb of 11 kb). The small size of micro-dystrophins, which may lack important functional subdomains present in the full-length dystrophin protein, may limit their clinical efficacy. Current dual AAV approaches to express larger “midi-dystrophin” (midi-Dys) proteins can either be inefficient or rely on the expression of smaller truncated products. To overcome these limitations, we utilize an RNA-based dual AAV technology, called StitchR (Stitch RNA), to deliver and express midi-Dys transgenes up to 7.5 kb for the treatment of DMD. StitchR utilizes self-cleaving ribozymes to efficiently generate a single large mRNA through precise trans-ligation of two precursor RNAs delivered by separate AAV vectors. Here, we designed numerous StitchR-based midi-Dys transgene sequences sized between 5.6 to 7.5 kb based upon either rational design or their occurrence in Becker muscular dystrophy (BMD) patients with mild clinical phenotypes. We then tested their expression in human skeletal muscle cells from healthy donors. We demonstrate robust expression of multiple different StitchR-based midi-Dys constructs with protein levels exceeding endogenous dystrophin levels in these primary human cells. Optimization of the N- and C-terminal dual AAV sequences has further improved midi-Dys protein expression and enabled robust packaging of the midi-Dys StitchR sequences into AAVs; these optimizations include refining the location of split sites, novel codon utilizations, and the screening of additional AAV regulatory elements. To test the efficacy of this approach in an *in vivo* DMD model, we delivered a 7.1 kb midi-Dys controlled by the muscle specific creatine kinase 8 (CK8) promoter via dual AAVs at total vector dose of 2e14 vg/kg (1e14 vg/kg of each vector) to mdx mice using either AAV9, MYO4A, AAVMYO2, or AAVMYO3. MYO4A-StitchR-midi-Dys treatment offered the greatest level of muscle protection as assayed by muscle force after repeated eccentric contractions of the gastrocnemius 6-7 weeks after AAV treatment. The muscle force of MYO4A-StitchR-midi-Dys treated mdx mice performed similar to healthy wild type control mice and was significantly greater than AAVMYO2-StitchR-midi-Dys ($p < 0.0001$), AAVMYO3-StitchR-midi-Dys ($p < 0.001$), AAV9-StitchR-midi-Dys ($p < 0.0001$), and vehicle treated mdx mice ($p < 0.0001$). AAVMYO2 and AAVMYO3 treatment with StitchR-encoded midi-Dys also offered significantly improved muscle force correction compared to the AAV9 condition at a matched dose ($p < 0.0001$), supporting enhanced myotropism of all three vectors (MYO4A, AAVMYO2, and AAVMYO3) compared to AAV9. In the same study, lower total doses of MYO4A-StitchR-midi-Dys (5e13 vg/kg and 1e14 vg/k) offered significant muscle protection and performed similar

(and not statistically different) from the higher 2e14 vg/kg dose conditions of the AAVMYO2 and AAVMYO3 capsid treatments. Additional measures of midi-Dys protein expression and muscle size and function in the StitchR-midi-Dys-treated mdx mice correlate with these muscle force findings. Together, these data highlight the potential efficacy of a StitchR-based gene therapy for the treatment of DMD and support its further development.

Study the Effect of Shear Stress on Adeno-associated Virus Structure via Molecular Dynamics Modeling

Jayden Liang[1 2], Leila Sharifi[1], Bodhisattwa Chaudhuri[1 2]

[1]*University of Connecticut, School of Pharmacy, Department of Pharmaceutical Sciences, Storrs, United States*,
[2]*University of Connecticut, Department of Chemical & Biomolecular Engineering, Storrs, United States*

Abstract Text Introduction
Shear exposure present during the processes behind adeno-associated virus (AAV) manufacturing is a common stressor linked to capsid destabilization and aggregation. However, determining the specific mechanistic contribution of shear remains experimentally challenging because it often occurs alongside interfacial stresses (air–liquid and solid–liquid), as well as equipment-specific hydrodynamic effects.

Methods
Here, we employ coarse-grained molecular dynamics (CG-MD) to quantify how controlled Couette-like shear influences the shape and stability of AAV8 capsids. A genome-containing AAV8 capsid was simulated with the MARTINI force field in explicit solvent at 300 K under periodic boundary conditions. Couette flow was imposed by deforming the simulation box in the xy direction through GROMACS. Using a cubic box of 62.86 nm, deformation rates of 0.1 and 0.5 nm/ps correspond to approximate shear rates of $\dot{\gamma} = 1.6 \times 10^9\ s^{-1}$ and $\dot{\gamma} = 8.0 \times 10^9\ s^{-1}$, respectively. Capsid responses were evaluated using root mean square deviation (RMSD), radius of gyration (Rg), and an elongation metric computed from axis-resolved gyration components, $E = \max(Rg_x, Rg_y, Rg_z)/\min(Rg_x, Rg_y, Rg_z)$. These quantitative measures were complemented by structural snapshot analysis.

Results
At the lower shear rate, the capsid remained nearly spherical with an elongation metric of E around 1.02, a lower RMSD, and a more compact radius of gyration. By contrast, increasing the shear rate induced pronounced and sustained anisotropic deformation, with E = 1.12, together with higher RMSD plateau and an increased radius of gyration. These changes were consistent with structural snapshots showing a transition from a spherical, compact morphology to a more elongated and less compact state. Overall, these results indicate that the mechanical response of AAV8 is strongly dependent on the imposed shear rate.

Conclusion
This framework provides a quantitative means of assessing AAV mechanical sensitivity under controlled shear. It can also be extended to establish deformation thresholds and evaluate formulation strategies designed to mitigate shear-induced capsid distortion during gene therapy manufacturing.

A

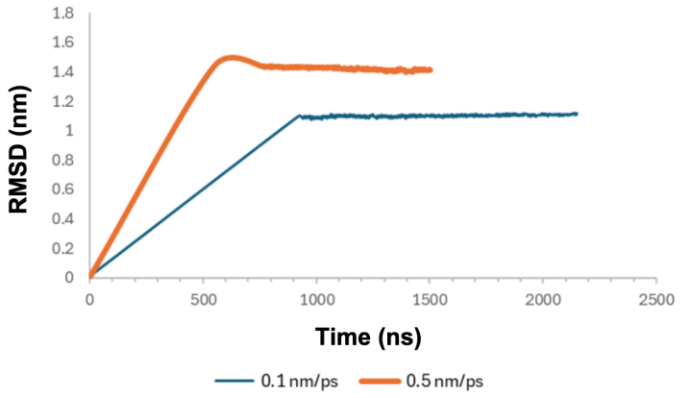

B

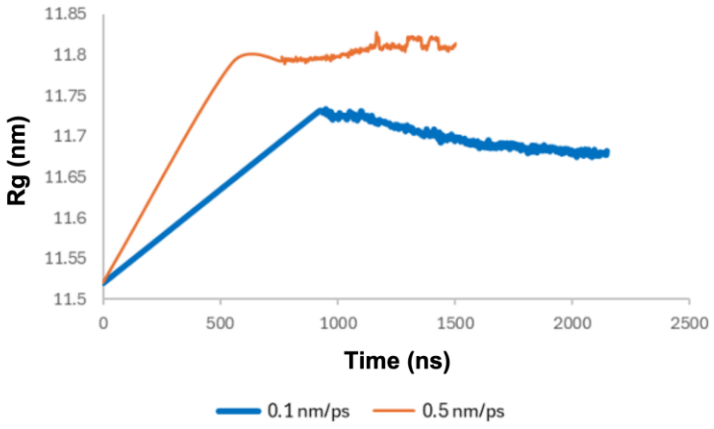

Figure 1. Effect of shear rate on AAV8 capsid structural stability and compactness.

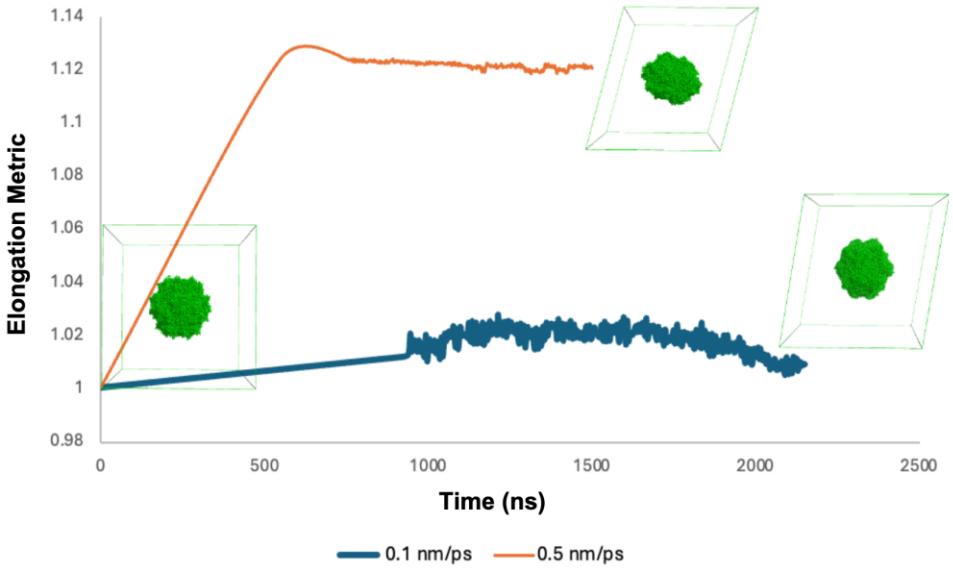

Figure 2. Shear-rate-dependent deformation of AAV8 capsids under controlled Couette flow.

Figure 1. Effect of shear rate on AAV8 capsid structural stability and compactness. (A) Root mean square deviation (RMSD) and (B) radius of gyration (Rg) of AAV8 capsids under deformation rates of 0.1 and 0.5 nm/ps.

Figure 2. Shear-rate-dependent deformation of AAV8 capsids under controlled Couette flow. Capsid elongation metric over time at deformation rates of 0.1 and 0.5 nm/ps, with representative structural snapshots illustrating shear-dependent changes in capsid morphology.

Three Novel CNS-Targeting AAV Capsids Identified from Human Genome AAV Displaying System

Chunyan He[1], Shijun Zhang[1]

[1]*GenAssist Ltd, Suzhou, China*

Abstract Text

Introduction:

Adeno-associated virus (AAV) mediated gene therapy holds great promise for treating central nervous system (CNS) and neuromuscular disorders. However, wild-type capsids like AAV9 suffer from limited blood-brain barrier (BBB) crossing efficiency and severe off-target liver accumulation. Current capsid engineering strategies suffer from low screening efficiency due to low library abundance or poor underlying science. To overcome these limitations, we developed a human genome AAV displaying system, named as Human-Originated Peptide Evolution (HOPE) platform. Human genome contains all the information of the ligands to receptors on cell membrane. We assume that ligand-containing AAV capsids may gain the cell entry function through interacting with their receptors. In this study, we aim to utilize in vivo NHP CNS enrichment and in vitro receptor precision screening approaches to obtain cross-BBB CNS capsids.

Methods:

Briefly, random sequences from human genome were cloned and then inserted between amino acids 588 and 589 in parental AAV9 library capsid. For neurotropic capsid discovery, the library first underwent two rounds of CNS enrichment of non-human primates (NHPs). The top 68 variants from the two-round NHP CNS sub-library were selected for barcoding and AAV packaging. The pooled barcoded AAV variants were injected i.v into NHP for tissue specificity analysis after 3 weeks. STAC BBB was chosen for positive control. Meanwhile, the two-round NHP CNS sub-library was further enriched in nominated BBB-crossing receptor overexpressing HEK293T to achieve known receptor medicated AAV CNS variants.

Results:

Among 68 AAV variants in NHP validation study, 8NHP9 and 8NHP10 showed powerful functional RNA transduction across multiple brain regions compared to AAV9. The tissue transduction profile of 8NHP10 was similar to STAC BBB, high CNS transduction and low in muscles and DRG, while 8NHP9 showed enhanced transduction in muscle/CNS/DRG. Meanwhile, both 8NHP10 and 8NHP9 exhibited strong liver de-targeting in biodistribution. The preliminary receptor characterization study showed that 8NHP10 may interact with TfR for BBB crossing. In receptor overexpressing HEK293T screening system, 8BBB16 exhibited strong non-TfR Receptor 4-dependent transduction with 285-fold and 72-fold of PUC19 control at the RNA and DNA levels, respectively. This indicates that 8BBB16 may interact with Receptor 4 to enter the cells. The potential of 8NHP10&9 and 8BBB16 to cross human

BBB is being evaluated in Transwell system containing hCMEC/D3 and primary human astrocytes as well as biodistribution study in mice.

Conclusion:

We successfully identified three CNS-targeting AAV capsid leads from HOPE platform only through two to three rounds enrichment, indicating the high screening efficiency of HOPE platform. 8NHP9 and 8NHP10, the two new capsids identified from NHP screening system, can target CNS tissues with minimal liver toxicity whereas the receptor-targeted 8BBB16 provides a highly specific mechanistic pathway for BBB crossing delivery of therapeutic load.

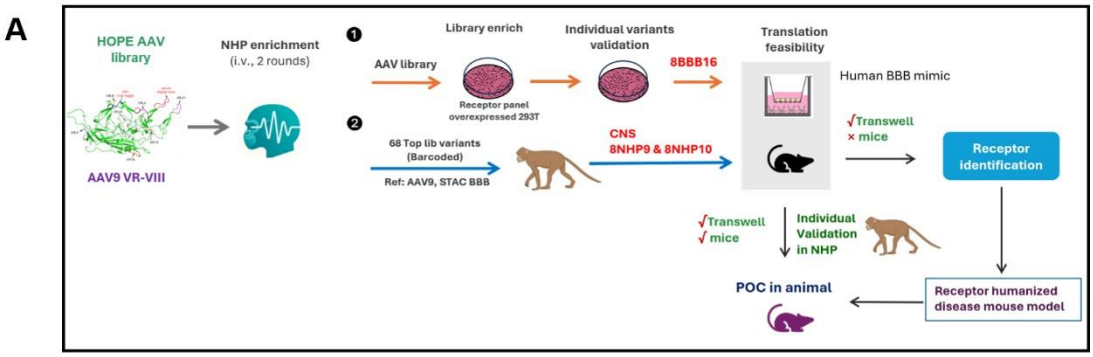

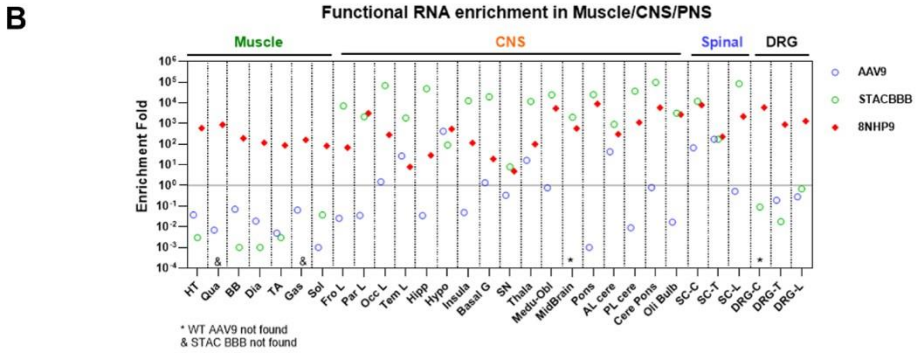

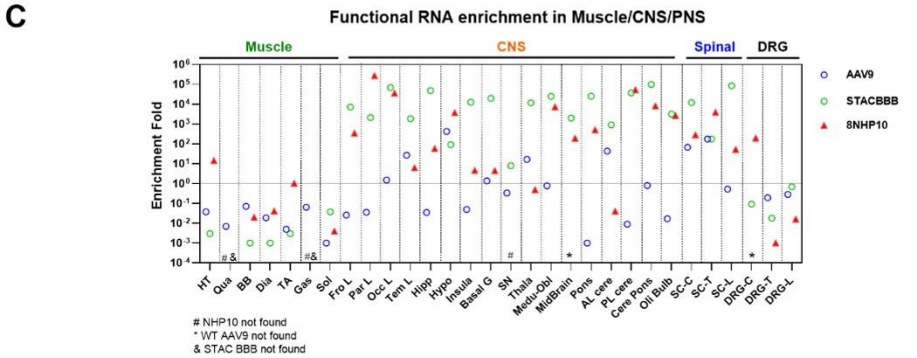

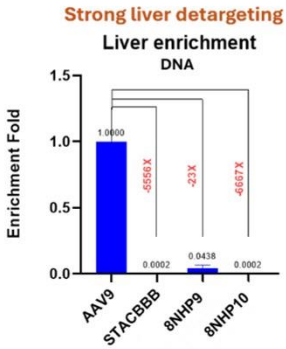

Fig 1. Characterization of CNS-Targeting AAV capsids in NHP

Leading AAV candidates (1-3 unique barcodes per variant) were pooled and i.v injected into 4kg NHP. Tissues were collected at Week 3 for NGS. The relative enrichment for each capsid in each tissue was normalized to the ratios in the pooled injected AAV product. Functional RNA enrichment was calculated as: Functional RNA enrichment = tRNA enrich (lib norm)* (tRNA ratio/tDNA ratio), t, tissue. **A.** Workflow of the three integrated systems for CNS capsid screening; **B.** 8NHP9 exhibited robust CNS/PNA/Muscle transduction in NHP; **C.** 8NHP10 demonstrated powerful and selective functional RNA transduction across multiple brain regions in NHP;**D.** 8NHP9 and 8NHP10 demonstrated significantly reduced liver targeting in NHP.

Genetic factors and early detection biomarkers associated with acute liver injury following AAV gene therapy

Janson White[1], Yeting Zhang[1], Sohrab Khan[1], Wenjing Xu[1], Ben Evans[1], Connor French[1], Tatiana Chachkovskyy[1], Wesley Beuck[1], James Richardson[1], Louise Rodino-Klapac[1], Rachael Potter[1]

[1]*Sarepta Therapeutics, Cambridge, United States*

Abstract Text

Delandistrogene moxeparvovec, an rAAVrh74 vector-based gene therapy approved for ambulatory patients in the US and select countries, has been shown through multi-year studies to stabilize or slow the progression of Duchenne muscular dystrophy (DMD). Acute liver injury (ALI) is a recognized adverse event associated with systemic adeno-associated virus (AAV) gene therapy, but host factors that may influence susceptibility remain incompletely understood.

Whole-genome sequencing (WGS) data was analyzed to identify genetic factors associated with ALI. Participants (N=158) with DMD treated with delandistrogene moxeparvovec with available WGS data were included from ENDEAVOR (NCT04626674) and EMBARK (NCT05096221) clinical trials. Each participant was assigned a single peak ALI severity of none, mild, moderate or severe based on highest observed severity during follow-up using prespecified ALT, GGT, GLDH, and total bilirubin thresholds.

HLA alleles were investigated for association with ALI. Longitudinal IFN-γ ELISpot analyses and cytokine profiling (EMBARK participants only; n=120) was also explored at Week 4 in participants with moderate/severe ALI. Together, these findings aim to identify potential markers of increased ALI susceptibility that warrants further investigation.

Sponsorship: This study was sponsored by Sarepta Therapeutics, Inc., Cambridge, MA, USA and funded by Sarepta Therapeutics, Inc., Cambridge, MA, USA. Editorial assistance was provided by Nucleus Global, in accordance with Good Publication Practice (GPP) 2022 guidelines (https://www.ismpp.org/gpp-2022) and was funded by Sarepta Therapeutics, Inc., Cambridge, MA, USA.

Disclosures: JW, YZ, SK, WX, BE, CF, TC, WB, JR, LRK, RP are employees of Sarepta Therapeutics, Inc. and may have stock options.

Apolipoprotein E Facilitates Enzyme Replacement Therapy Across the Blood-Brain Barrier via Polymeric Nanoparticles

Noah Arnold[1], Amelia Weber[1], Bridget Sehorn[1], Ariana Bachini[1], Lucian Williams[2], Vishnu Narendranath[1], Centrea Haddon[1], Amanda Gross[3], Jessica Larsen[1 2]

[1]Clemson University, Chemical and Biomolecular Engineering, Clemson, United States, *[2]Clemson University, Bioengineering, Clemson, United States*, *[3]Auburn University, Scott Ritchey Research Center, Auburn, United States*

Abstract Text

Lysosomal Storage Disorders (LSDs), though rare, are devastating conditions caused by genetic mutations leading to the dysfunction of lysosomal enzymes. These mutations result in enzyme misfolding, rendering the enzyme incapable of breaking down substrates, which subsequently accumulate within lysosomes, impairing cellular function and leading to cell death. Enzyme replacement therapy (ERT) has been successful in ameliorating symptoms of patients with non-neuropathic LSDs, making it a viable therapeutic approach. Patients receive intravenous (IV) infusions of endogenous enzymes that are either present at low concentration, missing entirely or misfolded, and therefore dysfunctional due to their genetic disease. Despite its promise in the clinic, ERT cannot be used to treat neuropathic LSDs due to the blood-brain barrier (BBB) which prevents the passage of recombinant enzymes. One such LSD is GM1 gangliosidosis (GM1), caused by mutations in the gene encoding ß-galactosidase (ßgal). Infantile and juvenile forms of GM1 are particularly severe, with early mortality. In my lab, we use nanoparticle vesicles, called polymersomes (PSs), to transport enzymes across the BBB. Specifically, Apolipoprotein E (ApoE), a cholesterol transporter, is bound to the surface of PSs and facilitates transcytosis across the blood-brain barrier (BBB). This nanoparticle directed IV ERT therapy (NanoDIVERT) has the potential to provide non-gene modifying treatment option for patients.

PSs are formed at diameters of 147 ± 17 nm with highly uniform size distributions, demonstrated by a polydispersity index of ~0.08. They efficiently encapsulate and deliver Cy5, a dye, across the BBB in $\beta gal^{-/-}$ mice, a model for GM1 gangliosidosis. These studies have demonstrated that ApoE functionalization of PSs made from PEG-b-PLA increased brain delivery when compared to unfunctionalized PSs. PSs were loaded with Cyanine 5 (Cy5) and injected via tail vein to simulate systemic administration of the platform. Results showed significant increases in CNS uptake in mice affected with GM1 compared to the unfunctionalized PSs. Uptake of functionalized and unfunctionalized PSs *in vivo* was confirmed using the in vivo imaging system and quantified using post-mortem organ homogenization to determine the percent of injected dose in each tissue (Figure 1A and B). The addition of ApoE statistically increased brain uptake in GM1-affected mice, with 3.34 ± 0.77% injected dose/g in the brain. Furthermore, we identified that the company used when purchasing PEGPLA, even at the same molecular weight, can dramatically change polymersome performance (Figure 1C, D, E). Investigation into differences is ongoing. Additionally, the inflammatory contributions of unfunctionalized, ApoE-functionalized, and ApoE-functionalized + enzyme-loaded PSs were examined by isolating leukocytes and staining with antibodies for specific markers. CD11b was stained for myeloid lineage while CD86 was stained for antibody activation states. While still very early, preliminary stains

show that ApoE functionalized enzyme-treated mice show the highest levels of myeloid cells present but the lowest levels of myeloid activation in the brain (Figure 1F and G). No significance is yet obtained. Preliminary data in this model shows that an injection of 2400 mg ApoE tagged PSs/kg with human enzyme leads to restoration of βgal activity up to 30% of normal wild type mouse levels, which is highly encouraging. Scaling up to the feline model, we observed that the same dose led to βgal activity levels up to 85% normal. NanoDIVERT has also extended its applicability to GM2 gangliosidosis, with the encapsulation of both hexosaminidase A and hexosaminidase B.

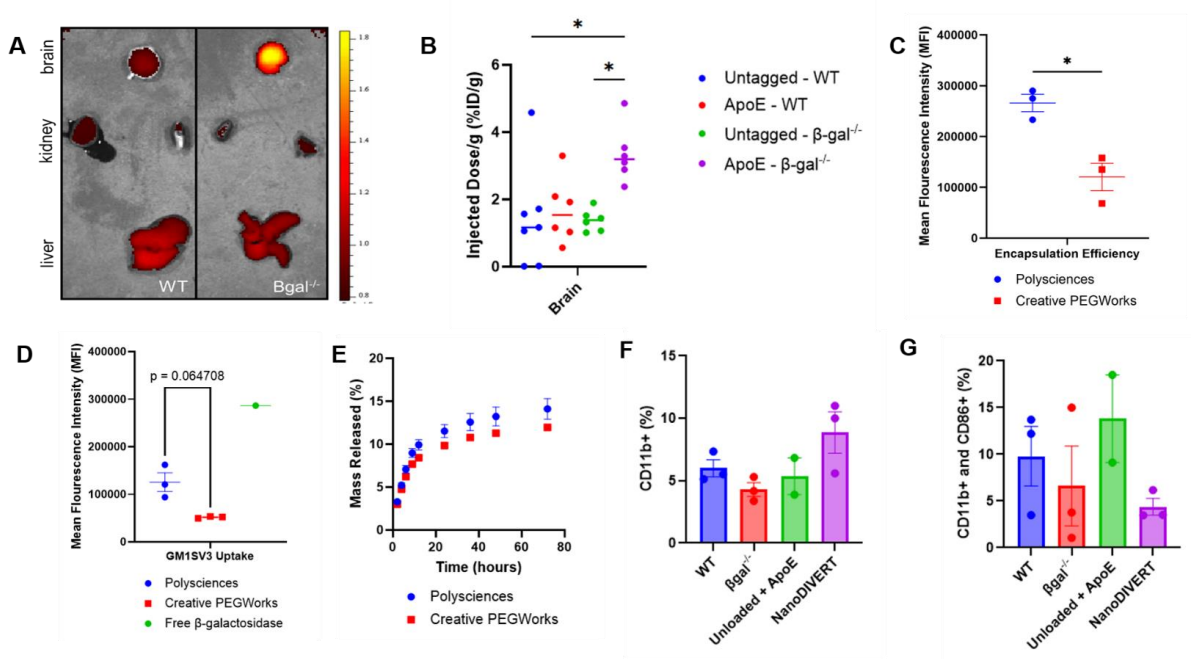

Figure 1. ApoE Polymersome Characterization. A) IVIS comparison of mouse organs post-mortem after treatment with ApoE functionalized polymersomes. Brain accumulation in diseased models is significantly altered. B) Percent injected dose per gram analysis of various mouse disease states and polymersome states Notably, functionalization with ApoE in diseased models leads to a significant accumulation of polymersomes within the brain. C) Quantified mean fluorescent intensity demonstrates that fluorescent enzyme loading efficiency is different depending on the company from which the polymer is ordered, with one company showing higher MFI than another, despite the exact same synthesis method. D) Uptake studies demonstrate that even at the same fluorescent enzyme dose, one company's polymer-based polymersome results in greater uptake *in vitro* (GM1SV3 – feline affected GM1 fibroblasts). E) Release studies highlight that Polysciences-based PEGPLA may be more pH responsive than Creative PEGWorks, despite having the same molecular weight of PLA. F) Percent of myeloid lineage leukocytes in various disease states and with different polymersome states. G) activation levels of myeloid lineage leukocytes in various disease states and with different polymersome states.

Oral Abstracts - Clinical Translation

One and Done: Agile CMC Strategies for N-of-1 Gene Therapies

Susan D'Costa[1]

[1]*Genezen, Lexington, United States*

Abstract Text

Introduction: The rapid expansion of gene and gene-modified cell therapies has exposed significant limitations in traditional Chemistry, Manufacturing, and Controls (CMC) paradigms, particularly for ultra-rare diseases. Single-patient (N-of-1) gene therapies offer a pragmatic pathway to deliver potentially life-saving treatments where no standard of care exists. However, conventional manufacturing approaches—designed for scalability and population-based trials—are poorly suited to the timelines, economics, and personalization required for N-of-1 investigational new drug (IND) applications. This work outlines an agile, risk-based CMC framework tailored to enable rapid development and clinical delivery of personalized gene therapies.

Methods: An agile CMC approach developed leveraging platform viral vector manufacturing processes, clinically validated reagents, and a risk-based process development strategy. Key elements included early proof-of-concept (POC) studies to assess construct-specific yield potential, use of platform GMP processes to minimize customization, and prioritization of clinically relevant critical quality attributes. Analytical release testing emphasizes platform-qualified assays and fit-for-use characterization methods to reduce cost and timelines. Where feasible, GMP-manufactured material may be used for preclinical studies to streamline development and regulatory alignment. Economic considerations focus on minimizing both direct manufacturing costs and indirect expenses such as plasmids, consumables, and safety testing.

Results: Application of this agile CMC framework will enable accelerated timelines from diagnosis to clinical dosing—often within 4-6months—while maintaining regulatory compliance and product quality. Platform-based manufacturing reduced process development burden and allowed sufficient GMP material generation despite limited process optimization. Streamlined analytical strategies shortened release timelines without compromising patient safety. This approach has supported multiple N-of-1 gene therapy programs, demonstrating feasibility across diverse constructs and indications while significantly reducing overall development costs compared to traditional paradigms.

Conclusion: Agile, platform-driven CMC strategies provide a viable and scalable solution for N-of-1 gene therapies, addressing the unique challenges of personalization, speed, and economics. By focusing on risk-based decision-making, standardized manufacturing platforms, and fit-for-purpose analytics, it is possible to deliver high-quality personalized gene therapies to patients with urgent unmet needs. This framework represents a critical evolution in CMC thinking and supports the broader adoption of individualized gene therapy development.

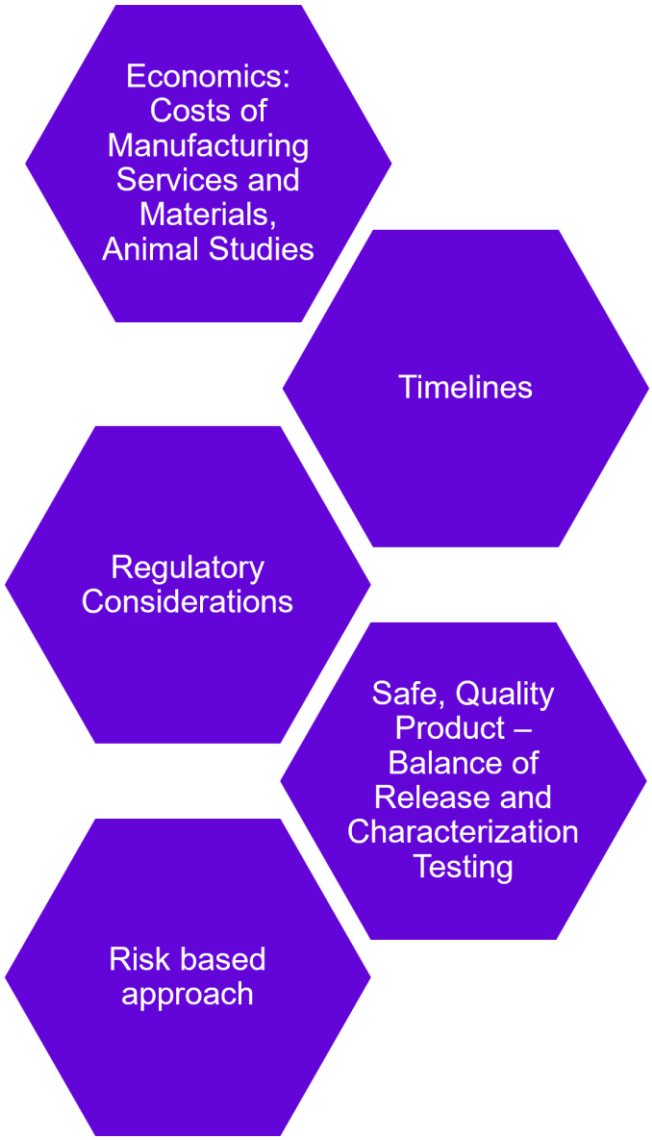
Economics: Costs of Manufacturing Services and Materials, Animal Studies
Timelines
Regulatory Considerations
Safe, Quality Product – Balance of Release and Characterization Testing
Risk based approach

Beyond FcγR Signaling: Fc-Scaffold Engineering Enhances mRNA-LNP Vaccine Immunity

Shani Benarroch[1], Dan Peer[1]

[1]*Dan Peer's Laboratory of Precision NanoMedicine, Shmunis School for Biomedicine and Cancer Research, George S. Wise Faculty of Life Sciences, Department of Materials Sciences and Engineering, Iby and Aladar Fleischman Faculty of Engineering, Center for Nanoscience and Nanotechnology, Cancer Biology Research Center, Tel Aviv University, Tel Aviv, Israel*

Abstract Text

The global landscape of infectious disease management has been fundamentally altered by the establishment of lipid nanoparticle (LNP) encapsulated messenger RNA (mRNA) vaccines. The clinical success of this platform during the COVID-19 pandemic highlighted its potential for rapid vaccine development and scalable manufacturing. While mRNA-LNP vaccines have demonstrated remarkable success against viral infections, their application to bacterial pathogens remains largely unexplored. A major limitation of this platform is the transient nature of antigen expression and rapid clearance, which may restrict antigen availability for effective immune activation. Fusion of antigens to the immunoglobulin Fc domain has emerged as a promising strategy to enhance vaccine efficacy; however, the mechanism underlying Fc-mediated enhancement in mRNA-LNP vaccines has yet to be defined. A better understanding of this mechanism could guide the rational design of potent mRNA vaccines.

In this study, we investigated the mechanism by which Fc-fusion enhances the performance of an mRNA-LNP vaccine encoding the *Yersinia pestis* bacterium F1 capsular antigen, a major protective antigen and key virulence factor. To this end, we designed a panel of Fc-engineered mRNA-LNP vaccines incorporating different Fc origins, IgG isotypes, and an aglycosylated Fc variant. We evaluated the relationship between Fc architecture, antigen pharmacokinetics, immunogenicity, and protective efficacy following lethal *Y. pestis* challenge in different mice strains. Fc-fusion significantly increased antigen pharmacokinetics, increasing systemic antigen exposure by more than 300-fold compared with the non-fused antigen and markedly prolonging antigen persistence in circulation. All mRNA-LNP vaccines encoding an Fc-fused *Y. pestis* F1 antigen elicited antigen-specific humoral and cellular responses, and provided effective protection against bubonic *Y. pestis* challenge. Notably, both wild-type mice vaccinated with aglycosylated Fc variant, with markedly reduced FcγR binding, and FcγR-deficient mice vaccinated with a murine Fc-fusion, demonstrated that enhanced immunogenicity is preserved in the absence of classical FcγR signaling.

Collectively, these findings support a model in which Fc engineering enhances mRNA-LNP vaccine performance, primarily through improved antigen stability and prolonged availability, and indicating protection is independent of classical FcγR engagement. Altogether, this study provided a mechanistic framework for the rational design of next-generation mRNA vaccines against bacterial pathogens.

Insights from Industry Stakeholders Can Help with Understanding Pathways to Convergence in AAV GTx Import Testing Requirements: Insights from Industry Stakeholders

Holly McCaleb[1], Lawrence Liberti[1]

[1]*University of Southern California, Alfred E. Mann School of Pharmacy and Pharmaceutical Sciences Department of Regulatory and Quality Sciences, Los Angeles, United States*

Abstract Text

Gene therapies (GTx) offer a promising new treatment for patients with genetic diseases that were previously considered untreatable by replacing the non-functional gene with a functional one. One of the most common types of GTx on the market and being evaluated in clinical studies are adeno-associated virus (AAV) GTx. AAV GTx are considered a type of biologic therapy in that they are manufactured from cells, grown in cell culture, and purified during downstream purification steps. However, their manufacture differs from typical biologics (like monoclonal antibodies, or mAbs) in some significant ways, including the smaller scale and lower yields of these manufacturing processes. These differences inherently limit the amount of material that can be generated in any given manufacturing campaign, in some cases quite significantly. Because of this limitation, access to gene therapies can be challenging because some Chemistry, Manufacturing, and Controls (CMC) regulatory requirements, considered standard for traditional biologics, represent a heavy burden for these modalities.

One noteworthy example of this type of regulatory burden is the requirement for import and/or registration testing, which can demand significant amounts of limited GTx material, leaving very little drug available for patients. Import testing (or registration testing) is the requirement that release testing be repeated in the specific country/territory prior to using the material for patients in that country, rather than relying on the release testing performed in the manufacturing country. Import testing was likely implemented to protect patients from counterfeit medicines, or potentially due to distrust of the results from the manufacturer or original market. However, global acceptance and harmonization of manufacturing expectations (ICH, cGMP, PIC/S, etc) are put in place to provide confidence in the manufacture and testing of material from most countries. With product quality system (PQS) expectations, confidence in the original release testing results increases, making import testing non-value-added.

Many global health authorities still require import testing to be performed on each lot that enters their territory before it can be given to any patients. This requirement can limit access to GTx because less material from each batch is available for patient dosing. Therefore, an alternative way to address import testing for these products is needed to ensure sufficient material remains available for therapeutic use. A survey will be conducted to evaluate factors that can encourage global regulatory conformance for gene therapy registration/licensing approvals, with the focus on the factors relating to review and approval of the CMC sections of the dossiers, and regional requirements (such as import and/or registration testing of drug product (DP)), all while ensuring no compromise to the standard for product quality. The survey will focus on key stakeholders such as GTx

manufacturers, regulators, clinical trial investigators, and patient/patient advocacy groups (PAGs), and will include questions covering demographics, experience with CMC challenges related to GTx submissions, approvals, and commercialization/patient access. As other CMC-related factors likely also contribute to the challenges with global access to GTx, the analysis of import testing impact will serve as a case study for evaluating ways to make AAV GTx accessible in more countries.

Oral Abstracts - Clinical Translation

P5 promoter-mediated incorporation explains REP/CAP manufacturing contaminants in patient liver biopsy after rAAV gene therapy.

Mark A Brimble[1 2], Shaoyuan Tan[2], Sarah Buddle[3 4], Li-An K Brown[4], Judith Breuer[3 4], Jeremy Crawford[2]

[1]Washington University in Saint Louis, Division of Allergy and Pulmonary Medicine, Department of Pediatrics, Saint Louis, United States, *[2]Saint Jude Children's Research Hospital, Host-Microbe Interactions, Memphis, United States*, *[3]Great Ormond Street Hospital NHS Foundation Trust, Department of Microbiology, Virology and Infection Control, London, United Kingdom*, *[4]UCL Great Ormond Street Institute of Child Health, University College London, Infection, Immunity and Inflammation Department, London, United Kingdom*

Abstract Text

Residual manufacturing DNA is a recognized impurity in recombinant adeno-associated virus (rAAV) gene therapies, raising questions about the origin, persistence, and biological consequences of these contaminants following patient treatment. Sequencing data from a patient treated with the AAV gene therapy Zolgensma for Spinal Muscular Atrophy recently revealed contaminating plasmid sequences from the vector manufacturing system within the patient's hepatocytes. The levels of wildtype gene components (REP/CAP) were remarkably high (0.5-1% of the therapeutic transgene). We hypothesized that these contaminants originated through the defined packaging mechanism of Rep-mediated, P5-associated, contaminant incorporation. Because the proprietary plasmid production sequences used for Zolgensma are not publicly available, the mapping references from the original study did not represent a ground truth to make this determination. We therefore conducted *de novo* assembly of the human-filtered dataset, which resolved two multi-kilobase contigs. By reanalyzing the original study data, we determined that an intact P5 promoter had been placed directly downstream of the AAV capsid gene in the manufacturing configuration. This contiguous contaminant sequence spanned the AAV REP and CAP genes, terminating downstream of the P5 Rep-binding-element at the Rep protein nicking site. A plasmid backbone contig likely originating from reverse packaging of the vector genome plasmid was also identified. Since P5-associated contaminants exist as heterogeneous lengths, we also examined sequences only partially aligned to the REP/CAP node to ascertain if recombination had occurred. 17% (9/46) of soft-clipped reads that partially mapped to REP/CAP sequence were linked to AAV ITR-derived sequence at heterogeneous positions across the REP/CAP contig, consistent with recurrent recombination between manufacturing-derived contaminants and rAAV-vector-genome-derived DNA. Further, analysis of ONT-data identified the P5 promoter as a preferred recombination breakpoint and was observed as a recombination junction in 5/16 reads (31.25%), with one ONT read containing two independent P5 sequences, indicating that a short P5-initiated contaminant fragment had recombined with a second larger one. We conclude that the positioning of native, intact AAV P5 promoter immediately downstream of the Capsid Gene contributes to the risk-profile of rAAV vectors via abundant transfer of wildtype rAAV genes to the patient. This is an actionable design choice and warrants evaluation in gene therapy products destined for the clinic.

Electrically active bilayer scaffold incorporating miR-126-loaded lipid nanoparticles for regenerative cardiac tissue engineering

Jekhan Saravanan[1 2], Shubhra Sinha[1], Allan Gamble[3], Azam Ali[2], Rajesh Katare[1]

[1]University of Otago, Department of Physiology, HeartOtago, North Dunedin, New Zealand, *[2]University of Otago, Centre for Bioengineering and Nanomedicine, Faculty of Dentistry,, North Dunedin, New Zealand*, *[3]University of Otago, School of Pharmacy, North Dunedin, New Zealand*

Abstract Text

Myocardial infarction (MI) causes irreversible cardiomyocyte loss, adverse ventricular remodelling, and impaired vascularisation, while the adult heart has limited regenerative capacity. MicroRNAs (miRNAs) regulate multiple pathways involved in post-ischaemic repair, including angiogenesis, inflammation, and cell survival; however, their therapeutic application is limited by rapid degradation and inefficient cellular delivery. We developed a multifunctional electrospun bilayer scaffold incorporating miR-126-loaded lipid nanoparticles (LNPs) to enable localised miRNA delivery while providing structural and electrical support for cardiac tissue repair.

LNPs were prepared using a microfluidic platform and loaded with the pro-angiogenic miR-126 mimic. The nanoparticles were incorporated into an electrospun bilayer scaffold consisting of a polyvinyl alcohol-silk fibroin (PVA-SF) inner layer and a poly(lactic-co-glycolic acid) (PLGA) outer layer, with reduced graphene oxide (rGO) incorporated to provide electrical conductivity. The scaffold was characterised for fibre morphology, chemical composition, thermal behaviour, mechanical properties, and electrical functionality. Biological performance was evaluated using endothelial cells and cardiac cells through cytocompatibility, cellular uptake, and migration assays.

The formulated LNPs exhibited favourable physicochemical characteristics for miRNA delivery, with a mean hydrodynamic diameter of 103.29 ± 0.64 nm (mean ± SD), polydispersity index (PDI) below 0.3, indicating a relatively uniform particle size distribution, and a positive zeta potential of +29.23 ± 0.43 mV, consistent with a cationic formulation capable of facilitating interactions with negatively charged cellular membranes. Quantitative PCR demonstrated increased intracellular miR-126 levels, with human umbilical vein endothelial cells (HUVECs) treated with miR-126-loaded LNPs showing a 24.64 ± 0.45% increase in miR-126 expression relative to the control group.

Scanning electron microscopy revealed a well-defined fibrous architecture, demonstrating successful formation of the electrospun bilayer scaffold. Fourier transform infrared spectroscopy confirmed the presence of the constituent polymers within the bilayer scaffold. Mechanical characterisation demonstrated that the scaffold possessed the required structural integrity and flexibility for cardiac tissue-engineering applications, while thermal analysis confirmed the thermal stability of the constituent materials. Cytocompatibility assessment further demonstrated high cell viability, indicating that the selected materials and fabrication process did not induce cytotoxic effects. HUVECs treated with the miR-126-LNP-incorporated bilayer scaffold achieved 88.79 ± 13.46% wound closure at 24 h, representing a significant increase compared with the control group ($P < 0.0001$) and

supporting a strong pro-migratory response. Incorporation of rGO generated an electrically active scaffold, supporting its potential to facilitate electrical signal transmission within damaged myocardium.

Together, these findings demonstrate the feasibility of integrating localised miR-126 delivery, nanofibrous structural support, and rGO-mediated electrical functionality within a single bilayer scaffold. Increased intracellular miR-126 expression, high cytocompatibility, and significantly enhanced endothelial migration further support the regenerative potential of this approach. By combining localised miRNA delivery with structural and electrical functionality, this multifunctional platform addresses multiple challenges associated with post-MI repair and provides a promising foundation for further evaluation in cardiac tissue regeneration.

Oral Abstracts - Delivery and Targeting

In vivo generation of therapeutic insulin-producing cells by direct reprogramming gene therapy for diabetes

Masahito Matsumoto[1]

[1]*Juntendo University, Diagnostics and Therapeutic of Intractable Disease, Tokyo, Japan*

Abstract Text

Restoring durable endogenous insulin production without ex vivo cell manufacturing or transplantation remains a major challenge in regenerative therapy for diabetes. We developed direct cell fate conversion (DIVER), a regenerative gene therapy strategy designed to generate therapeutic insulin-producing cells directly from somatic cells without passage through a pluripotent stem cell state. DIVER combines the pancreatic lineage factors Ngn3, Pdx1, and MafA with a newly identified reprogramming factor, K-factor, to induce pancreatic islet-like insulin-producing cells in a single step. In vitro, the optimized DIVER program achieved greater than 80% conversion toward an insulin-producing phenotype. Functional activity was demonstrated by transplantation of DIVER-induced cells into streptozotocin-induced type 1 diabetic mice, resulting in significant reductions in blood glucose and HbA1c. We next translated this concept into an in vivo gene therapy approach using AAV-mediated delivery of the reprogramming program to directly convert resident somatic cells into insulin-producing cells within diabetic animals. In vivo delivery produced a rapid and marked improvement in hyperglycemia within days, while histological analyses demonstrated robust generation of insulin-positive reprogrammed cells in treated tissues. Inclusion of K-factor substantially enhanced somatic cell reprogramming, supporting its key role in establishing an efficient insulin-producing cell fate. These findings provide proof of concept for a fundamentally different therapeutic architecture: rather than using gene therapy solely to replace or supplement a defective gene product, DIVER uses gene delivery to generate a new therapeutic cell population directly within the body. By bypassing pluripotent stem cells, ex vivo cell manufacturing, and transplantation, in vivo DIVER has the potential to overcome major scalability and implementation barriers associated with current cell replacement strategies. Our study establishes direct in vivo cell reprogramming as a regenerative gene therapy paradigm for diabetes and provides a platform for extending gene therapy from molecular correction to therapeutic cell generation in vivo.

Fresh, Fast, and Released: First Operational Evidence of a Tiered QC Framework Enabling Same-Day Batch Release Across Two Autologous Cell Therapy Platforms

Sagi Nahum[1], Devanshi Doshi[1]

[1]*CellVira, Analytical Development and CMC, Germantown, United States*

Abstract Text

Fresh, Fast, and Released: First Operational Evidence of a Tiered QC Framework Enabling Same-Day Batch Release Across Two Autologous Cell Therapy Platforms

Sagi Nahum[1], Devanshi Doshi[1]

[1]CellVira, Germantown, Maryland, United States

Introduction

Decentralized and point-of-care (POC) manufacturing of autologous cell therapies has gained traction as a strategy to shorten vein-to-vein time and deliver fresh, non-cryopreserved products closer to the patient. Despite this momentum, translating these approaches into GMP-compliant frameworks capable of supporting fresh infusion remains a critical unmet challenge. The primary bottleneck is no longer manufacturing but quality control. Conventional compendial sterility testing requires 7 to 14 days; culture-based mycoplasma methods take weeks. Same-day or next-day fresh release is structurally impossible under standard approaches. To address this challenge, we previously developed and published a tiered quality management architecture and distributed QC execution strategy designed specifically to resolve this constraint. This platform has since supported decentralized POC production for over 200 patients in real-world clinical settings. Here we report the first operational implementation of this framework across two biologically distinct autologous cell therapy products manufactured within the same GMP-certified mobile facility.

Methods

Manufacturing was performed at a POC reference site operating within a mobile clean room unit, following structured technology transfer from a central Control Site according to the published tiered model (). Two product platforms were included: an investigational autologous anti-CD19 CAR-T product (lentiviral vector, 10-day closed system process) and tumor-infiltrating lymphocytes (TILs, rapid expansion protocol). The same QC release strategy was applied to both products: mycoplasma was detected by an FDA cleared qPCR-based assay qualified on-site, replacing weeks of culture-based testing with a same-day result; endotoxin was measured by cartridge-based rapid LAL within hours; sterility was conducted by direct inoculation at a GMP-accredited external laboratory, decoupling the infusion decision from the 14-day compendial read; and potency was assessed by automated

cytotoxicity and functional cytokine release. For CAR-T, Vector Copy Number and VSV-G quantification were retained at the Control Site as an inter-site analytical anchor. CAR-T fresh product stability was evaluated at 0, 24, and 36 hours post-harvest under refrigerated transport conditions.

Results

Eight consecutive qualification batches (4 CAR-T, 4 TILs) were completed and released at the POC site. All batches passed pre-defined release criteria across identity, purity, viability, microbial safety, and potency. No batch failures occurred. QC release decisions were reached within 36–48 hours post-harvest for all products, within the clinically viable fresh infusion window. CAR-T product maintained full stability of viability, CAR+ phenotype, and cytotoxic function through 36 hours post-harvest, confirming feasibility of a point-of-care infusion model. TIL batches showed consistent tumor-reactive function at release. Analytical comparability between the POC reference site and the Control Site was confirmed for CAR-T vector-specific parameters.

Conclusion

These results provide the first operational evidence that a peer-reviewed, tiered QC framework can enable GMP-compliant, same-day batch release for autologous cell therapies manufactured at the point of care. By integrating decentralized quality management with distributed QC execution and rapid analytical methods, the framework operationally addresses the QC constraints that have historically limited fresh decentralized delivery. The approach holds across two biologically distinct products manufactured at the same mobile facility. A platform with this architecture has already supported over 200 patient treatments in real-world settings. Eight releases. Two products. One mobile unit. All fresh.

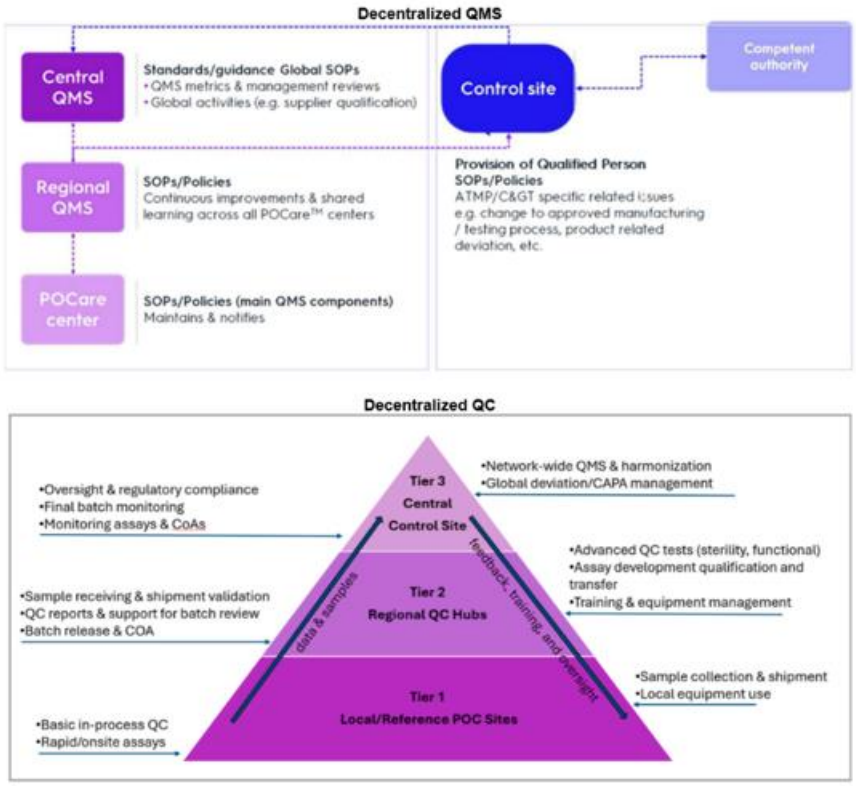

Figure 1. Mechanisms for control and oversight in a decentralized CGT manufacturing network. The upper panel illustrates the hierarchical QMS governance structure; the lower panel depicts the tiered QC oversight model supporting standardized testing, data review, and regulatory compliance across decentralized manufacturing sites.

Enabling Decentralized Lentiviral Vector Manufacturing: Advancing Best Practice Through Distributed QC and Centralized Governance

Devanshi Doshi[1], Sagi Nahum[1]

[1]*CellVira, Analytical Development and CMC, Maryland, United States*

Abstract Text

Enabling Decentralized Lentiviral Vector Manufacturing: Advancing Best Practice Through Distributed QC and Centralized Governance

Devanshi Doshi[1], Sagi Nahum[1]

[1]CellVira, Maryland, United States

Background
Lentiviral vector (LVV) characterization is among the most analytically demanding activities in cell and gene therapy manufacturing, often requiring more than 15 distinct assays to assess identity, potency, purity and safety. Many of these tests are performed by specialized laboratories using different platforms, quality systems, and, in some cases, across multiple jurisdictions, creating significant challenges for analytical consistency, data integration, and batch release. As LVV manufacturing becomes increasingly distributed across external CDMOs, QC must enable consistent analytical execution, data integrity, specifications, and release decisions across sites.

Unlike autologous drug products, LVV is typically manufactured as multi-lot material by an external CDMO and supplied across manufacturing networks. This creates a distinct QC challenge: the sponsor retains ultimate responsibility for product quality and regulatory compliance, while analytical testing and laboratory execution may occur outside the sponsor's direct operational control. Our decentralized QC model for CGT provides a foundation for distributing analytical execution while maintaining centralized oversight.

Operational Gap
The decentralization of LVV QC introduces operational dependencies that are not addressed solely through individual assay requirements. Sample allocation across multiple release tests, limitations in parallel testing, and differences in laboratory readiness can affect testing timelines and material utilization. These challenges are further amplified when testing is performed by external laboratories, as method qualification/validation, kit availability, laboratory capacity, and scheduling must align with manufacturing and release timelines. Concurrently, translating regulatory expectations requires clear alignment of Quality Target Product Profile (QTPP), specifications, testing responsibilities, quality agreements, release, and disposition decision rights across sponsor-CDMO interfaces. This creates a need for integrated QC governance connecting analytical strategy, laboratory capability, and quality decision-making.

The Dual-Layer Governance Strategy

We present a tested two-layer governance model that converts the QTPP from a static CMC document into an operational architecture for decentralized LVV QC. The first layer is a sponsor-owned, version-controlled QTPP that defines the intended LVV quality profile and establishes an attribute-by-attribute assessment of CQAs. The QTPP also establishes the sponsor's regulatory classification position and reference-standard strategy, creating a common technical baseline across external manufacturing partners and a basis for consistent quality expectations.

The second layer is a Decision Rights Matrix (DRM) that operationalizes the QTPP by defining three control elements for key manufacturing, analytical, quality, and regulatory decisions: final approval authority, notification window, and change-control owner. Decision categories include CQA acceptance-criterion changes, confirmed OOS results, batch-record deviations, CQA linked analytical method changes, batch release, core process-parameter changes, and technology transfer.

Together, the QTPP and DRM establish a direct linkage between what quality attributes must be controlled, how they are evaluated, and who has authority to make quality decisions. This linkage enables attribute-level determination of which LVV testing can be decentralized, which requires centralized confirmation, and which remains characterization-only, while incorporating ongoing site-by-site comparability assessment using in-process and release data.

Conclusion

A scalable decentralized LVV QC strategy begins with a simple principle: distribute testing, not the definition of quality. The tested two-layer model couples a sponsor-owned QTPP with a Decision Rights Matrix to establish a common quality target and predefined decision authority across distributed manufacturing and analytical sites. By defining quality and decision rights prospectively, the model reduces reliance on site-specific interpretation and enables decentralized execution without compromising centralized quality oversight. Its application across CDMOs, laboratories, and jurisdictions offers a scalable approach for the evolving LVV supply chain and provides a foundation for extending decentralized QC beyond drug product to the starting material node that enables the broader CGT manufacturing network.

Oral Abstracts - CNS

An optimized lipid-siRNA platform for intrathecal gene silencing in deep brain structures

Alexander Sorets[1], Nora Francini[1], Joshua Park[1], Adam Abdulrahman[1], Alexander Ligocki[1], Cristian Carvajal Tapia[1], Ethan Lippmann[1], Craig Duvall[1]

[1]*Vanderbilt University, Nashville, United States*

Abstract Text

Introduction: Advances in understanding the molecular causes of neurodegenerative disease, coupled with increasingly precise therapeutics, herald a new era for treating historically incurable neurological disorders. Realizing this potential, however, requires delivering these therapies to the brain regions and cell types where disease manifests. Short interfering RNAs (siRNAs) are especially promising for Huntington's disease (HD) and other gain-of-function disorders, producing potent, durable, and highly specific silencing of target transcripts. Yet for siRNAs administered into cerebrospinal fluid (CSF), the central challenge is reaching deep brain structures such as the striatum, the primary site of pathology in HD.

This problem stems from a fundamental trade-off between tissue penetration and cellular uptake. Unconjugated siRNA disperses well through tissue but, owing to its hydrophilicity, is poorly internalized. In contrast, strategies that enhance uptake, such as cholesterol conjugation, generate steep concentration gradients at CSF-brain interfaces that limit distribution to deep structures (Figure 1A). We therefore sought to develop a lipid-siRNA conjugate that enhances cellular uptake while preserving the favorable tissue dispersion of unconjugated siRNA.

Methods: We generated a library of lipid-siRNA conjugates (Figure 1B) spanning a range of hydrophobicities and screened them by intrathecal injection in rats, a physiologically relevant model of human administration, measuring both delivery and huntingtin (Htt) silencing (mRNA and protein) in deep brain structures. To visualize biodistribution, Cy5-tagged conjugates were injected intrathecally (60 nmol) and the spinal cord and brain were analyzed histologically at 48 hours, comparing the optimized lead with a previously published, more hydrophobic construct (L2-Gen1); parallel staining of unlabeled siRNA controlled for Cy5-dependent artifacts. In an independent dose-response study, rats received intrathecal conjugate targeting Htt (60 and 90 nmol), and knockdown was quantified in the cerebellum and striatum as representative superficial and deep structures.

Results: Striatal Htt mRNA silencing followed a U-shaped dependence on hydrophobicity, with an optimum at an intermediate structure we term L2-Gen2 (Figure 1C). To understand why L2-Gen2 silenced Htt so effectively in the striatum, we examined biodistribution histologically. We found that the more hydrophobic L2-Gen1 accumulated along CSF-CNS interfaces, whereas L2-Gen2 dispersed deeper and more homogeneously through the tissue, distributing throughout the striatum, a notoriously difficult deep structure to reach (Figure 1D); the same pattern was seen with non-fluorescently tagged L2-Gen2, confirming it was not a Cy5 artifact. To assess the robustness and reproducibility of L2-Gen2, we performed an independent dose-response study. Here, we again observed potent and dose-responsive HTT

protein knockdown by L2-Gen2 in both the cerebellum and striatum (Figure 1E). In data not shown, we have further demonstrated durable silencing in microglia (>75% knockdown at 6 weeks), a historically hard-to-target cell type.

Conclusions: By screening a library of lipid-siRNA conjugates in a rat intrathecal model, we identified L2-Gen2, a conjugate whose balanced hydrophobicity overcomes the deep-delivery barrier that has limited oligonucleotide therapeutics (a representative subset of the library is shown). More than a single therapeutic, this establishes hydrophobicity tuning as a design principle and L2-Gen2 as a tunable platform for durable siRNA silencing throughout the deep CNS.

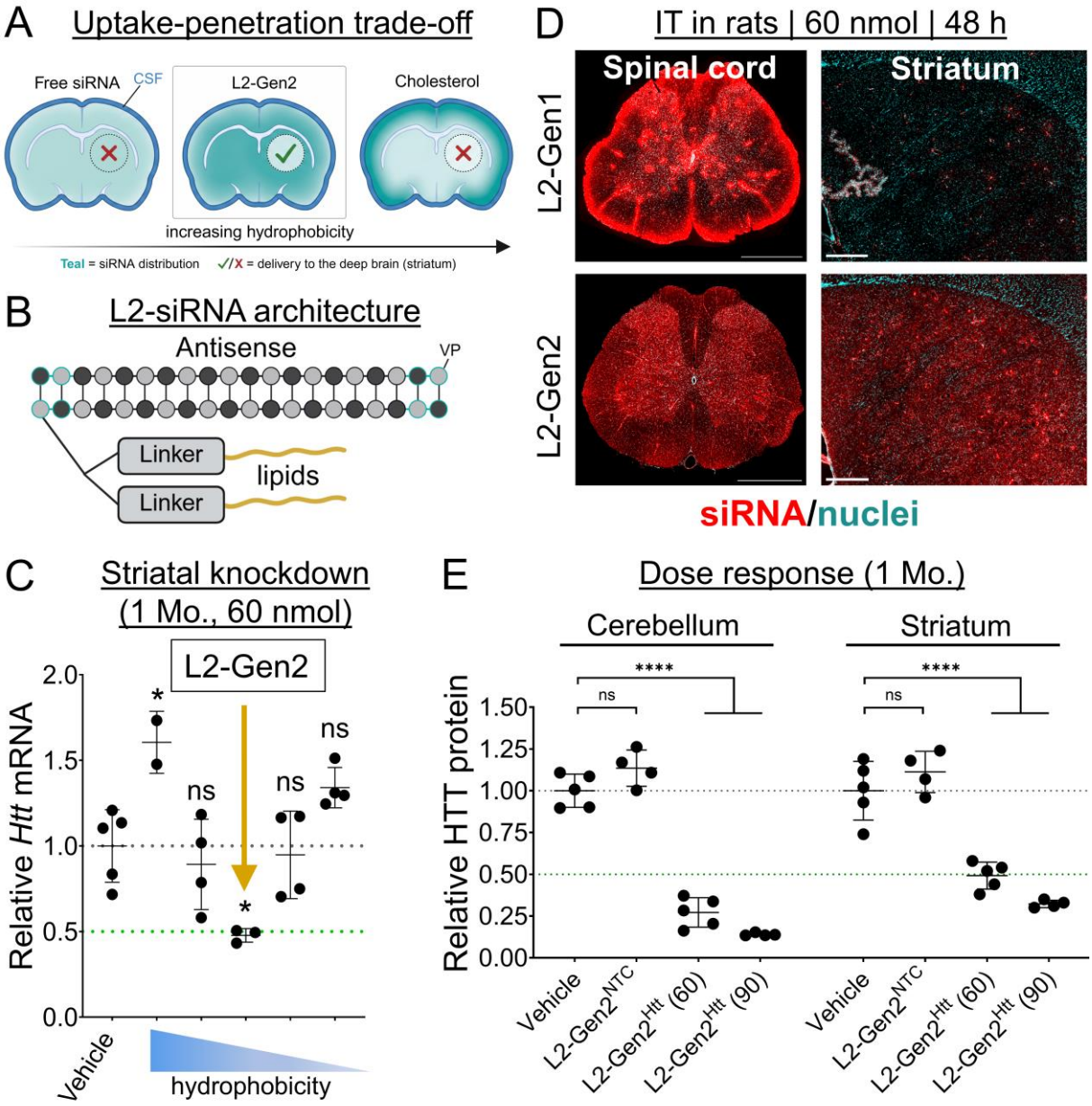

Figure 1: An optimized lipid–siRNA conjugate (L2-Gen2) enables intrathecal huntingtin silencing in deep brain structures.

Figure one: An optimized lipid–siRNA conjugate (L2-Gen2) enables intrathecal huntingtin silencing in deep brain structures. (A) The uptake–penetration trade-off: as conjugate hydrophobicity increases (left to right), siRNA distribution shifts from broad but poorly retained (free siRNA) to superficial (cholesterol); an intermediate sweet spot, L2-Gen2, reaches the deep striatum. (B) L2-siRNA architecture: a chemically modified siRNA joined

through two linkers to lipids (L2). Color key: 2′-F (dark) and 2′-Ome (light gray) nucleotides; phosphodiester (black) and phosphorothioate (teal) linkages; VP, 5′-vinylphosphonate. (C) Striatal *Htt* mRNA one month after intrathecal delivery (60 nmol) across conjugates spanning a hydrophobicity gradient; silencing peaks at L2-Gen2 (arrow). n = 3-5 rats; mean ± SD; *p < .05; ns = non-significant; One-way ANOVA (Dunnett's correction). (D) CNS biodistribution of Cy5-labeled L2-Gen1 vs L2-Gen2 (intrathecal, 60 nmol, 48 h) in spinal cord and striatum. Scale bars = 500 µm for both spinal cord and striatum. (E) Dose-responsive HTT protein knockdown by L2-Gen2 in cerebellum (superficial) and striatum (deep) vs vehicle and non-targeting control (NTC); 60 and 90 nmol. n = 4-5 rats; mean ± SD; ****p < 0.0001, ns = non-significant; One-way ANOVA (Dunnett's correction).

Oral Abstracts - Delivery and Targeting

Bispecific adaptor proteins enable disease-specific targeting with cognate engineered cells

Zachary Eidman[1], Jonathan Brunger[1]

[1]*Vanderbilt University, Biomedical Engineering, Nashville, United States*

Abstract Text

Chronic inflammatory diseases, a broad class of diseases including Alzheimer's disease (AD), arthritis, diabetes, and cardiovascular disease, are some of the world's most significant public health burdens and are estimated to affect nearly 125 million Americans. Although there are effective, non-pharmaceutical interventions to reduce risk and treat symptoms in some cases of inflammatory diseases such as type II diabetes and atherosclerosis, other inflammatory diseases like rheumatoid arthritis (RA) require disease-modifying drugs to help reduce symptoms and treat the pathogenic inflammatory dysregulation. Furthermore, other inflammatory diseases such as AD and osteoarthritis (OA) have limited effective and clinically approved disease-modifying drugs, demonstrating a need for novel therapeutics to treat these conditions.

A major roadblock in many regenerative engineering efforts is inflammation and its role in disrupting the natural healing of tissue. Our lab has previously developed a cytokine-responsive cell therapy platform termed native MATRIX (nMATRIX). In this work, we developed synthetic Notch receptors (synNotch) outfitted with extracellular binding domains that selectively bind to inflammatory cytokines. As synNotch receptors are derived from the juxtacrine Notch receptor, they require a small amount of force to cleave the intracellular transcription factor and activate downstream gene expression and do not readily signal with soluble molecules. To enable signaling with soluble cytokines, we developed a mAb-decorated biomaterial platform that captures and presents soluble cytokines to cognate synNotch cells that recognize a distinct, non-overlapping epitope of the ligand. This was the first reported approach demonstrating soluble, monomeric cytokines can be used as a synNotch-class ligand.

As a biomaterial-based approach is not feasible for various disease applications, we have developed a protein-based strategy that builds on our previous approach but instead uses matrix-bound disease markers as an immobilizing strategy. We have developed bispecific adaptor proteins that consist of two distinct binding domains that allow for binding of a cytokine of interest (e.g. IL-1β) and a disease-specific marker (e.g. amyloid beta) that acts as an interface between diseased tissue and our cytokine-responsive engineered cells (Figure 1A). This strategy acts as Boolean AND gate such that inflammatory cytokines and a disease marker both need to be present to enable engineered cell transgenic signaling. To demonstrate this strategy was viable, we designed anti-GFP/anti-Aβ bispecific adaptors to interface with our previously described anti-GFP engineered synNotch cells. After plating these cells on wells treated with adsorbed $A\beta_{42}$, we dosed with varying doses of adaptor protein and demonstrated significantly upregulated signaling only when the adaptor protein and GFP were present (Figure 1B). Similarly, when swapping the anti-GFP binding domain for an anti-IL-1β domain to produce an AD targeting adaptor, we demonstrated high levels of

synthetic IL-1β receptor activation, with an inductance of over 70x over baseline (Figure 1C). Furthermore, this data shows that productive signaling only occurs when $A\beta_{42}$, IL-1β, and adaptor protein are all present, and that minimal activation occurs when any single component is missing. To demonstrate the modularity of this system, we also developed an RA-targeting adaptor with anti-collagen II (CII, a marker of damaged collagen) and anti-IL-6 binding domains. When testing with IL-6 responsive engineered cells, we showed a dose dependent activation when treating with a range of adaptor protein doses and 1nM IL-6 (Figure 1D). Lastly, to show this system works with cell-bound markers, we created an anti-fibroblast activation protein (FAP) and anti-IL-1β adaptor variant. FAP has been implicated in atherosclerosis and is upregulated in various cancers such as glioblastoma. To test this construct, we produced a FAP overexpression Jurkat line and co-cultured IL-1β-responsive cells with these cells and various doses of adaptor and IL-1β (Figure 1E). Like previous experiments, we showed that proficient synthetic receptor activation only occurs when both adaptor protein and cytokine are present. Furthermore, this system is robust and works with varying levels of protein and cytokine.

These data indicate we can engineer bispecific adaptor proteins that act as a disease-specific targeting mechanism for engineered cell therapies. These constructs can bind to two distinct targets simultaneously, enabling Boolean logic gated therapeutic responses in diseased tissues. This approach is highly modular and robust and can be adopted for other use cases using the same framework. Ultimately, we envision this platform as a “plug and play” tool for specific sense and response responses in a wide variety of contexts.

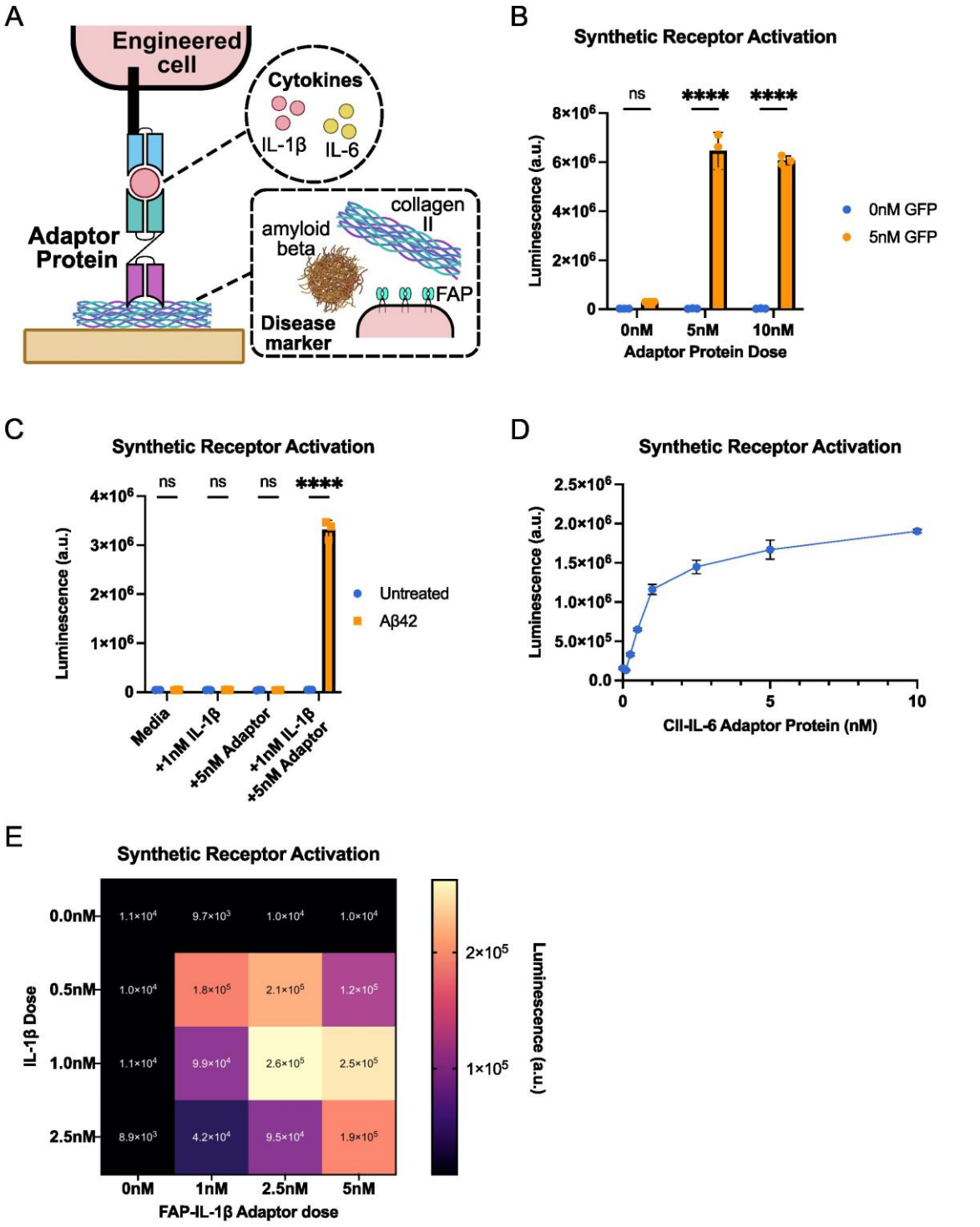

Figure 1. (A) Schematic of bispecific adaptor protein platform. Inflammation-responsive synNotch cells only activate in the presence of static disease markers and cytokines. (B) GFP-responsive synNotch mouse mesenchymal stem cells activate on adsorbed Aβ42 (1μg) when treated with Aβ-GFP adaptor protein and 5nM GFP. (C) IL-1β-responsive synNotch engineered HEK293 activation when treated with IL-1β and Aβ-IL-1β adaptor protein when plated on untreated surfaces or surfaces coated with Aβ42. (D) IL-6-synNotch engineered HEK293 activation when plated on collagen II and treated with varying doses of CII-IL-6 adaptor protein and 1nM IL-6. (E) Heat map showing activation of IL-1β-responsive engineered synNotch Jurkat T cells in response to varying doses of FAP-IL-1β adaptor protein and IL-1β, when co-cultured with FAP overexpression Jurkats. Receptor activation for all described experiments was measured via BrightGlo luminescence assay measuring firefly luciferase production by the co-engineered inducible reporter gene circuit. Two-way ANOVA with Tukey's multiple comparisons. n=3. ****p<0.0001

Oral Abstracts - Clinical Translation

Will It Reach Patients? An AI Model Predicts Clinical Translation of Gene Therapies from Modifiable Preclinical Design Choices

Maria Mascarenhas[1], Luana de Mambro[1], Cynthia Bartolomeo[1], Camila Kaleka[2], Diego Astur[2], Pedro Debieux[2], Moisés Cohen[2], Roberta Stilhano[1]

[1]Santa Casa de São Paulo, São Paulo, Brazil, [2]Israelita Albert Einstein Hospital, São Paulo, Brazil

Abstract Text

Gene therapy has begun to deliver what it promised. Single administrations now durably alter the course of inherited, neuromuscular, ocular, hematologic and metabolic diseases for which no disease-modifying treatment existed, and the modality is no longer limited by whether the biology can work. It is limited by how little of the work ever reaches a patient. Only a small fraction of the gene therapies that succeed in animals arrives at a registered clinical trial. That loss is expensive, it is slow, and it is largely invisible, because the studies that stop are rarely the ones that get discussed. We asked whether what separates the programs that advance from those that do not is, in measurable part, how the preclinical study was designed, and whether those choices can be identified early enough to shape the next study rather than to judge the last one.

We built a case-control study of preclinical gene therapy programs matched by disease. Of 675 curated publications, 479 were eligible and 454 were extracted from the full text; no study entered the analysis on the strength of its abstract. The unit of analysis is the development program rather than the article, so a laboratory publishing repeatedly on the same target and disease counts once. A program was a case when the same development lineage, the same target and mechanism, and the same disease reached a registered interventional trial. Controls were programs that did not, restricted to work published in 2020 or earlier so that at least six years had elapsed for a trial to appear. The final dataset comprised 352 programs across 95 disease targets, 159 cases and 193 controls, each described by 52 methodological variables.

The evidence is statistical before it is computational. Each variable was tested individually against translational progression with correction for multiple comparisons, and 25 of the 52 were significant at a false discovery rate below 5%. Programs that used a route of administration feasible in humans were far more likely to advance (odds ratio 21.38; 95% CI, 2.85-160.15), as were those testing a product representative of the one intended for the clinic (12.19; 2.78-53.40), evaluating in non-human primates (15.27; 3.54-65.94), holding translational funding (4.38; 2.74-7.00), treating after the disease was established rather than pre-emptively (3.84; 2.24-6.58), using a large animal model (3.63; 2.02-6.53), replicating findings independently (2.78; 2.09-3.71), planning a dose-response (2.52; 1.60-3.96), performing formal toxicology (2.51; 1.61-3.92) and protecting the invention by patent (2.37; 1.41-4.00).

Combining these variables in a gradient boosting model with nested cross-validation, the outer folds grouped by disease target so that no target appears in both training and test, discrimination reached an area under the ROC curve of 0.852 (95% CI, 0.802-0.895), with an

area under the precision-recall curve of 0.850 against 45% prevalence and a Brier score of 0.153 (P < .001). Confidence intervals came from cluster bootstrap resampling diseases and significance from blocked permutation of the outcome within disease. Programs in the top decile carried a positive likelihood ratio of 42.5. Logistic regression on the same variables reached 0.835, so the signal lies in the variables and not in the complexity of the algorithm. Critically, a model restricted to the 43 variables that already exist before any animal is treated performed identically (0.852; 0.801-0.894). The prediction does not require the experiment to have been run.

The most consequential result is what carries that signal. Isolated from everything else, design choices that require no additional funding discriminated as well (0.757; 0.694-0.812) as indicators of resources and program maturity (0.757; 0.707-0.802). Replicating a finding, treating an established disease, planning a dose-response and reporting a viable route are decisions made on paper, and they carry as much information about eventual translation as money and infrastructure do.

Discrimination held for in vivo gene addition and replacement (0.877; n = 289) and gene editing (0.840; n = 24); the ex vivo and silencing subgroups are too small to support use. Because the curated sample is enriched for programs that advanced, the model ranks a study against comparable studies rather than estimating an absolute probability of success. Applied to four Brazilian programs still in planning, it produced specific, low-cost design recommendations and declined to score one project outside its domain. Translational failure is usually discussed as a problem of money and infrastructure. These data locate a substantial and measurable part of it somewhere earlier and far cheaper: in the choices a researcher makes while the study is still a protocol.

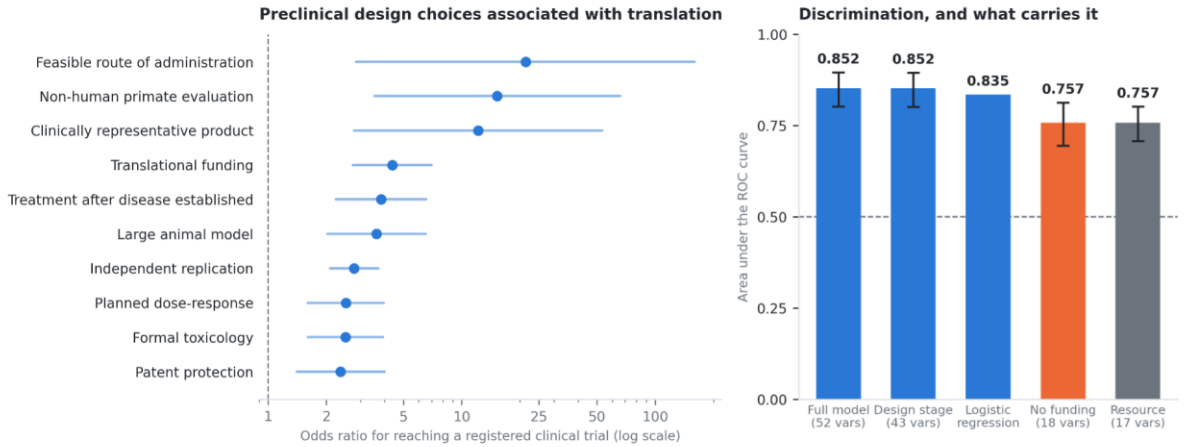

Figure 1. Left: odds ratios (95% CI) for reaching a registered clinical trial. Right: AUROC by variable set; design choices needing no funding match resource indicators.

Oral Abstracts - CNS

Amyloid-β- and tau-responsive synthetic receptors to build a programmable Alzheimer's disease therapy

Madeline Spetz[1], Hyosung Kim[1], Alexander Ligocki[1], Dylan Conger[1], Swathi Shekharan[1], Rebecca Embalabala[1], Ethan Lippmann[1], Jonathan Brunger[1]

[1]*Vanderbilt University, Nashville, TN, United States*

Abstract Text

Alzheimer's disease (AD) is a progressive, neurodegenerative disorder characterized by the aggregation of the proteins amyloid-beta (Aβ) and tau. AD currently lacks an effective treatment. To address the gap in available treatments, in recent years, there has been increased interest in cell-based therapies for AD, including chimeric antigen receptor (CAR)-microglia or -astrocytes. The goal of these cell therapies is to clear amyloid-β (Aβ), the protein that abnormally aggregates in AD, by phagocytosis. Notably, Aβ clearance is also the goal of anti-Aβ monoclonal antibody (mAb) passive immunotherapy, which has been extensively investigated for the treatment of AD. Some of these – lecanemab and donanemab – have been FDA-approved on the basis of their ability to clear Aβ; however, their ability to provide meaningful cognitive benefit remains controversial.

We have developed a new, modular cell therapy approach for AD utilizing the synthetic Notch (synNotch) platform, where we have replaced the extracellular recognition domain with the single chain variable fragment (scFv) of Aβ and tau monoclonal Abs that have been tested in clinical trials for AD. We replaced the Notch intracellular domain with a synthetic transcription factor (TF), so that recognition of Aβ or tau drives the expression of a transgene (Fig. 1A). This response transgene is entirely programmable; therefore, we can use this response to produce therapeutic transgenes like neuronal growth factors or anti-inflammatory factors. This programmable response, which can be independent of Aβ clearance, is unlike a CAR, which activates cell-type-specific effector functions such as phagocytosis of Aβ and unselective cytokine production.

A synNotch receptor constructed from the anti-Aβ antibody bapineuzumab detects synthetic Aβ as indicated by the expression of the response transgene SEAP (Fig. 1A); Sem-Notch (constructed from the anti-tau mAb semorinemab) detects recombinant human tau (Fig. 1B). Both Aβ- and tau-responsive receptors function in brain cells that are relevant in the progression of AD. Sem-Notch functions in iPSC-derived microglia (Fig. 1C). Bap-Notch allows iPSC-derived human astrocytes to recognize Aβ isolated from human brain bank donors with cerebral amyloid angiopathy (CAA) (Fig. 1D). Bap-Notch astrocytes programmed to respond to Aβ with anti-inflammatory transgenes soluble TNF receptor (sTNFR1) and IL-1 receptor antagonist (IL-1Ra) attenuate the expression of reactive astrocyte genes consistent with the chronic inflammation found in AD (Fig. 1E).

Finally, to circumvent potential challenges associated with delivery of the synNotch receptors to brain cells like astrocytes or microglia, we expressed both Aβ- (Bap-Notch) and tau-responsive (Sem-Notch) receptors in mesenchymal stromal cells (MSCs) – cells that are already the basis for Lomecel-B, an investigational therapy for AD. Bap-Notch mMSCs also

recognize Aβ *in vivo* when transplanted directly to the brains of aged 5xFAD mice, as indicated by mCherry transgene expression in transplanted cells surrounding Aβ plaques (Fig. 1F). Preliminary data indicates that Sem-Notch MSCs transplanted to aged PS19 tauopathy transgenic mice recognize tau (not shown).

In sum, our platform is easily portable to multiple cell types and is not restricted to phagocytes, regulates functions distinct from Aβ clearance, and is entirely programmable. This approach repurposes antibodies existing anti-Aβ or -tau mAbs, including those that have failed clinical trial, allowing us to build receptors that can detect either Aβ or tau.

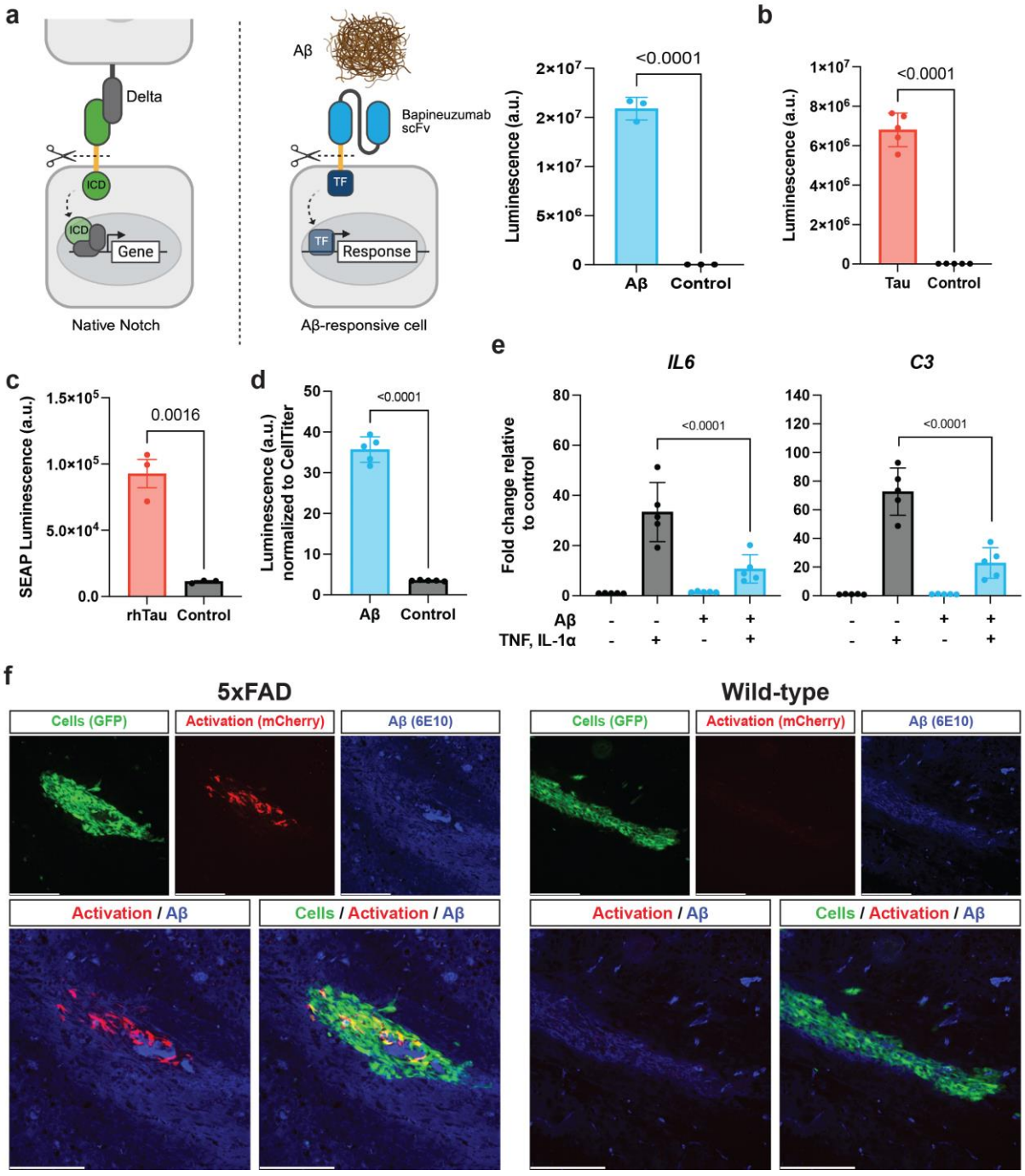

Figure 1: Aβ and tau synNotch receptors drive programmed responses. (a) Schematic of Notch and synNotch. Notch recognizes its ligand Delta, resulting in cleavage of the transmembrane core and releasing the intracellular domain to the nucleus for target gene regulation. Bap-Notch was constructed by replacing the Notch1 extracellular domain with the bapineuzumab single chain variable fragments (scFvs) and the intracellular domain (ICD) with the tet-transactivator synthetic transcription factor (TF). SEAP activity assay measuring output of Bap-Notch mMSCs in response to immobilized synthetic $A\beta_{42}$, compared to no Aβ control condition. **(b)** SEAP activity assay measuring output of Sem-Notch mMSCs in response to immobilized full-length recombinant tau. **(c)** SEAP activity assay measuring

output of Sem-Notch iPSC-derived microglia in response to recombinant tau. **(d)** SEAP activity assay measuring output of Bap-Notch astrocytes in response to human human Aβ seeds. **(e)** qPCR measuring *IL6* and *C3* expression in Bap-Notch astrocytes with Aβ-driven sTNFR1-IL-1Ra transgene. **(f)** Cryosections of 5xFAD and WT brains showing transplanted Bap-Notch mMSCs (green), Aβ (blue), and Aβ-driven mCherry expression (magenta). Scale bar = 200 μm.

Towards treating prostate cancer using an engineered human sodium/iodide symporter (NIS) protein and 188ReO4-

Haswitha Sabbineni[1], Nancy Carrasco[1]

[1]*Vanderbilt University, Nashville, United States*

Abstract Text

The sodium/iodide symporter (NIS) is the plasma membrane protein that actively transports iodide (I^-) into the thyroid, as well as various clinically approved radiotracers used for imaging [such as pertechnetate ($^{99m}TcO_4^-$), radioiodide ($^{123}I^-$), and tetrafluoroborate ([^{18}F] BF_4^-)] and for therapeutic purposes [e.g., $^{131}I^-$ and preclinically approved perrhenate ($^{186/188}ReO_4^-$)]. For over 80 years, targeted internal radiation therapy (*TIRT*) has been used successfully to treat thyroid cancer: administered radioiodide ($^{131}I^-$) is selectively accumulated in thyroid cancer cells by NIS. NIS-mediated TIRT is a promising approach to treating prostate cancer when NIS has been exogenously expressed in prostate cancer cells by gene transfer. Prostate cancer is the second deadliest cancer in men in the United States and Europe. Localized prostate cancer is typically treated with prostatectomy or definitive radiotherapy (*RT*), but these treatments *fail* to cure 20-40% of patients. For metastatic castration-resistant prostate cancer (mCRPC), there are only a very few effective agents available with unique mechanisms, all of which improve survival *only modestly*, by ~4 months, in randomized trials.

For NIS-based TIRT to be successful against prostate cancer, three challenges must be overcome: **(i)** the thyroid must be protected from β-radiation, **(ii)** the immune response must be mitigated, and **(iii)** the treatment must be tissue-specific. To tackle these challenges, we have engineered a NIS protein (*PF-NIS*) by replacing two amino acids that are close to the substrate cavity (the substitutions are L253P and V254F). PF-NIS transports oxyanions (such as $^{186/188}ReO_4^-$ and $^{99m}TcO_4^-$), but virtually no I^-. We have shown *in vitro* that cells expressing wild-type NIS (WT-NIS) do not die when treated with $^{186}ReO_4^-$ and saturating concentrations of non-radioactive iodide (100 µM I^-), because WT-NIS does *not* transport oxyanions in the presence of excess I^-. In contrast, cells expressing PF-NIS do die under those conditions, because PF-NIS does *not* transport I^-.

Plasmid generation and polyplex preparation: We subcloned the cDNA coding for PF-NIS or WT-NIS under the PSA promoter into the *mini-vec* plasmid backbone. Polyplexes were prepared with polyethyleneimine (jetPEI) and a plasmid consisting of the PF-NIS cDNA under a PSA promoter, and they were characterized using dynamic light scattering (DLS) and scattering electron microscopy (SEM) to determine their size and zeta potential.

Animal model: For our prostate cancer model, we used immunodeficient (Nu/Nu) mice subcutaneously engrafted with human lymph node prostate carcinoma (LNCaP) cells, and tumor volumes were measured using vernier calipers. Once the tumors had reached volumes of ~200 mm^3, mice were injected with polyplexes either intratumorally (IT) or intravenously (IV), and after 48 hours, mice were treated with $^{188}ReO_4^-$ IV. NIS expression in tumor cells was quantitated by SPECT-CT imaging. To determine the effects of NIS-mediated $^{188}ReO_4^-$ treatment on thyroid physiology and that of other organs, blood was collected from

mice and serum was obtained to quantitate their TSH, T_4, and T_3 levels and to run blood chemistry panels. After the mice were perfused with 10% formalin, different organs (e.g., salivary glands, thyroid, liver, spleen, heart, and lungs) were collected and stained with hematoxylin and eosin (H&E) to examine their morphology.

PF-NIS-expressing LNCaP cells transport more oxyanions than PF-NIS-expressing Cos-7 cells, because PSA is promoter-specific. Tumors shrank significantly more in the mice treated with PF-NIS and $^{188}ReO_4^-$ than in the negative control groups (which received saline). Furthermore, I^- protected the thyroids of these mice from the effect of $^{188}ReO_4^-$. At the endpoint of the experiment, we did not detect any changes in the morphology of the thyroid by H&E and immunofluorescence. We saw normal levels of TSH and T_4 which indicate that I^- protected the thyroid from $^{188}ReO_4^-$.

These studies will establish a therapeutic strategy for treating prostate cancer with an engineered NIS molecule (PF-NIS) using the β-emitter $^{188}ReO_4^-$. This strategy will offer the advantage of not rendering mice or (eventually) patients hyperthyroid, as their thyroids will be protected with I^- rather than by administering thyroid hormones. If successful, this approach will pave the way to successfully treating several other extrathyroidal cancers besides prostate cancer with PF-NIS and $^{188}ReO_4^-$.

Oral Abstracts - CNS

Oncolytic herpes simplex viral vectors restricted to cell-to-cell spread enhance therapeutic outcomes in preclinical glioblastoma models

Anna Sparks[1], Bonnie Hall[2], Trevor J. Hancock[1], William F. Goins[2], Joseph C. Glorioso[2], Joseph W. Jackson[1]

[1]*University of Tennessee Graduate School of Medicine, Department of Medicine, Knoxville, United States*, [2]*University of Pittsburgh School of Medicine, Department of Microbiology and Molecular Genetics, Pittsburgh, United States*

Abstract Text

Glioblastoma (GBM) is an aggressive brain malignancy that is resistant to current treatment modalities with only ~5% of patients surviving after 5 years. In recent decades, oncolytic herpes simplex virus (oHSV) vectors have been designed to treat GBM but have been met with varying and overall limited success. Previously, our group has implemented the use of an oHSV armed with interleukin-12 (IL-12), a potent cytokine capable of inducing intratumoral proinflammatory immune responses, as a GBM therapeutic to enhance the effectiveness of oHSV vectors. This IL-12-armed vector (oHSV:IL-12) has demonstrated a positive therapeutic benefit when used in the murine CT2A and GL261N preclinical glioma models with 17% and 30% overall survival, respectively, and enhances TCR diversity within the tumor mass compared to controls. However, this effect appears to be dose dependent as enhanced survival was only observed following administration of $1x10^7$ PFU of oHSV:IL-12 whereas mice administered $1x10^6$ PFU did not exhibit any therapeutic benefit. As control vectors without IL-12 did not provide a therapeutic benefit in either scenario, we hypothesized that the amount of oHSV derived IL-12 is the driver of therapeutic efficacy. One approach to enhance the amount of oHSV derived IL-12 is enhance oHSV spread/persistence in the tumor environment. To achieve this goal, we engineered the HSV glycoprotein gK to restrict viral spread in a cell-to-cell manner through the formation of syncytia within the tumor mass. In both murine and human glioma cell lines, the oHSV:gK vector enhanced tumor cell death in comparison to control oHSV. When armed with IL-12, oHSV:gK increased the overall survival of mice in the CT2A model to 40% when administered at the lower dose of $1x10^6$ PFU, at which no positive impact on survival was observed using the unmutated oHSV:IL-12. Moving forward we will analyze the persistence of the oHSV:gK and oHSV:gK:IL-12 vectors in murine GBM models, perform immunological characterization, and evaluate the therapeutic efficacy of this vector at alternative doses. These data represent a potential new avenue to exploit oHSV vectors for GBM therapy.

Oral Abstracts - Delivery and Targeting

Cell-specific and genomic site-specific engineering enables safe and potent in vivo TRAC-CAR T cell generation in mice and non-human primates

Jonas Fowler[1], Connor Tsuchida[1], Abdullah Syed[1], Justy Gomez Guagua[1], Isha Ukani[1], Ayesha Shabbir[1], Juan Hurtado Koolik[1], Cole Ingamells[1], Cloelia DeCioccio[1], Steven Long[1], Nathan Kipniss[1], June Dense[1], Itzia Zaleta-Linares[1], Phil Storm[1], Alex Qu[1], Mildred Unti[1], Beeke Wienert[1], Thomas Gardner[1], Miranda Meeuwsen[1], Eleazar DeAlmeida[1], Benjamin Cook[1], Anastasiia Kamenska[1], Paul Westberg[1], James Whitney[2], Jennifer Hamilton[1]

[1]*Azalea Therapeutics, Berkeley, United States*, [2]*Boston College, Department of Biology, Boston, United States*

Abstract Text

Introduction: In vivo chimeric antigen receptor (CAR) T cell therapies are rapidly advancing into the clinic and showing early signs of success, but current modalities have key limitations. mRNA-based therapies rely on transient expression that may lack the durability needed to effectively clear tumors. More durable, randomly integrating approaches such as retargeted lentiviral therapies carry the risk of insertional oncogenesis or cis-antigen masking in off-target transduced malignant cells, both of which are compounded by the *in vivo* distribution of lentiviral vectors compared to traditional *ex vivo* CAR T cell therapy. Here, we present a novel platform that generates TRAC-CAR T cells in humanized mouse models as well as non-human primates (NHPs) via the delivery of dual vectors mediating both cell-specific and genomic site-specific engineering.

Methods: Our dual vector platform relies on CRISPR-mediated homology directed repair (HDR) for site-specific integration of a CAR transgene into the *TRAC* locus of T cells *in vivo*. CD3-targeted enveloped delivery vehicles (EDVs) activate T cells and deliver Cas9 ribonucleoprotein that generate a double-stranded DNA break at the *TRAC* locus. Concurrently, a T cell tropic AAV (AAV-T) delivers a promoterless HDR template encoding a CAR transgene for precise integration at the cut site resulting in T cell specific, uniform expression of the CAR from the endogenous *TRAC* promoter. To test the EDV and AAV-T dual vector platform, particles designed to integrate a CD19-targeted CAR into human T cells were first validated *in vitro* and subsequently delivered via a single intravenous dose into immunodeficient mice engrafted with human PBMCs and the B cell leukemia cell line, NALM6. Peripheral blood samples were collected to analyze TRAC-CAR T cell expansion and contraction while bioluminescent imaging was performed to track NALM6 tumor burden over time. To assess feasibility in an immunocompetent setting without lymphodepletion, six NHPs were intravenously administered surrogate EDV and AAV-T particles designed to similarly integrate a CD20-targeted CAR in the *TRAC* locus of NHP T cells. Peripheral blood and biopsies of the lymph node and bone marrow were analyzed to confirm TRAC-CAR T cell generation and determine the depth of target B cell depletion.

Results: EDV and AAV-T robustly and preferentially edit human T cells over off-target cell types *in vitro*. Furthermore, CAR transgenes artificially integrated at the *TRAC* locus of off-target cell types are not expressed *in vitro*. In mice, we observed both EDV and AAV-T dose-dependent generation of CD19-targeted TRAC-CAR T cells resulting in NALM6 tumor clearance followed by TRAC-CAR T cell contraction. Upon subsequent tumor rechallenge without particle re-dosing, TRAC-CAR T cells were able to re-expand and clear the tumor

again. Long-read sequencing confirmed a precise *in vivo* integration at a single genomic locus. Similarly in NHPs, dosing surrogate EDV and AAV-T was well tolerated and resulted in CD20-targeted TRAC-CAR T cell expansion and subsequent contraction after deep CD20+ B cell depletion in the peripheral blood, lymph nodes and bone marrow of all six animals that were treated. Genomic analyses of mouse and NHP tissue samples confirmed genomic site-specific integration of the CAR transgene at the *TRAC* locus with no off-target expression or integration in non-T blood cells detected.

Conclusions: Our EDV and AAV-T dual vector platform enables T cell-targeting and genomic-site specific editing to generate TRAC-CAR T cells *in vivo* that are capable of eliminating successive tumors in a humanized mouse model as well as achieving deep B cell depletion in an immunocomponent NHP model without the need for prior lymphodepletion. In addition to the efficacy of TRAC-CAR T cells, we also observed T cell specific transduction and expression *in vitro*, as well as genomic integration specificity *in vivo*. This novel approach represents a major milestone in development of *in vivo* CAR T therapies as it uniquely allows for the safe, precise and effective integration of a CAR transgene specifically into the TRAC locus of T cells *in vivo*. Importantly, it enables the generation of potent and durable TRAC-CAR T cells, while eliminating the risk that random integration can pose including insertional oncogenesis for any on- or off-target cell transduced *in vivo* as well cis-antigen masking in malignant cells.

Oral Abstracts - CNS

AAV-ChP: A Novel AAV Capsid with Specific Tropism for Choroid Plexus Epithelial Cells In Vitro and In Vivo

Qizhao Wang[1], Jiyi Xu[2], Cheng Xu[1], Shoupeng Wei[2], Bing Wang[1], David Lovinger[2], Li Zhang[2], Daozhan Yu[1]

[1]AAVnerGene Inc, Rockville, United States, *[2]National Institute on Alcohol Abuse & Alcoholism, Bethesda, United States*

Abstract Text Choroid plexus epithelial cells (ChPE) are the primary source of cerebrospinal fluid (CSF) production. Emerging evidence suggests that the choroid plexus (ChP) plays a much broader role than previously appreciated. Beyond CSF production, the ChP functions as a detoxification interface that removes harmful circulating substances and as an immunological surveillance hub that regulates immune-cell access to the central nervous system. Clinical studies have linked ChP dysfunction to major neurological disorders, including neurodegenerative disease, stroke, major depression, and alcohol use disorder. However, ChP research has been substantially limited by the lack of effective cell-type-specific gene-delivery tools. AAV5 is the currently used serotype for ChP targeting; however, following intracerebroventricular (ICV) injection in rodents, its transduction is not restricted to ChPE cells, This CNS tropism limits its utility for precise molecular dissection of ChPE function. To address this challenge, we transduced the ATHENA-I AAV capsid barcode library (including hundreds of common AAV serotypes and engineering variants) into human primary ChPE cells and performed next generation sequencing (NGS) to quantify the abundance and expression of individual capsid variants. Through this screen, we identified a novel capsid from our engineered capsid pool, designated AAV-ChP, that exhibited preferential tropism for ChPE cells. Compared with AAV5, AAV-ChP achieved approximately 13-fold higher vector DNA levels and 50-fold higher RNA levels. The enhanced transduction efficiency was further confirmed by individual transduction experiments using AAV-ChP and AAV5 vectors carrying a CMV-mCherry reporter. RNAscope analysis. We then compared AAV-ChP with AAV5 in a mouse model following ICV administration. In contrast to AAV5, RNAscope analysis showed that AAV-ChP-mediated transgene expression was largely confined to the ventricular compartment, with no detectable signal outside the ventricles. Single-cell RNA sequencing further confirmed this remarkable specificity, showing that approximately 92% of mCherry-positive cells were ChPE cells. The preferential and highly specific ChPE transduction of AAV-ChP has also been confirmed across multiple disease models using different reporter genes or genes of interesting. This AAV-ChP capsid provides a valuable tool for investigating ChPE function under both physiological and pathological conditions and offers a highly specific and efficient gene-delivery platform for targeting ChP-associated CNS diseases.

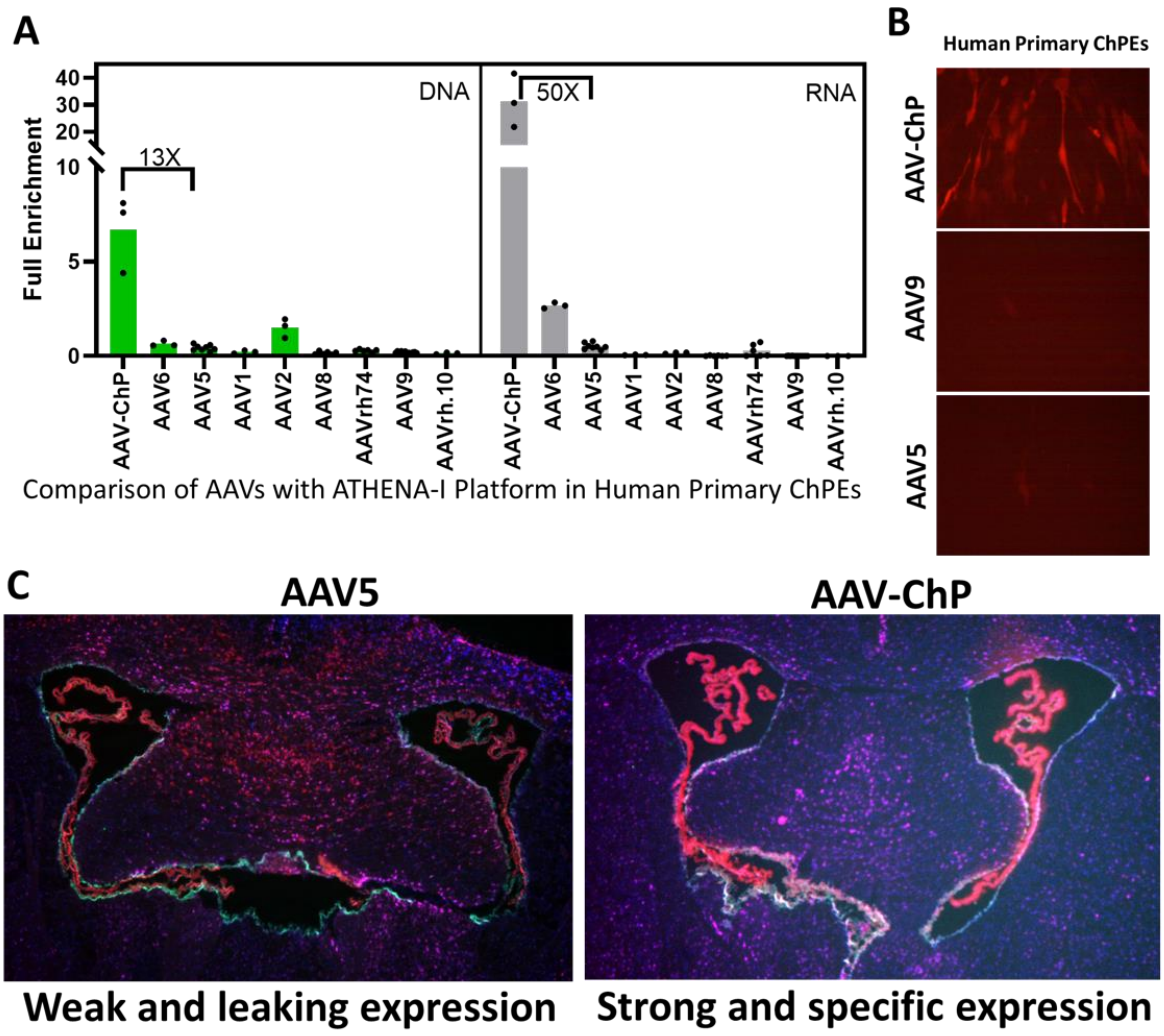

Figure 1. AAV-ChP exhibits preferential transduction of choroid plexus epithelial (ChPE) cells in vitro and in vivo. (A) AAV-ChP demonstrated enhanced transduction of primary human ChPE cells compared with AAV5, as assessed by vector DNA and transgene RNA levels using NGS-based barcode analysis. (B) Enhanced transduction of primary human ChPE cells was further confirmed using AAV-ChP and AAV5 vectors carrying a CMV-mCherry reporter. (C) Following intracerebroventricular (ICV) administration in mice, AAV-ChP-mediated mCherry expression was strongly localized to the choroid plexus, whereas AAV5-mediated expression extended into other brain regions. Representative brain sections show colocalization of AAV-ChP-mediated mCherry expression (red) with the ChPE/epithelial marker FoxJ1 (green). Aquaporin-4 (AQP4; magenta) was used to visualize surrounding brain structures.

AAVone2.1 single-plasmid platform enables >80% full AAV particles and titers up to 1 × 10^16 vg/L across diverse capsids

Jiantao Zhang[1], Yuyan Wang[1], Yu Liu[1], Jason Yu[1], Lemin Wang[1], Rongze Yang[1], Qizhao Wang[1]

[1]*AAVnerGene Inc, Rockville, United States*

Abstract Text

Adeno-associated virus (AAV) manufacturing remains a critical bottleneck for *in vivo* gene therapy, particularly for high-dose systemic indications where vector demand directly affects clinical feasibility, manufacturing costs, and patient access, necessitating superior vector quality and scalable economics. Conventional triple-plasmid transfection systems (AAVtri) rely on the independent delivery of helper, Rep/Cap, and vector-genome plasmids, leading to spatial, temporal, and stoichiometric mismatches during production. These mismatches contribute to low productivity, batch variability, and a high proportion of empty particles at harvest. We previously developed AAVone1.0, a single-plasmid AAV production system integrating adenoviral helper genes, Rep/Cap genes, and the AAV vector genome into a single construct. While AAVone1.0 eliminated spatial mismatch and increased AAV productivity by approximately 2- to 4-fold, it only modestly improved full-particle ratios, indicating that temporal and quantitative coordination remained key barriers to efficient genome packaging. To better synchronize AAV genome replication with capsid protein availability, we engineered AAVone2.1, a second-generation single-plasmid platform. Across a broad panel of natural AAV serotypes, including AAV1, AAV6, AAV8, AAV9, AAVrh.10, and AAVrh.74, as well as engineered capsids, including AAV-DJ, AAVmyo, AAV-ShD, AAV-9P31, AAV-PHP.eB, and AAV-BI-hTFR1, AAVone2.1 consistently improved packaging efficiency at harvest. Notably, AAVone2.1 increased the full-particle ratio to greater than 70% for the majority of tested capsids, including 82.1% for AAV1, 79.2% for AAV8, and 82.6% for AAV-DJ. Overall, the full-particle ratios achieved with AAVone2.1 ranged from 50% to 85%, compared with the typical ranges of 20% to 50% observed with AAVtri systems and 25% to 55% with AAVone1.0. For a 2.8 kb vector genome, AAVone2.1 consistently outperformed both AAVtri and AAVone1.0 across all tested capsids and producer cell lines, including VPC2.0 and HEK293one, in both productivity and purification recovery. When combined with process optimization, including HEK293 producer cell development, optimized transfection reagents and parameters, and production enhancers, AAVone2.1 generated crude production titers up to 1 × 10^16 vg/L. These findings demonstrate that precise calibration of AAV production-component architecture can simultaneously improve vector yield, increase full-particle ratio, and streamline manufacturing. By reducing reliance on intensive downstream full/empty separation across both natural and engineered capsids, AAVone2.1 offers a scalable single-plasmid platform with the potential to lower the cost of goods and expand global access to GMP-grade AAV gene therapies.

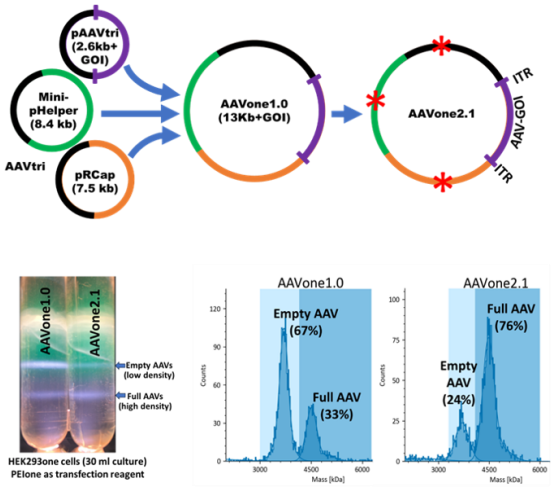

Serotype	Genome	Full Particle Ratio at Harvest (%)		
		AAVtri	AAVone1.0	AAVone2.1
AAV1	2.8kb	33.1	50.4	82.1
AAV2	2.8kb	29.0	32.0	52.0
AAV6	2.8kb	49.0	53.4	72.4
AAV8	2.8kb	42.6	48.2	79.2
AAV9	2.8kb	33.9	37.6	73.4
	4.3kb	33.4	30.4	61.5
	4.7kb	30.1	29.1	54.0
AAVrh.10	2.8kb	32.8	41.6	72.7
AAVrh.74	2.8kb	24.4	44.3	60.2
AAV-DJ	2.8kb	29.4	51.5	82.6
AAV-ShD	2.8kb	23.1	48.0	74.2
AAV-9P31	2.8kb	34.0	N/A	77.2
AAVmyo	2.8kb	30.4	N/A	73.4

Figure 1. AAVone2.1, a single-plasmid AAV production platform, improves full-particle packaging across diverse capsids. (A) Schematic comparison of the AAVone platform design, in which adenoviral helper genes, AAV Rep/Cap genes, and the AAV vector genome are integrated into a single production plasmid to improve coordination of vector genome replication and capsid assembly. **AAVone2.1**, a modified version of the **AAVone1.0 backbone**, significantly improves the full-particle ratio, as well as AAV productivity. (B) Representative analytical profiles showing improved full-particle enrichment with AAVone2.1 compared with conventional AAVtri or earlier AAVone1.0 platform configurations. (C) **Summary of full-particle ratios at harvest across natural AAV serotypes and engineered capsids.** AAVone2.1 achieved >70% full AAV particles across multiple capsids—with some exceeding 80%—while maintaining high production titers.

Amplification-free AAV titer and high-throughput gene editing quantification by CRISPR kinetics: analytical qualification of a one-hour assay for CMC workflows.

Charles Blanluet[1]

[1]*QUiCKR Bio, Long Island City, United States*

Abstract Text

Introduction

Vector genome titer is a release-defining attribute in AAV manufacturing, while on-target editing efficiency is the key readout in gene editing development and manufacture. Both depend on reference methods, ddPCR and NGS respectively, that impose amplification bias, multi-step workflows, and turnaround measured in shifts or days. When results arrive hours to days after sampling, they can no longer inform in-process decisions, so these measurements function as retrospective records rather than process controls.

Methods

QUiCKR (Quantification Using initial CRISPR Kinetic Rates) quantifies DNA targets from the initial velocity of Cas12 trans-cleavage against a fluorescent reporter. A target-specific gRNA is designed to a 20-nucleotide site. Initial rates are fit and converted to concentration against a calibrator. For AAV titer, the workflow is amplification-free and comprises five steps: PK/DNase treatment (40 min), dilution (5 min), plating (5 min), 37 °C incubation and read (10 min), and automated analysis. Results return in under one hour with approximately 20 minutes hands-on, on standard 384-well qPCR instrumentation with no dedicated capital equipment. Side-by-side workflow mapping against ddPCR (~8 h), including the same PK/DNase step in both, gives roughly an 8-fold reduction in time to result for titer. For gene editing, the workflow substitutes target amplification for the PK/DNase step upstream of the same kinetic readout, quantifying editing efficiency as single-nucleotide substitution fraction from amplicons generated from extracted genomic DNA.

Results

Formal qualification of the gene editing application was performed at a CRO against five parameters with pre-specified acceptance criteria. Editing was delivered by AAV vector, and accuracy was assessed across 24 vector lots and the resulting gene-edited panels versus ddPCR and NGS ($R^2 > 0.90$); repeatability across 3 vector lots in 6 replicates (%CV < 10%); intermediate precision across 3 vectors by 3 runs by 3 operators (%CV < 10%); linearity and dynamic range across 3 vectors at 10 dilutions ($R^2 > 0.90$); and specificity across 3 vectors and 3 probes (zero false positives). Data generated meet these criteria. The finalized matrix with parameter-level results will be presented.

Independent customer data from three industry sites meet the accuracy, repeatability, and linearity criteria for standalone AAV titer quantification. Comparison against ddPCR gave R^2 = 0.94 and 0.93 across 21 AAV lots spanning 6.5×10^{10} to 6.9×10^{13} vg/mL at the first site, with run-to-run agreement of R^2 = 0.96 between two independent runs, indicating that method

reproducibility exceeds cross-method agreement with ddPCR. An independent 7-vector panel at the second site gave $R^2 = 0.943$ ($r = 0.971$, log–log), with mean absolute error of 15.9% of mean ddPCR titer and MAPE of 13.6%. Intra-assay precision across 5 vectors at that site ranged from 1.53% to 12.60% CV, mean near 8%. At the third site, quantification of process intermediates and purified drug product across 13 samples spanning 3.8×10^{11} to 7.5×10^{13} vg/mL gave $R^2 = 0.99$ against site-reported ddPCR values. In dual-probe configuration, ITR and WPRE were quantified concurrently across a dilution series of 3 source vectors, tracking concordantly from 2.3×10^{13} down to approximately 10^{10} vg/mL.

Conclusion

A single CRISPR-kinetic readout serves two distinct analytical needs. In AAV vector manufacturing, it quantifies genomic titer amplification-free in under one hour for in-process and release testing. In gene editing workflows, it quantifies on-target editing efficiency from amplicons at scale, where NGS is the incumbent method. Formal qualification of the AAV-delivered editing workflow meets pre-specified accuracy, precision, linearity, and specificity criteria, and independent customer data from three industry sites corroborate titer performance at ddPCR-level agreement. Same-hour titer results enable in-process decisions rather than retrospective confirmation.

Genome editing using targeted lipid nanoparticles for Mantle Cell Lymphoma therapy

Lior Stotsky-Oterin[1 2 3], Dan Peer[1 2 3], Itai Benhar[1 2 3]

[1]Shmunis School of Biomedicine and Cancer Research, Tel Aviv University, Tel Aviv, Israel, *[2]Center for Nanoscience and Nanotechnology, Tel Aviv University, Tel Aviv-Yafo, Israel*, *[3]Cancer Biology Research Center, Tel Aviv University, Tel Aviv, Israel*

Abstract Text

Mantle Cell Lymphoma (MCL) is an aggressive, rare B-cell malignancy, genetically characterized by the t(11;14) translocation that leads to overexpression of Cyclin D1. MCL patients are mostly diagnosed at advanced stages and present with a disseminated disease that frequently involves the bone marrow. Despite recent advances in chemotherapy and immunotherapy, virtually all patients eventually relapse with resistance to prior treatments, rendering MCL incurable with current therapies. Therefore, new therapeutic strategies are most needed. Sry-Related High-Mobility-Group Box 11 (SOX11) has emerged as a key transcription factor in the pathogenesis of MCL as it is highly expressed in ~90% of patients, while absent in mature B-cells. Its specific expression in MCL, particularly in aggressive forms, suggests that in addition to its value as a diagnostic and prognostic biomarker, SOX11 may serve as a potential therapeutic target. CRISPR-Cas9 is a powerful tool for specific gene editing that holds great promise in treating various conditions, including hematological malignancies. We aim to harness CRISPR-Cas9 technology to specifically knockout SOX11 using αCD38-targeted lipid nanoparticles (LNPs) co-encapsulating Cas9 mRNA and a sgRNA as a novel potential therapy for MCL. First, we demonstrated that SOX11 knockdown using siRNA-LNPs leads to significant cell death of MCL cell lines, validating SOX11 as a therapeutic target. To utilize the CRISPR-Cas9 system, we screened for multiple sgRNAs and found an efficient candidate reaching ~80% editing in MCL cells. Next, we screened different LNP formulations, optimized LNP composition, and identified a formulation that efficiently delivered CRISPR-Cas9 RNA into ~95% of the treated MCL cells. Combining both, SOX11-CRISPR LNPs led to efficient gene editing that consequently resulted in ~95% cell death. To enhance target specificity, we developed a novel targeting platform named Lipidated Antibody Nanoparticle Delivery (LAND), comprised of a lipidated αCD38 single-chain variable fragment (scFv), and produced as micelles from E. Coli. These micelles were then incorporated into the LNPs, enabling enhanced internalization and efficiency in MCL cells *in vitro*, as well as selective binding to MCL cells within the bone marrow population *ex vivo*. Furthermore, to evaluate the therapeutic efficacy of our targeted CRISPR-LNPs *in vivo*, we established a novel disseminated xenograft MCL model that demonstrates significant bone marrow involvement as in most MCL cases. Finally, we performed a biodistribution evaluation of the targeted LNPs, showing localization of the αCD38-LNPs in the femurs of MCL-bearing mice. Our potential ability to disrupt essential gene expression *in vivo*, specifically in MCL cells, demonstrates the feasibility of genome editing as a targeted therapeutic strategy and may open new avenues for treating this devastating disease and other hematological malignancies.

Oral Abstracts - Delivery and Targeting

Bispecific VSV-G Engagers: A Platform for Targeted in vivo Gene Delivery.

Menachem Rubinstein[1], Diana Gataulin[1], Gopal Naik Nenavath[2], Nandakumar Packiriswamy[2], Gideon Schreiber[1], MD Sharif Hasan[2], Tatenda Kadungure[2], Harshitha Anantharama[2], Pragati Jain[2], Patrycja Lech[3], Luis Blancas-Mejia[3], Hamid Salimi[2], Kah-Whye Peng[3], Stephen Russell[3]

[1]Weizmann Institute Of Science, Rehovot 76100, Israel, *[2]Imanis Life Sciences, Rochester MN, United States*, *[3]Vyriad, Rochester MN, United States*

Abstract Text

Introduction

VSV-G-pseudotyped lentiviral vectors (LVVs) are widely used for ex vivo CAR T-cell therapy and gene therapy. These vectors enter a broad range of cell types through the ubiquitously expressed LDL receptor (LDLR) and other LDLR family members (Fig. 1A). LVV-based ex vivo therapies have transformed the treatment of B-cell malignancies and monogenic disorders, but their broader application is constrained by complex, costly, and patient-specific manufacturing procedures. These limitations have stimulated the development of in vivo approaches in which vectors are reengineered to target specific cell types. However, such modifications can reduce transduction efficiency and vector yield and compromise vector stability. Previously, we identified a soluble N-terminal fragment of LDLR (sLDLR) that inhibits VSV-G-mediated transduction by competing with cell-surface LDLR for vector binding (Fig. 1B).

Methods

Building on this observation, we developed a general targeting strategy that preserves the potency of unmodified VSV-G-pseudotyped LVVs while redirecting them to specific cell types. The approach uses reversible engagers comprising VSV-G-binding CR domains of LDLR fused to a ligand or antibody recognizing a cell-type-specific receptor. The engager blocks native LDLR-mediated entry while redirecting the vector to the target receptor. Following endocytosis, the engager dissociates, releasing fully functional VSV-G-pseudotyped LVV, thereby enabling efficient genetic cargo delivery (Fig. 1C).

For T-cell targeting, we fused the VSV-G-binding region of sLDLR (CR1–3) to an anti-CD3 scFv. To increase avidity for the native trimeric VSV-G spike, we generated a trimeric engager, $(\alpha CD3–VL–sLDLR)_3$, using a GCN4-derived trimerizing leucine-zipper peptide (Fig. 1D).

Results

The trimeric anti-CD3 engager selectively transduced non-preactivated human T cells within PBMCs, achieving transduction efficiencies of up to 70% (Fig. 1E). In NSG immunocompromised mice bearing human OPM-2 multiple myeloma tumors, systemic administration of LVV complexed with the trimeric engager generated CAR T cells in vivo and induced rapid tumor regression, with tumor signals declining to near-background levels within 21 days (Fig. 1G,H).

Conclusion

Reversible LDLR-based engagers provide a modular strategy for directing unmodified VSV-G-pseudotyped LVVs to selected cell types while preserving their high transduction efficiency. By separating cell targeting from vector engineering, this approach may provide a scalable platform for in vivo CAR T-cell generation and other forms of targeted in vivo gene therapy.

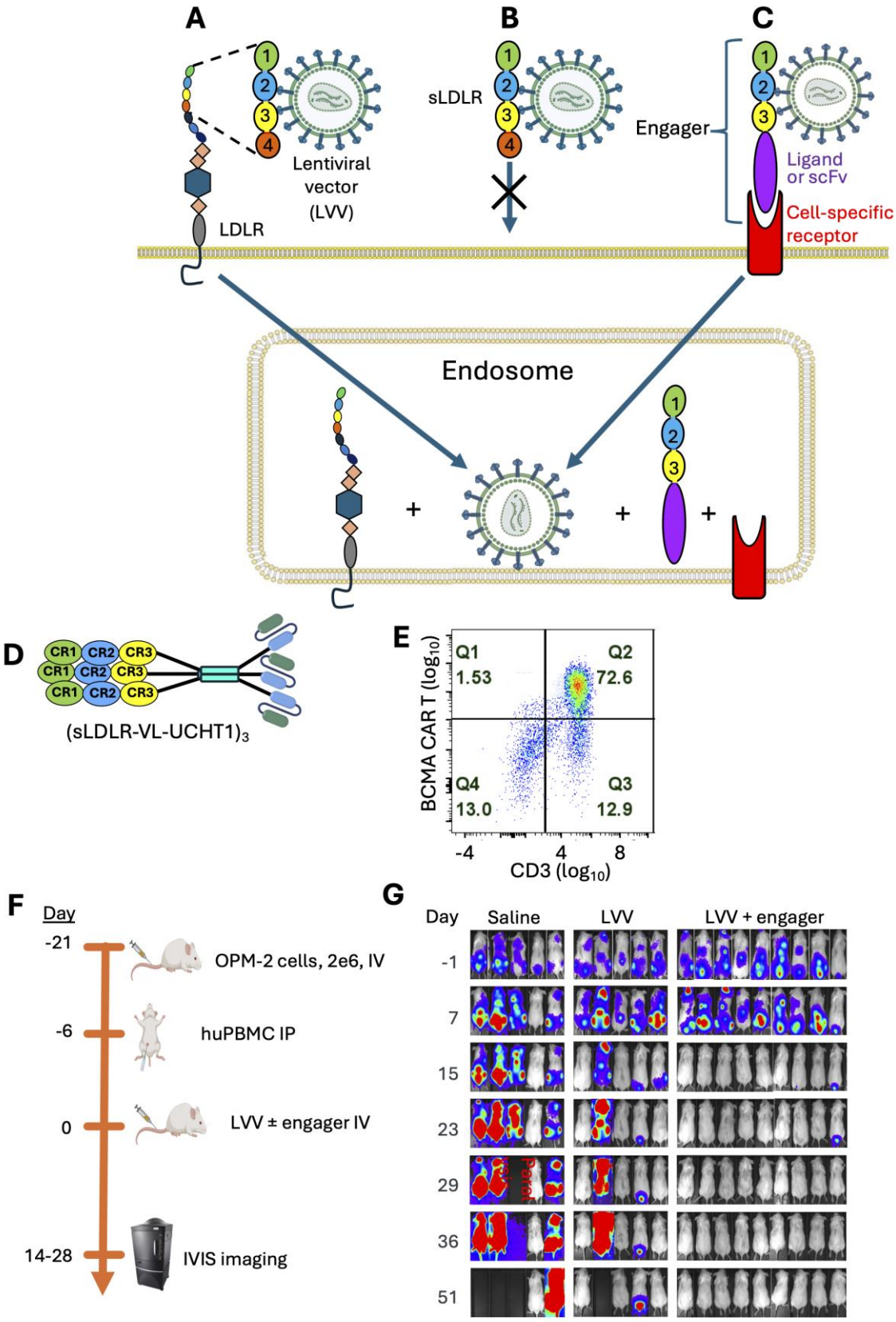

Figure 1. Schematic representation of the reversible engager approach and its use for in vivo CAR T. A. Entry of a lentiviral vector (LVV) through the LDL receptor. B. sLDLR competitively inhibits LVV entry to cells. C. Engager-mediated entry of LVV through a cell-specific receptor

and inhibition of its entry through LDLR. At the endosome, LVV is detached from the engager and effectively fuses with the endosomal membrane. D. Scheme of the trimeric engager (âCD3-VL-sLDLR)$_3$. E. Percentage of GFP-expressing T cells transduced in PBMC with LVV + 6.7 nM engager, gated on live/CD45+ cells. F. Workflow of the study with NSG mice. G. Clearance of BCMA+ OPM-2 tumors by T cells generated in vivo by LVV ± engager.

Rescuing the Guardian of the Genome: An LNP-Based Approach to Restore p53 Activity

Aviad Elisha[1 2 3], Dan Peer[1 2 3]

[1]Shmunis School for biomedicine and cancer reserach, Tel Aviv University, The George S. Wise Faculty of Life Sciences, Tel Aviv-Yafo, Israel, *[2]Center for Nanoscience and Nanotechnology, Tel Aviv University, Tel Aviv-Yafo, Israel*, *[3]Cancer Biology Research Center, Tel Aviv University, Tel Aviv-Yafo, Israel*

Abstract Text

Mutations in TP53 are among the most common alterations in human cancers and frequently result in loss of tumor suppressor activity through dominant-negative effects. This dominant-negative interference of mutant p53 with wild-type p53 limits the effectiveness of strategies based solely on wild-type p53 delivery. Here, we describe a dual silencing-and-replacement approach designed to overcome this limitation by simultaneously suppressing endogenous mutant p53 and restoring functional p53 expression.

In cancer cell models with distinct TP53 backgrounds, delivery of wild-type TP53 mRNA alone produced mutation-dependent effects, with reduced efficacy observed in dominant-negative contexts. In contrast, co-delivery of TP53-targeting siRNAs with engineered wild-type TP53 mRNA enhanced cytotoxicity and apoptotic signaling, consistent with functional reactivation of the p53 pathway. This combined strategy shifted dominant-negative cell line toward a TP53-null–like response profile and improved downstream pathway engagement.

To enable therapeutic application, we developed lipid nanoparticles (LNPs) that optimized for co-encapsulation and delivery of both RNA components. The formulation supported efficient RNA delivery, strong target knockdown, and robust mRNA expression with minimal cytotoxicity. Notably, the optimized formulation resulted in significantly lower cell viability following combination treatment compared to either agent alone. Finally, the optimized formulation was injected to tumors bearing mice and the particles were accumulated mainly in the tumor lesions. Further analysis revealed that 26% of cancer cells in the tumor were positive for both mRNA an siRNA

These findings support a mutation-agnostic RNA therapeutic approach for restoring p53 function in cancers harboring dominant-negative TP53 mutations. The mutation-agnostic design may enable application across a broad range of malignancies in which TP53 dysfunction is prevalent, including high-grade serous ovarian cancer, triple-negative breast cancer, non-small cell lung cancer, and other tumors in which TP53 alterations frequently co-occur with driver mutations such as BRCA1/2.

Programmable DNA integration with New-to-Nature tools using Computational Protein Design

Elizabeth Kellogg[1], Hailey Wallace[1], Seong Guk Park[1], Adam Smiley[1], Tuba Şevik[1], Shubham Dubey[1], Shirin Fatma[1], Samuel Vo[1], Ethan Creed[1], Alexandre Zanghellini[1]

[1]*Saint Jude Children's Research Hospital, Memphis, United States*

Abstract Text

Precise insertion of large DNA cargo at defined genomic sites, without inducing double-strand breaks, remains a major limitation of current genome-editing technologies. Here we address this challenge by using *de novo* protein design to create highly active, new-to-nature RNA-guided transposons. The resulting system, NovoCAST, is the simplest CRISPR-associated transposon (CAST) described to date. NovoCAST exhibits sharply defined integration profiles, up to 3 orders of magnitude increase in activity relative to native CASTs, and exceptionally high on-target specificity. Structural and biochemical analyses confirm that the designed proteins fold and function as intended. Finally, we demonstrate robust programmable genomic integration in human cells, underscoring the translational potential of this approach. Together, these results establish *de novo* protein design as a powerful strategy for building efficient, precise genome-integration systems and provide a foundation for the development of clinically relevant, programmable gene integration tools.

Therapeutic Delivery of siRNA Targeting TERT by Fab-directed Ionizable Lipid Nanoparticles against Neuroblastoma

Zhongkun Zhang[1], Yufei Wang[1], Siyu Yao[1]

[1]*Southeast University, School of Public Health, Nanjing, China*

Abstract Text

Introduction

Neuroblastoma (NB) is a pediatric solid tumor arising from neural crest cells of the sympathetic nervous system. Despite progress in multimodal therapy, outcomes for high-risk NB remain poor. RNA interference using siRNA delivered by targeted lipid nanoparticles (tLNPs) offers a strategy to suppress otherwise undruggable oncogenic drivers, but its application in NB has been hindered by inefficient delivery to neural tissues. This study developed Fab-conjugated lipid nanoparticles targeting GD2 for enhanced siRNA delivery to NB, providing a potential precision siRNA therapy against pediatric solid tumor.

Methods

The fragment antigen-binding region of an anti-GD2 antibody (GD2Fab) was purified and conjugated to various ionizable lipid nanoparticles (GD2FabLNPs). Comparisons were made among unconjugated LNPs, full anti-GD2 monoclonal antibody-conjugated LNPs (GD2mAbLNPs), and GD2FabLNPs. siRNA targeting telomerase reverse transcriptase (siTERT) was encapsulated into GD2FabLNPs using ethanol injection. Different NB cell lines (SH-SY5Y, Neuro-2a, etc.) were treated with GD2FabLNP-siTERT in vitro to assess siRNA uptake, mRNA downregulation, and cell viability. Xenograft and syngeneic NB mouse model were developed to evaluate the NB-specific delivery efficiency, antitumor activity, and safety of GD2FabLNP-siTERT upon intravenous administration.

Results

GD2FabLNP significantly enhanced siRNA uptake in NB cells compared with unconjugated LNPs and GD2mAbLNPs. Among tested ionizable lipids, a cyclic tertiary amine LNP, achieved the highest delivery efficiency, outperforming DLin-MC3-DMA and SM-102. siTERT delivered by GD2FabLNPs significantly downregulated TERT mRNA and reduced NB cell viability. Intravenous administration of GD2FabLNP-siTERT in NB xenograft models led to robust, tumor-specific siRNA delivery and substantial inhibition of tumor growth, demonstrating superior efficacy and delivery specificity of GD2FabLNP compared with unconjugated LNPs and GD2mAbLNPs.

Conclusion

GD2FabLNPs provide an efficient siRNA delivery platform to NB, highlighting siTERT as a promising therapeutic modality to treat NB. these findings highlight the strong therapeutic potential of siTERT against NB and suggested a superior tLNP platforms for cancer treatment using Fab-conjugated LNPs instead of mAb-conjugated LNPs.

uPAR-Directed CAR T-Cell Therapy Remodels the Pathologic Muscle Niche and Improves Skeletal Muscle and Respiratory Function in Preclinical models of Duchenne Muscular Dystrophy

Hamayl Afzal[1]

[1]*Duke University, Durham, United States*

Abstract Text

Introduction: Duchenne muscular dystrophy (DMD) is a progressive and fatal neuromuscular disease characterized by muscle degeneration, chronic inflammation, fibrosis, and progressive loss of skeletal and respiratory muscle function. Although dystrophin-restoring gene therapies have demonstrated clinical potential, their effects are limited by challenges including incomplete tissue correction and treatment-associated toxicities. Moreover, these approaches do not directly target the persistent inflammatory and fibrotic muscle microenvironment that contributes to impaired regeneration and functional decline. We hypothesized that selectively targeting pathogenic cell populations within the dystrophic muscle niche could provide a complementary therapeutic strategy.

Methods: Using single-cell transcriptomic profiling of dystrophic muscle, we identified urokinase plasminogen activator receptor (uPAR) as a surface marker enriched on subsets of macrophages and fibro-adipogenic progenitors (FAPs) exhibiting inflammatory and fibrogenic phenotypes. We generated uPAR-directed chimeric antigen receptor (CAR) T cells and evaluated their therapeutic activity in a murine model of DMD. Treatment effects were assessed using histopathological, molecular, regenerative, and functional endpoints, including skeletal muscle force, fibrosis, and diaphragmatic and respiratory function.

Results: uPAR-directed CAR T cells selectively targeted uPAR-expressing pathogenic cell populations within dystrophic muscle and remodeled the pathological muscle microenvironment. CAR T-cell treatment reduced inflammatory and fibrotic pathology, enhanced muscle regeneration, and improved skeletal muscle force. Importantly, treatment also reduced diaphragmatic fibrosis and improved measures of respiratory function, addressing a major source of morbidity and mortality in DMD. The therapeutic effects were associated with remodeling of the cellular niche rather than direct targeting of dystrophin-deficient myofibers.

Conclusions: These findings establish uPAR-directed CAR T-cell therapy as a potential niche-remodeling immunotherapy for DMD. By targeting pathogenic inflammatory and fibrogenic cell populations, this approach addresses disease mechanisms that remain largely unaddressed by dystrophin-restoring therapies and may provide a complementary strategy for improving muscle regeneration and function. The improvement in diaphragmatic and respiratory outcomes further supports the translational potential of targeting the dystrophic muscle microenvironment as a therapeutic strategy for DMD.

Origami-Driven Insights into BAFF-R: Computational Exploration for Next-Generation CAR T-Cell Targeting

Rhea Gupta[1]

[1]*The Overlake School, Redmond, United States*

Abstract Text

Introduction: Chimeric antigen receptor (CAR) T-cell therapy has demonstrated substantial efficacy in B-cell malignancies, but antigen escape, including CD19 loss, remains an important mechanism of relapse. B-cell activating factor receptor (BAFF-R; TNFRSF13C) is a mature B-cell survival receptor expressed across multiple B-cell malignancies and has demonstrated preclinical potential as an alternative CAR T-cell target. However, productive antigen recognition depends not only on binding affinity but also on epitope accessibility and the spatial organization of receptor-ligand interactions. We developed an integrated computational framework to characterize BAFF-R antibody recognition and investigate DNA origami as a programmable platform for nanoscale organization of recognition elements.

Methods: The human BAFF-R sequence (UniProt Q96RJ3) was structurally modeled using AlphaFold 3 and evaluated for membrane topology and extracellular accessibility using PROTTER and ChimeraX. Twelve antibody structures (1CR9, 1IL1, 1IQW, 1NLB, 2HRP, 2UYL, 2XQB, 3QEG, 4A6Y, 4H20, 6IDH, and 6KDH) were computationally screened against BAFF-R using HDOCK, with additional docking using HADDOCK and GRAMM. Predicted interfaces were characterized with PLIP for hydrogen bonds, hydrophobic contacts, salt bridges, and π-stacking interactions. PRODIGY was used to estimate protein-protein binding free energy. The leading candidate was further evaluated using Protein-Sol and AmyloGram for predicted solubility and aggregation propensity. A nanoHUB model was used for exploratory simulation of tumor-cell dynamics under varying immune-response parameters. DNA-origami structures were designed using caDNAno and visualized with oxView and ChimeraX to model programmable positioning of multiple recognition elements at defined nanoscale geometries.

Results: HDOCK scores ranged from −9.3 to −15.9, with 4H20 producing the most favorable predicted score (−15.9). PRODIGY independently identified 4H20 as the most favorable complex within the tested panel, with a predicted binding free energy of approximately −25 kcal/mol, compared with approximately −15 kcal/mol for 1CR9. PLIP analysis of the predicted 4H20-BAFF-R complex identified approximately 13 hydrogen bonds and 11 hydrophobic interactions, together with additional π-stacking and salt-bridge contacts. Protein-Sol predicted predominantly favorable residue-level solubility characteristics, while AmyloGram identified limited regions exceeding its aggregation-associated threshold. Cross-platform docking supported the presence of a structurally plausible extracellular interaction interface, although docking and affinity scores represent computational predictions rather than experimentally measured binding parameters. DNA-origami modeling demonstrated that recognition elements could be positioned at programmable distances and orientations, establishing a geometric framework for investigating multivalent BAFF-R engagement. In the nanoHUB simulation, increased immune-response parameters produced more rapid

reductions in simulated cancer-cell populations; this model was exploratory and did not directly reproduce BAFF-R CAR T-cell biology.

Conclusions: Within the evaluated computational panel, 4H20 demonstrated the most favorable predicted BAFF-R recognition profile based on docking score, predicted binding energetics, and intermolecular contact density. The study further establishes a computational framework connecting target structural analysis with programmable nanoscale organization. We hypothesize that appropriately spaced BAFF-R recognition elements could increase the probability of simultaneous receptor engagement and alter effective avidity relative to unstructured monovalent recognition. This hypothesis remains experimentally unvalidated; the present study does not demonstrate enhanced receptor clustering, CAR T-cell activation, or therapeutic efficacy. Future studies will experimentally measure 4H20-BAFF-R binding kinetics, validate predicted interface residues, characterize DNA-origami folding and antibody conjugation, and compare conventional versus spatially organized BAFF-R recognition for effects on antigen binding and CAR T-cell activation. This approach provides a testable framework for incorporating nanoscale molecular geometry as an additional design variable in next-generation cellular immunotherapy.

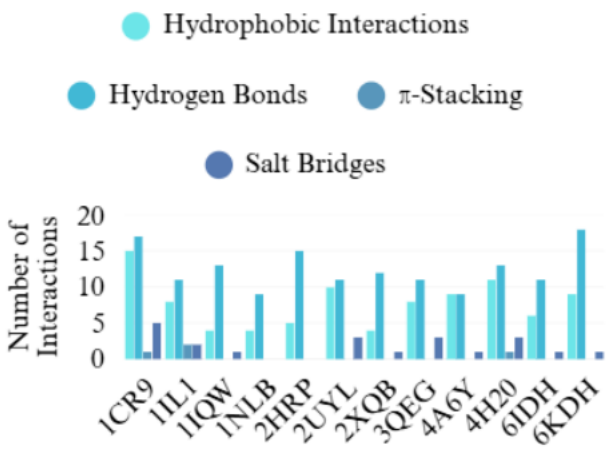

Figure 1: This figure shows the average ***number of interactions between the BAFF-R protein and the various antibodies*** *used in this research, this data was obtained using the PLIP webserver.*

1. The Protein–Ligand Interaction Profiler (PLIP) was used to analyze predicted intermolecular contacts within selected BAFF-R–antibody complexes.

The purpose of this analysis was to determine whether favorable docking predictions were accompanied by chemically plausible intermolecular contacts.

The predicted antibody-binding interface consisted of residues located within the extracellular region of BAFF-R. These residues represent computationally predicted contact residues and should not be interpreted as experimentally confirmed antibody epitopes.

Polymeric Nanoparticle Mediated Delivery of NF1 Attenuates Mammary Tumor Growth in a Heterozygous NF1 Deletion Rat Model

Ashlee Colbert[1], Erik Westin[2], Keara White[2], Deeann Wallis[3], Robert Kesterson[2], Cherry Gupta[1]

[1]Battelle, Columbus, United States, *[2]Louisiana State University, Baton Rouge, United States*, *[3]University of Alabama, Birmingham, United States*

Abstract Text

INTRODUCTION: Neurofibromatosis type 1 (NF1) is caused by loss-of-function mutations in the NF1 tumor suppressor, which encodes neurofibromin, a RAS GTPase-activating protein. Neurofibromin loss sustains RAS-MAPK signaling and drives tumor growth, and RAS-pathway inhibitors have shown limited durable efficacy. Restoring functional NF1 expression is a direct, mechanistically targeted alternative. Polymeric nanoparticles (PNPs) offer a non-viral, scalable platform for intratumoral gene delivery, but in vivo proof-of-concept for PNP-mediated Nf1 replacement in solid tumors has not been demonstrated. We evaluated whether a single intratumoral injection of a PNP-formulated mouse Nf1 plasmid suppresses spontaneous tumor growth in Nf1-deficient rats.

METHODS: Female NF1+/- rats, which develop spontaneous mammary tumors with high penetrance (onset 2-4 months of age), were monitored 2-3 times weekly. Upon tumor detection, tumors received a single intratumoral injection of PNP (formulation E7) carrying an expressing mouse Nf1 plasmid (mNf1; n=10 tumors), PNP carrying a non-expressing (stop-codon) Nf1 plasmid (STOP; n=6 tumors), or saline vehicle (n=8 tumors); STOP and saline were analyzed together as controls (n=14). Caliper tumor volumes were collected 2-3 times weekly for up to ~50 days post-injection and expressed as log2 change from baseline (Day 0). Analyses included per-timepoint two-group comparisons, area-under-the-curve (AUC) of cumulative growth burden, per-tumor log-linear (exponential) growth-rate estimation, and a shared-parameter joint longitudinal-survival model linking tumor trajectory to humane-endpoint culling. Secondary (non-injected) tumors were tracked for off-target effects.

RESULTS: In the initial cohort, Nf1-treated tumors grew significantly slower than saline controls, with separation emerging by Day 4 ($p=0.023$; Days 5 and 7, $p=0.045$ and 0.047) and cumulative AUC burden ~51% lower in treated tumors (mean AUC 73.4 vs 110.7 log2-units; $p=0.038$ by Day 20). In the expanded cohort, the exponential growth rate was approximately halved in Nf1-treated tumors (~7%/day) relative to pooled controls (~13%/day). Objective regressions, including complete responses to undetectable volume, occurred in a subset of Nf1-treated tumors but not in saline controls; a single regression in the non-expressing STOP arm indicates a low background rate of spontaneous regression and underscores the value of the included controls. The joint model identified tumor burden as the dominant driver of culling—each one-unit increase in log tumor volume raised the culling hazard approximately 7.8-fold (HR 7.78, 95% CI 2.66-22.65; $p<0.001$)—with a consistent directional treatment benefit on tumor growth and longer time-to-endpoint in Nf1-treated animals. Enrollment is

ongoing toward the biostatistically recommended target, and final results will be available prior to the conference.

CONCLUSIONS: These data provide in vivo proof-of-concept that non-viral, PNP-mediated intratumoral delivery of Nf1 produces biologically meaningful tumor-growth suppression and objective regressions in an Nf1-deficient mammalian model, with activity specific to the expressing construct relative to non-expressing and vehicle controls. The approximately two-fold reduction in growth rate, early onset of effect, and complete responses are consistent with sufficient intratumoral transfection to restore functional neurofibromin activity. These findings establish a foundation for a non-viral gene-replacement approach to NF1-associated tumors and motivate multi-dose dosing regimens, expression/mechanistic validation, and a powered confirmatory study.

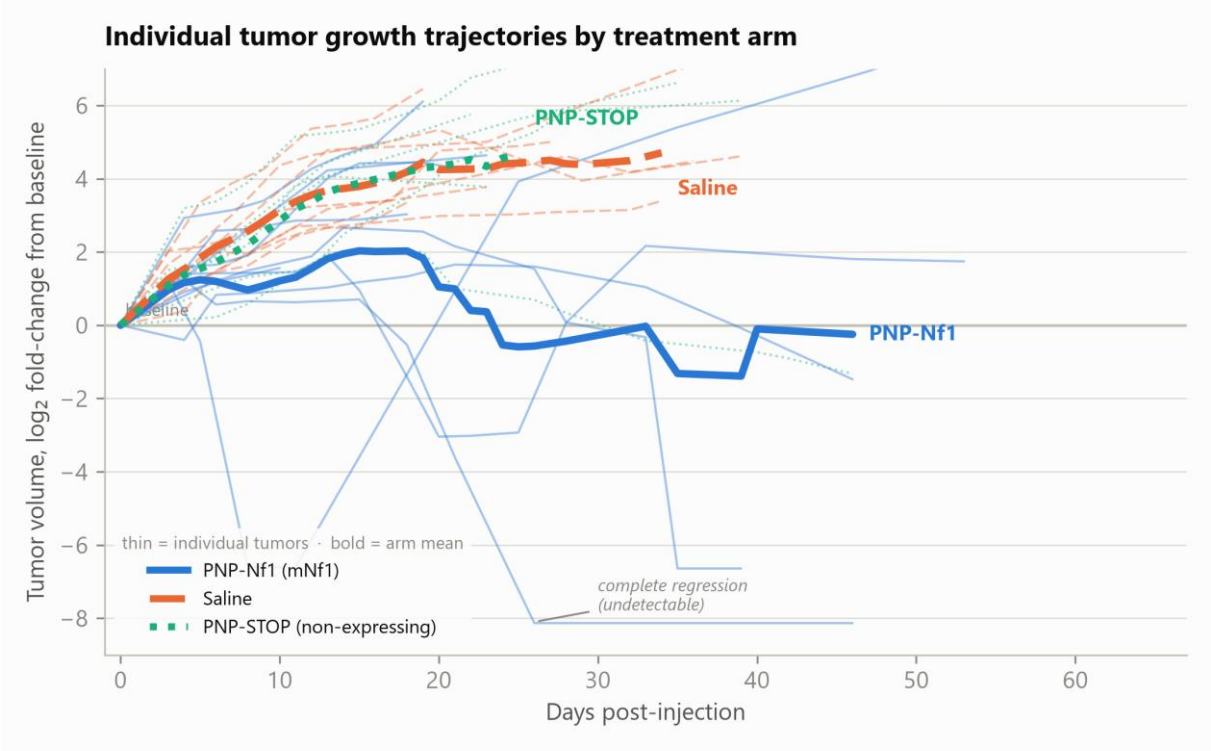

Figure 1. Single intratumoral dose; n=10 mNf1, 8 saline, 6 STOP tumors. Values=1 (undetectable) plotted at log_2FC floor.

Redefining AAV manufacturing using stable producer cell lines as a new paradigm

Gang Li[1], Chien-Ting Li[1], Michael Haller Friedrich[1], Tam Duong[1], Vijetha Bhat[1], Bingnan Gu[1]

[1]*Lonza, Houston, United States*

Abstract Text Introduction: AAV (Adeno-associated virus) - based gene therapies hold immense potential and have emerged as one of the fastest evolving therapeutic modalities. Yet, manufacturability of these next-generation therapeutics remains a challenge, with process scalability and the increasing cost of goods as limiting factors for making broader therapeutic access feasible.

Methods: Our AAV producer cell line (PCL) technology is based on a proprietary approach, in which all of the AAV-producing components are stably integrated into a cell line and AAV production is triggered using a small molecule inducer. This platform has been evaluated across multiple AAV products, and at scales up to pilot-scale bioreactors, for various target product profiles such as genomic titers, packaging efficiency, infectivity and purity.

Results: The established platform process enables the consistent generation of productive PCL clones across several serotypes and genes of interest while meeting or exceeding product quality attributes of traditional transient transfection methods, making it an excellent alternative to simplify and optimize AAV production efficiency, increase scalability, and improve batch consistency.

Conclusions: This approach resulted in the development of a highly productive, scalable, helper virus-free stable cell line system capable of enabling large scale clinical and commercial manufacturing of AAV with reduced complexity and lowered costs of goods.

Ligand conjugation to native AAV capsids enables TfR1-mediated CNS delivery without capsid engineering

Lavaniya Kunalingam[1], Maia Marchand[1], Adeline Muscat[1], Genny Amadei[1], Ludmila Juricek[1], Kamélia Kara-Ali[1], Corentin Deschamp[1], Maureene Beaunol[1], Delphine Compere[1], Adrien Savy[1], Emmanuelle Jordi[1], Alexandre Simon[1], Lolita Petit[1], Emmanuel Galène[1], Patricia Françon[1], Julien Spatazza[1], Davide Monteferrario[1]

[1]*Coave Therapeutics, Paris, France*

Abstract Text

Precise delivery of gene therapy vectors to specific tissues and cell types remains a major challenge, particularly following systemic administration of AAV vectors. Current approaches rely on capsid engineering to modify tropism, with targeting moieties encoded within the capsid sequence. While this strategy has enabled major advances in targeted gene transfer, each new therapeutic application requires the development of a new engineered capsid, limiting modularity and scalability while increasing development and CMC burden.

To address these limitations, Coave Therapeutics developed ALIGATER™, a proprietary chemical conjugation platform enabling on-demand receptor-mediated retargeting of AAV through the controlled attachment of tissue-specific targeting ligands to the AAV surface. By specifying tropism through ligand choice, the ALIGATER™ platform enables targeting to be defined without necessarily genetically modifying the AAV capsid sequence. Ligands are screened for translationally relevant binding properties, including receptor affinity, specificity, binding kinetics and cross species reactivity, after which ligand loading and surface presentation are optimized for each AAV backbone. The ALIGATER™ platform is being deployed across multiple targeting programs, with the present work focusing on its application to systemic central nervous system (CNS) delivery.

We applied the ALIGATER™ platform to develop AAV9 conjugated with a transferrin receptor 1 (TfR1)-targeting ligand (coAAV9). Leveraging high expression of TfR1 on CNS endothelial cells and its key role in mediating transcytosis across the blood-brain barrier (BBB), we aimed to enhance CNS biodistribution following systemic administration. A panel of TfR1-binding ligands was characterized by surface plasmon resonance (SPR), identifying candidates with favorable binding profiles toward both human and non-human primate (NHP) TfR1. Conjugation to AAV9 followed by dot blot confirmed preservation of ligand binding, enabling identification of candidates for functional testing. In vitro screening in human and NHP TfR1-expressing cell lines further refined ligand selection and enabled optimization of conjugation density to maximize coAAV transduction efficiency, showing a substantial improvement over unconjugated AAV9.

Selected vectors were then evaluated in vivo following systemic administration in humanized TfR1 knock-in mice. Optimized coAAV9 achieved robust CNS targeting, with approximately 50-fold higher vector levels in the brain and 10-fold higher levels in the spinal cord, accompanied by over 150-fold increase in transgene expression, compared with unconjugated AAV9. Histological analysis of brain sections spanning multiple levels further

demonstrated broad distribution of transgene expression across the brain. These results demonstrate that ligand conjugation can substantially enhance and redirect systemic AAV9 delivery to the CNS. A dedicated NHP study is planned to assess whether the cross species binding profile translates into enhanced CNS delivery in a large animal model, providing an important step toward evaluating the translational potential of this approach.

Together, these findings support the ALIGATER™ platform as a modular platform to overcome the limitations of capsid-defined tropism and enable programmable AAV delivery across tissues, with the potential to accelerate scalable and translatable precision gene delivery across diverse therapeutic areas.

Tuned for CNS Delivery – Enhancing Receptor-Mediated Transcytosis with Affinity-Tunable Anti-TfR1 VHHs

Anette Sommer[1], Fenna van Rijt[1], Devarshi Kapadia[1], Noel Smith[2], Remon van Geel[1]

[1]Lonza Oss B.V., Kloosterstraat 9, Oss, Netherlands, *[2]Lonza, Saffron Walden, United Kingdom*

Abstract Text

Introduction

The blood-brain barrier (BBB) remains a major obstacle to the development of biologics for central nervous system (CNS) disorders. Receptor-mediated transcytosis through transferrin receptor 1 (TfR1) has emerged as a promising strategy to enhance brain delivery; however, the relationship between receptor affinity and BBB transport efficiency remains an important design consideration for CNS-targeted therapeutics.

Methods

A panel of anti-TfR1 VHH shuttle variants with low, medium, and high receptor affinity was incorporated into a common bispecific antibody format. Molecules were expressed, purified, and characterized prior to evaluation in an in vitro BBB model. Transcytosis performance was compared across affinity variants to assess the impact of receptor engagement on transport across the endothelial barrier.

Results

Affinity-dependent differences in BBB transport were observed across the anti-TfR1 VHH variants. Comparative analysis demonstrated that receptor affinity significantly influences transcytosis efficiency and supports identification of shuttle configurations that maximize BBB passage while maintaining therapeutic antibody architecture. These findings establish affinity tuning as a critical parameter in the rational design of TfR1-mediated CNS delivery systems.

Conclusions

Systematic optimization of TfR1-binding affinity provides a practical strategy to enhance receptor-mediated transcytosis of biologics across the BBB. The results support the development of next-generation CNS delivery approaches and demonstrate the potential applicability of affinity-tunable TfR1 shuttles across antibody, bispecific, antibody-oligonucleotide conjugate (AOC), Adeno-Associated Virus (AAV), targered Lipid Nano Particles (LNPs) and other bioconjugate modalities.

Intent™Xpress: A Highly Efficient, Stable LNP Transfection Reagent for Nucleic Acid Delivery into Cell Lines and Primary Human Immune Cells

Aarushi Jain[1], Zhao Han[1], Haritha Menon[1], Matthew Gold[1], Athaliah Gervacio[1], Kieran Murray[1], Jennifer Nguyen[1], Maria Albaba[1], Yury Karpov[1], Jun Liu[1], Rajesh Krishnan[1], Natalia Martin Orozco[1]

[1]*Providence Therapeutics Holdings Inc, Calgary, Canada*

Abstract Text

Lipid nanoparticle (LNP)-based delivery has emerged as a leading platform for intracellular nucleic acid delivery, yet efficient and reproducible transfection of primary human immune cells remains a persistent technical challenge. Hard-to-transfect cell types including monocytes, T cells, and NK cells are poorly served by commercial reagents, which frequently exhibit low efficiency, cytotoxicity, and cumbersome preparation requirements.

Providence Therapeutics Holdings Inc. has developed Intent™Xpress, a novel LNP transfection reagent optimised for high-efficiency, low-toxicity delivery of nucleic acid payloads across a broad range of cell types. Using a Design of Experiments (DoE)-guided formulation discovery approach, Intent™Xpress was rationally developed to maximise intracellular delivery while preserving cell viability. The formulation self-assembles within 5 minutes at room temperature upon mixing with the nucleic acid payload requiring no specialised equipment, media modification, or additional preparation steps enabling a simple, reproducible, and scalable transfection workflow.

Comparative evaluation against leading commercial transfection reagents demonstrated superior performance across multiple cell lines and primary human immune cells, including monocytes, T cells, and NK cells, with high cell viability maintained across all conditions tested. The platform accommodates multiple nucleic acid payload classes; mRNA, pDNA, siRNA and supports simultaneous co-delivery in a single transfection step, highlighting its versatility across diverse intracellular delivery applications.

From a formulation standpoint, Intent™Xpress exhibits outstanding storage stability: the standalone reagent is stable at room temperature for ≥10 months; the reagent encapsulating the nucleic acid remains stable for up to 5 weeks at room temperature and 12 weeks at -80 °C, properties that distinguish it from conventional LNP formulations and support practical, cold-chain-independent deployment.

Intent™Xpress offers a robust, versatile, and shelf-stable LNP transfection platform for nucleic acid delivery into cell lines and primary human immune cells.

High-Yielding, High Purity Chemical Synthesis of RNA to 300 Nucleotides

Madeleine Dellinger[1]

[1]*Cirena, Inc., Boulder, United States*

Abstract Text

More than a decade ago, our laboratory developed a robust method for synthesizing long RNA molecules in the solid phase; approximately 100–300 or more nucleotides in length that matched or exceeded available methods for long DNA synthesis. However, the approach was never broadly commercialized. New CRISPR applications now require guide RNAs longer than those supported by conventional RNA synthesis techniques introduced in the late 1980s. Here, we describe a modern method for the de novo chemical synthesis of RNA and chemically modified RNA. The method supports next-generation CRISPR systems and modification strategies designed to improve base-editing efficiency while reducing unintended bystander editing. Using 2'-O-thionocarbamate-protected nucleoside phosphoramidites (TC), we synthesized thousands of pegRNAs of up to 250 nucleotides, along with circular RNAs and lncRNA subunits of up to 300 nucleotides. These products were generated in multimilligram quantities with standard commercial 96- and 192-column synthesizers. We also developed a high-yield, affinity-assisted, single-step chromatographic purification process that can be scaled to clinical quantities and used for *in vivo* screening. Because this phosphoramidite-based synthesis does not require final deprotection with hydrofluoric acid, it permits the site-specific addition of a broader range of stabilizing chemical modifications. Several of these modifications substantially improved pegRNA stability, specificity, and editing efficiency.

A Systemically Administered LNP Platform for Gene Editing in Cardiomyocytes

Andong Liu[1], Shaoli Liu[2], Ruilu Feng[2], Xiaopeng Song[2], Zimo Liu[2], Lin Zhang[2], Yu Lu[2], Rui Mao[2], Jiani Lei[2], Kate Rosner[3], Hongming Chen[3]

[1]METiS TechBio, Hangzhou, China, *[2]METiS TechBio, Beijing, China*, *[3]METiS Therapeutics, Cambridge, MA, United States*

Abstract Text

Introduction: While lipid nanoparticles (LNPs) are a versatile and clinically validated non-viral platform for large gene payloads, achieving organ-specific delivery beyond the liver remains a significant hurdle in genetic medicine. Cardiomyocyte-targeted delivery is particularly challenging, yet overcoming this barrier could open therapeutic opportunities across a broad range of cardiovascular diseases (CVDs). Here, we report an antibody-modified targeted LNP (tLNP) that achieves unprecedented efficiency and specificity in delivering genetic payload to cardiomyocytes via intravenous administration.

Methods: We employed an AI-driven lipid design engine to identify LNPs with specific tissue tropism. Candidate LNPs were evaluated in an mTmG mouse model following intravenous administration, using Cre-mRNA to induce eGFP expression as a readout for functional intracellular delivery. Following the identification of lead lipids with heart-specific tropism, formulations were further optimized for enhanced cellular uptake and subsequently functionalized with antibody targeting ligands to generate targeted LNPs (tLNPs). To assess therapeutic potential, the optimized lead tLNP was used to deliver CRISPR-Cas9 machinery to quantify gene editing efficiency in the cardiomyocytes.

Results: Optimized LNP without ligand functionalization demonstrated ~70% cardiomyocyte delivery. Off-target expression in the liver and spleen was minimized to <10%, with the integration of miRNA binding sites into the mRNA UTR. Upon functionalization with a targeting ligand, the cardiomyocyte-tLNP (CM-tLNP) achieved near-complete (> 95%) cardiomyocyte transfection. Furthermore, delivery of CRISPR-Cas9 machinery resulted in significant genomic editing within the myocardium, demonstrating the robust therapeutic potential of the platform for cardiac applications.

Conclusion: Our findings demonstrate that combining AI-driven LNP discovery and ligand-mediated targeting can achieve highly specific extrahepatic LNP delivery via intravenous administration. The achievement of near-complete cardiomyocyte targeting and significant *in vivo* gene editing suggests that this tLNP platform could be a transformative tool for treating genetic heart disorders and other intractable heart diseases.

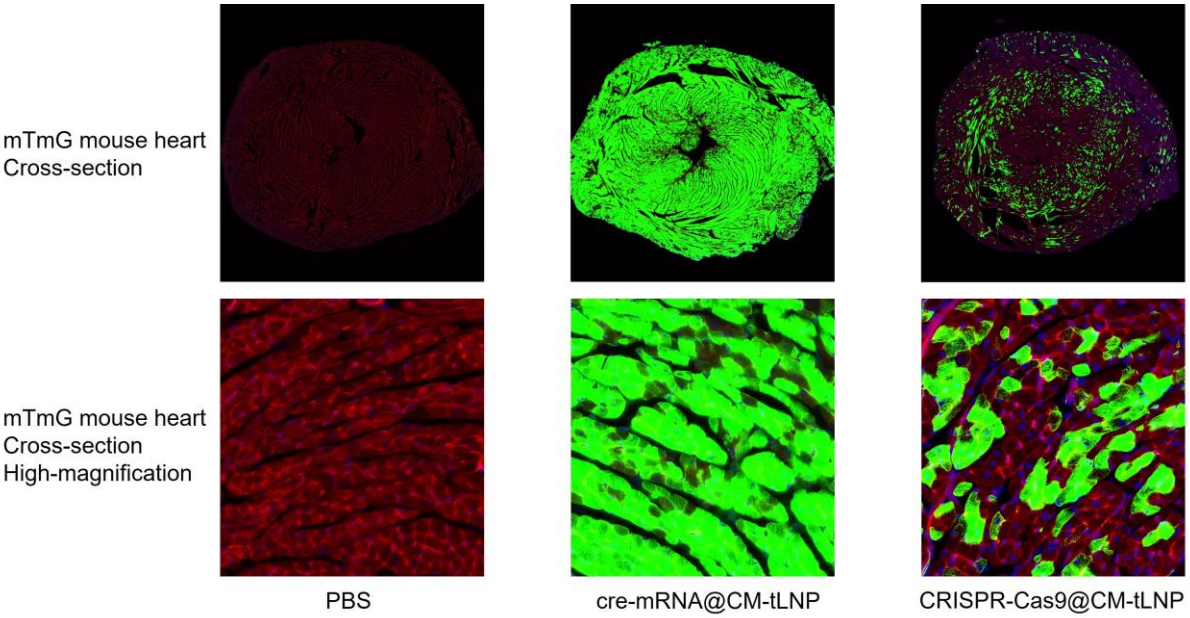
mTmG mouse heart
Cross-section
mTmG mouse heart
Cross-section
High-magnification
PBS
cre-mRNA@CM-tLNP
CRISPR-Cas9@CM-tLNP

Assessing clinically relevant safety outcomes and drive reverse translation strategies to limit unnecessary immune monitroing in critically ill patients

Vibha Jawa[1]

[1]*Epivax, Providence, United States*

Abstract Text

Background: Immunogenicity against chimeric antigen receptor (CAR) constructs can potentially compromise CAR T-cell expansion, persistence, and therapeutic efficacy. However, the clinical significance of anti-CAR antibody responses remains incompletely understood, particularly in patients with compromised immune function. Orvacabtagene autoleucel (orva-cel), a fully human B-cell maturation antigen (BCMA)-targeted CAR T-cell therapy, was evaluated in a phase 1/2 study in patients with relapsed or refractory multiple myeloma (RRMM). This study investigated the magnitude, specificity, and clinical relevance of treatment-emergent anti-CAR antibody responses.

Methods: Anti-CAR therapeutic domain-specific antibodies (ATAs) were monitored longitudinally in 157 orva-cel-treated patients. Immunogenicity assessments included antibody incidence, titers, immunoglobulin isotype characterization, and B-cell epitope mapping. In vitro immunogenicity risk assessment and epitope characterization were used to identify immunogenic regions within the CAR construct. Associations between ATA status, CAR T-cell expansion and persistence, and clinical outcomes were evaluated to understand the functional consequences of humoral immune responses.

Results: ATAs were detected in 44.6% of patients, with increasing incidence and titers over time. Epitope mapping identified five immunodominant consensus peptide sequences within the CAR therapeutic domain, recognized by both IgG and IgM antibodies. Notably, persistent IgM responses were observed in most ATA-positive patients, suggesting an atypical or potentially constrained humoral response. Despite the relatively high ATA incidence, antibody positivity was not associated with impaired CAR T-cell expansion or reduced patient survival. However, reduced CAR T-cell persistence was observed in ATA-positive patients. In vitro immunogenicity assessment and epitope mapping identified immunogenic hotspots within the CAR construct that may have contributed to the observed antibody responses. The limited functional consequences of these responses may reflect lymphodepletion, underlying disease-associated immune dysfunction, and impaired adaptive immune capacity in patients with RRMM.

Conclusions: These findings demonstrate that a high incidence of anti-CAR antibodies does not necessarily translate into clinically meaningful impairment of CAR T-cell activity or survival outcomes. Although ATAs were associated with reduced CAR T-cell persistence, their overall clinical impact appeared limited in this patient population. Integrating longitudinal clinical immunogenicity monitoring with mechanistic antibody characterization, epitope mapping, and in vitro risk assessment provides a more comprehensive framework for interpreting anti-CAR immune responses. These findings underscore the importance of considering patient immune status, disease biology, and functional outcomes when assessing immunogenicity risk and optimizing next-generation CAR T-cell therapies.

Metabolic determinants of recombinant protein productivity in CHO cells: a systems-level framework for improving yield and product quality of clinical therapeutic proteins and antibodies

Rita Singh[1 2], Niraj Kumar[1]

[1]Translational Health Science and Technology Institute, Faridabad, India, *[2]Jawaharlal Nehru University, Biotechnology, New Delhi, India*

Abstract Text Introduction

Chinese hamster ovary (CHO) cells manufacture most approved therapeutic proteins and monoclonal antibodies, yet raising volumetric and specific productivity without compromising product quality remains a central challenge in clinical biomanufacturing. Sodium butyrate (NaB) is used empirically across the industry to boost titre at 0.5-3.0 mM, but its therapeutic window is narrow: above 2-3 mM, cytotoxicity and impaired N-glycosylation fidelity emerge, and the threshold varies with clone, feeding strategy and culture format. Because the metabolic basis of the productive state has never been resolved across the full dose range, process developers lack both a rational basis for dose selection and measurable indicators of whether a culture has entered the productive window. We therefore asked whether that window can be defined quantitatively from cellular metabolism, and whether this yields monitoring biomarkers and rational cell line engineering targets translatable to manufacturing.

Methods

CHO-K1 cells were treated for 24 h with NaB at eight concentrations (0-8.0 mM), spanning sub-therapeutic, productivity-enhancing and cytotoxic ranges. Intracellular metabolites were extracted by a freeze-thaw and sonication protocol and profiled by LC-MS/MS on an Orbitrap Fusion Tribrid platform using C18 and HILIC separations in positive and negative modes, yielding 469 annotated features at MSI Level 1/2. A ten-stage pipeline was applied without pathway pre-selection: probabilistic quotient normalisation; principal component analysis; Welch t-test with Benjamini-Hochberg FDR per dose; ANOVA; Spearman dose-correlation; metabolite set enrichment analysis; KEGG topology analysis; Random Forest and LASSO regression for biomarker ranking; and KEGG/STRING network construction for target nomination.

Results

Three concentration-dependent metabolic states were resolved: sub-threshold (0-0.25 mM), productive (0.5-2.0 mM) and cytostressed (4.0-8.0 mM). Boundaries were derived a priori from the data and converged independently with the productivity-enhancing range established empirically in industry, providing a quantitative definition of the operating window. Differentially abundant metabolites expanded dose-dependently (82 to 243), with suppressed metabolites outnumbering induced ones 1.67:1 at 2.0 mM, indicating broad catabolic suppression rather than single-pathway activation. Suppression of fatty acid, amino acid and polyamine metabolites occurred alongside induction of TCA intermediates, glutathione-cycle metabolites and NAD-related species, a reorganisation consistent with

reallocation of resources from growth toward secretory function. Tryptophan metabolism was among the top enriched pathways (FDR 0.009): indole-derived catabolites declined, including indole-3-lactic acid (log2FC -1.43), a species previously reported to inhibit growth and productivity in fed-batch culture, while NMN and beta-NAD increased. Machine learning across all 469 features, independent of pathway assumptions, identified oxoproline (rho +0.946), serine, heptanoate, cyclohexanoic acid and indole-3-lactic acid as the most strongly dose-responsive metabolites, each anchoring a pathway mechanistically linked to secretory capacity, redox balance or carbon reallocation. Network analysis nominated SIRT1, HDAC1 and IDO1 as central regulatory nodes, with CPT1A and NAMPT additionally supported.

Conclusions

This work converts an empirical dosing practice into a quantitatively defined productive window and delivers two translational outputs: a compact panel of dose-responsive metabolites suitable for development as at-line indicators of process state, and a prioritised set of engineering targets (SIRT1, IDO1, CPT1A, NAMPT) for host cell line development. Both are directly relevant to improving titre and product consistency in the manufacture of therapeutic proteins and antibodies. Findings are associative and derived in a non-producer line; validation in recombinant producer lines under fed-batch conditions, with titre and glycosylation readouts, is the necessary next step.

Figure 1 | Pairwise PCA score plots: each NaB concentration vs. 0 mM control (95% confidence ellipses)

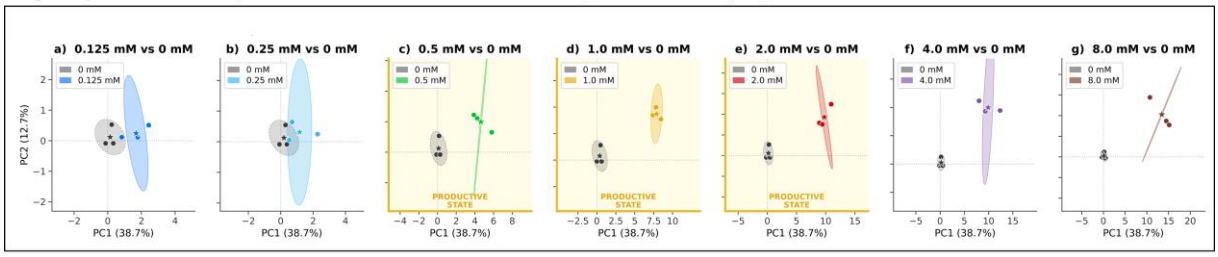

Figure 1. Pairwise PCA score plots for each sodium butyrate concentration versus 0 mM control, with 95% confidence ellipses. Three concentration-dependent metabolic states are resolved: sub-threshold (0-0.25 mM; panels a-b), NaB-responsive or productive (0.5-2.0 mM; panels c-e, shaded) and cytostressed (4.0-8.0 mM; panels f-g). PC1 38.7%, PC2 12.7%.

Figure 2 | Protein-protein interaction (PPI) network and node centrality ranking (KEGG/STRING, score > 0.700)

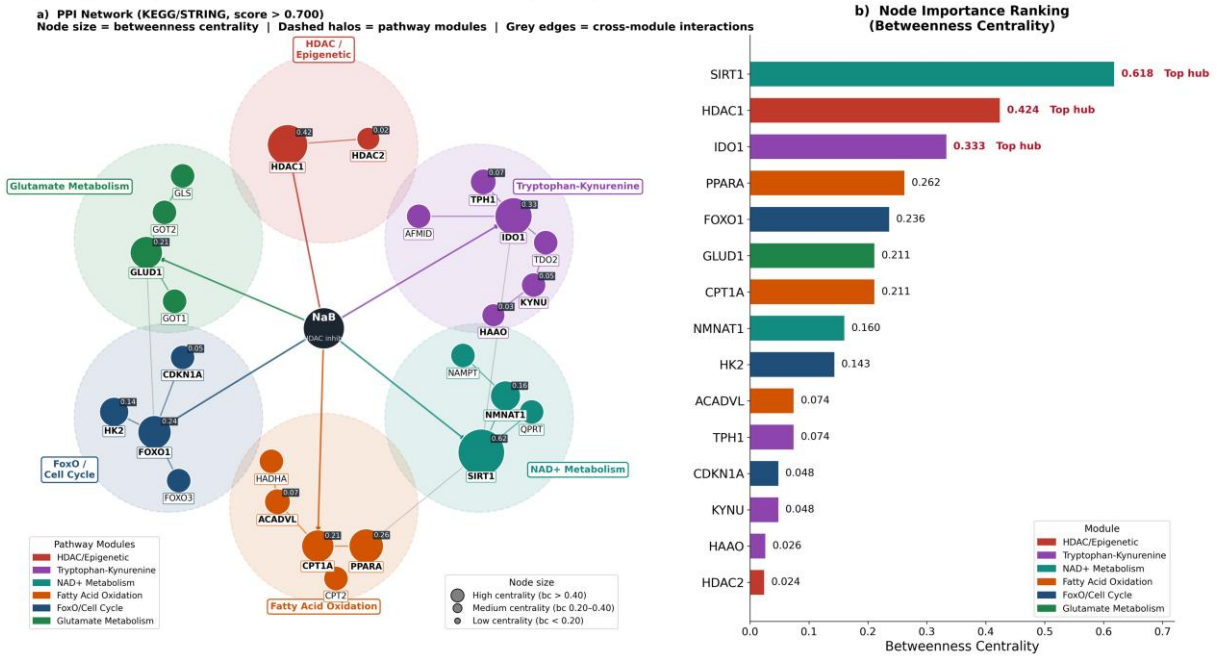

Figure 2. Protein-protein interaction network of regulatory genes from the top enriched pathway sets. (a) Network of 28 nodes across six functional modules: HDAC/epigenetic, tryptophan-kynurenine, NAD+ metabolism, fatty acid oxidation, FoxO/cell cycle and glutamate metabolism; node size reflects betweenness centrality and grey edges indicate cross-module interactions. (b) Node importance ranking by betweenness centrality, identifying SIRT1 (0.618), HDAC1 (0.424) and IDO1 (0.333) as top hubs. Network topology reflects inferred regulatory relationships; causal roles require experimental validation.

Figure 1. Pairwise PCA score plots for each NaB concentration versus 0 mM control with 95% confidence ellipses, resolving three metabolic states: sub-threshold (0-0.25 mM), productive (0.5-2.0 mM, shaded) and cytostressed (4.0-8.0 mM). PC1 38.7%, PC2 12.7%.

Figure 2. PPI network of regulatory genes from the top enriched pathway sets (KEGG/STRING, score > 0.700). (a) 28 nodes across six functional modules; node size reflects betweenness centrality, grey edges indicate cross-module interactions. (b) Node ranking by betweenness centrality: SIRT1 (0.618), HDAC1 (0.424) and IDO1 (0.333) are top hubs, followed by PPARA, FOXO1, GLUD1 and CPT1A. Topology is inferred; causal roles require validation.

Accelerating gene therapy development and manufacturing QA/QC with an FDA/CBER AMT-designated NanoMosaic analytics platform

Qimin Quan[1], Angad Garg[1]

[1]*NANOMOSAIC, WALTHAM, United States*

Abstract Text

The rapid expansion of the gene therapy landscape has fundamentally shifted the treatment paradigm for genetic disorders, moving genetic medicine toward industrialized, platform-based modalities. However, as these new therapies advance from ultra-rare, to rare and more common diseases, the inherent molecular heterogeneity of delivery vectors, particularly recombinant adeno-associated virus (rAAV) products, presents a severe bottleneck. Maintaining stringent process control and ensuring product quality requires a complex matrix of legacy analytical methodologies.

To address these challenges, the FDA/CBER Advanced Manufacturing Technology (AMT) designation was established to accelerate the integration of innovations that substantially improve manufacturing efficiency and product consistency. Adopting an AMT-designated platform provides a strategic regulatory pathway, mitigating CMC risks through prioritized FDA engagement and expedited IND/BLA reviews.

We developed an integrated, multi-analyte AAV platform using Nanoneedle technology and secured the FDA/CBER AMT designation, fulfilling criteria for significantly improving manufacturing processes, enhancing product quality, and reducing development timelines for gene therapies. Our platform enables the harmonized characterization of capsid attributes and viral genome integrity within a single, unified assay framework. Fig. 1 (A–B) illustrates densely integrated nanoneedles fabricated on a silicon chip and integrated into standard SBS well-plate format. Both capsid titer and transgene titers can be quantified using the nanoneedle-based, multi-omic detection (Fig. 1C). For genome quantification, the assay utilizes a dual-oligo hybridization mechanism where sequence-specific probe positioning defines the measured sub-population. Probes targeting the distal termini of the viral genome enable the direct detection of full-length transgenes - a significant advancement over conventional PCR methods that rely on short-amplicon surrogates to infer integrity. Simultaneously, capsid titers are determined via an integrated sandwich immunoassay on the same platform. By merging precise full-length transgene quantification with total capsid measurements, the platform provides automated empty/full/partial (E/F/P) ratios. As a case study to demonstrate the value of full-length quantification, both short-region and full-length transgene titers were measured for two constructs (Fig. 1D-F). Short-region and full-length titers differed significantly for the CAG promoter construct, but not for CMV, indicating substantial genome truncation in the CAG-promoter samples. We further resolved heterogeneous AAV sub-populations, including

truncated genomes, to pinpoint construct-specific vulnerabilities. The truncation locus, located around the ~700 bp position within the CAG region, was confirmed by long-read sequencing. The genome integrity is a critical quality attribute that directly indicates the potency. We demonstrated that the nanoneedle platform can be extended to quantify

transgene-derived RNA, enabling both genome integrity and RNA-based potency measurements on a single analytical platform. In Fig. 1G, ACTB mRNA copy number was quantified using a standard curve and was consistent with the expected estimate (Human Protein Atlas GTEx), indicated by the dotted line.

The nanoneedle platform enables the harmonized characterization of capsid attributes and viral genome integrity, RNA quantification within a single, unified assay framework. By merging precise full-length transgene quantification, total capsid measurements and RNA-based potency characterization, the platform provides viral vector quantifications and accurate genome integrity analysis (true empty/full/partial ratios), bridging the gap between physical titers and potency. This minimizes analytical variability, reduces process development costs, and provides high-fidelity data insights from upstream process development to release testing. Ultimately, integrating this AMT-designated technology early in development empowers manufacturers to strengthen product quality, minimize analytical variability, and significantly accelerate the timeline for bringing next-generation gene therapies to patients.

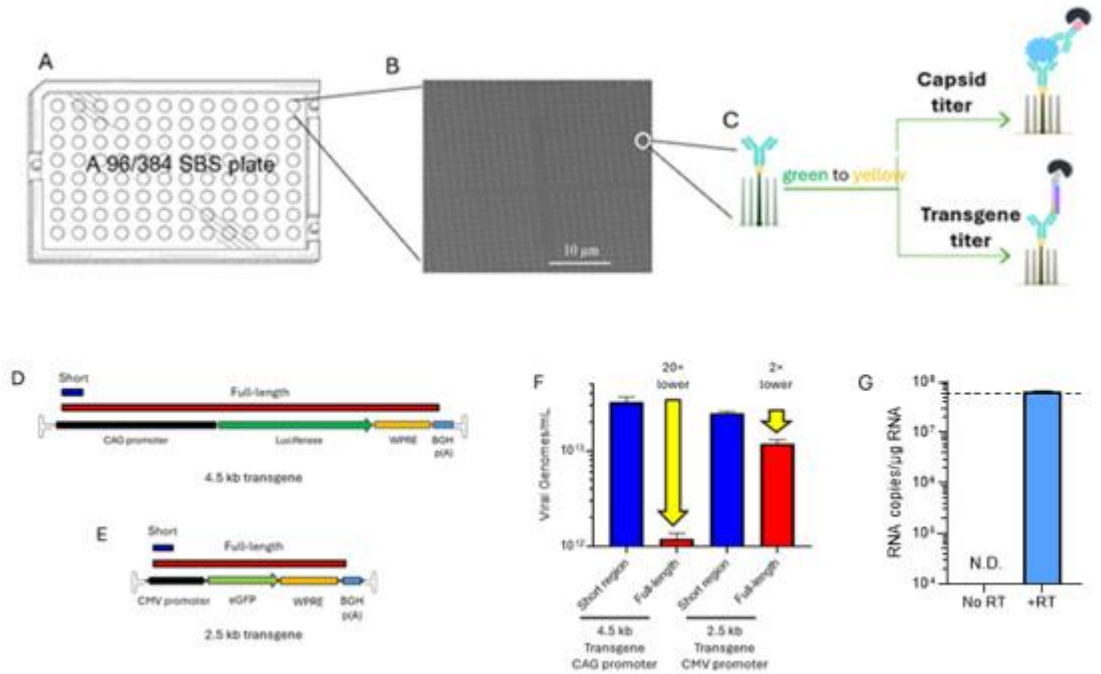

Fig. 1. A-B. Schematic of the SBS 96/384 plate with nanoneedles by scanning electron microscopy. **C**. Capsid and transgene titer quantifications using nanoneedle technology. **D-F.** Comparison of full-length (red) and short-region (blue) measurements of two constructs with CAG promoter (D) and CMV promoter (E) reveals a significant difference for the CAG promoter (but not for the CMV promoter sample), indicating a large population of truncated genomes in the CAG samples. **G.** ACTB mRNA copy number was quantified using a standard curve and was consistent with the expected estimate, indicated by the dotted line. (N.D.: Not detectable).

Polymer Nanoparticle Delivery of Therapeutic NF1 Signaling ERPs to Schwann Cells

Kenneth Sims[1], Danielle Huk[1], Andrea McCue[1], Ashlee Colbert[1], Jacqueline Grible[1], Emma Schmitz[1], Adele Guglielmi[2], David Segal[2]

[1]Battelle Memorial Institute, Columbus, OH, United States, *[2]University of California, Davis, Davis, CA, United States*

Abstract Text

Introduction: Development of a broadly applicable therapeutic approach for all individuals with Neurofibromatosis Type 1 (NF1) plus the ability to load and deliver large payloads remain as two key challenges to overcome for successful translation of an NF1 gene therapy to the clinic. To address these challenges, we have investigated the use of polymer nanoparticles (PNPs) to deliver targeted epigenetic regulatory proteins (ERPs) as transient therapeutic payloads that cause persistent downregulation of mitogen-activated protein kinases 1 and 2 (MEK1/2) in Schwann cells. By combining complementary strengths in CRISPR payload design and PNP delivery vehicle research and development across two collaborative institutions, we have significantly improved our CRISPR payload Map2k1 and Map2k2 repression capabilities while increasing our understanding of PNP cell uptake mechanisms in Schwann cells and enhancing PNP transfection efficiency approximately 10-fold *in vitro*. Overall, our iterative design-build-test-learn (DBTL) approach has significantly advanced the technology readiness level and therapeutic potential of our ERP-encoding payloads loaded and delivered by PNP delivery vehicles.

Methods: Approximately 20 CRISPR constructs with MPZ(0) promoters were generated and screened via qPCR to measure guide RNA (gRNA) repression capabilities for MEK1/2 gene expression and RAS/MAPK pathway activity. These constructs were directly compared to Selumetinib using Western blots for MEK and pERK levels. PNPs were synthesized via reversible addition–fragmentation chain transfer polymerization, purified, and characterized for monomer conversion, size (*i.e.*, diameter), polydispersity index (PDI), zeta potential, loading efficiency, cytotoxicity, and transfection efficiency *in vitro*.

Results: CRISPR constructs with two top performing gRNAs were found to have repressed Map2k1 and Map2k2 levels in Schwann cells by approximately 50%. CMyc levels were also observed to have decreased by ~60%. Western blot results showed these constructs reduced MEK levels more than Selumetinib, but Selumetinib reduced pERK levels to a greater extent once normalized to β actin. In addition, a top PNP design previously found to deliver nucleic acids to sciatic nerve tissue in wild type mice after intrathecal delivery was successfully reproduced across multiple DBTL rounds using scaled-out standardized manufacturing and characterization processes, showing no statistical difference in terms of diameter, PDI, or zeta potential when characterized via dynamic light scattering in aqueous conditions without cargo. The DBTL cycle evolution also resulted in this final PNP design improving Schwann Cell transfection efficiency by approximately 10-fold (*i.e.*, ~3% in DBTL iteration #1 to ~30% in

DBTL iteration #4). Cell uptake mechanism studies revealed that Schwann cells used clathrin mediated endocytosis to take up this PNP.

Conclusions: This set of studies assessed the CRISPR construct repression capabilities in Schwann cells *in vitro* as well as the manufacturing and characterization reproducibility of a top PNP design identified previously. The results obtained demonstrated successful repression of MEK1/2 gene expression and RAS/MAPK pathway activity *in vitro*. Moreover, the standardized manufacturing processes showed reproducible PNP production that led to identification of key cell uptake mechanism insights and a 10-fold improvement in Schwann cell transfection efficiency *in vitro*. However, additional work is needed to extend these results *in vivo*. The critical insights from these studies will help advance this epigenetic regulatory protein-loaded PNP therapeutic approach to NF1 focused preclinical studies as immediate next steps and ideally towards commercial and/or clinical nervous system gene therapy applications in the future.

First-in-human Phase 1 study of GF-CART01, a non-viral CD19/CD20 dual-targeted CAR T-cell therapy manufactured using the qCART™ Platform, in patients with relapsed/refractory B-cell malignancies

Shang-Ju Wu[1], Sareina Chiung-Yuan Wu[2 2], Howard Cheng[2 2], Ting-Wan Lin[2 2], Wei-Kai Hua[2 2], Jui-Cheng Tsai[2 2], Kuo-Lan Wen[2 2]

[1]National Taiwan University Hospital, Internal Medicine, Taipei, Taiwan, *[2]GenomeFrontier Therapeutics, CORP, New Taipei, Taiwan*

Abstract Text

Background: CD19-directed CAR T-cell therapies have revolutionized the treatment of relapsed/refractory B-cell malignancies, yet their long-term clinical benefit remains limited by disease relapse and treatment-related toxicities, including cytokine release syndrome (CRS) and immune effector cell-associated neurotoxicity syndrome (ICANS). Most patients eventually relapse within 1–2 years, underscoring the need for next-generation CAR T-cell therapies with improved durability, persistence, and safety. Emerging evidence suggests that sustained responses may be achieved through multi-antigen targeting to prevent antigen escape and CAR T-cell products enriched for stem cell memory T (T_{SCM}) cells, balanced CD8/CD4 ratios, and reduced exhaustion phenotypes. To address these challenges, GenomeFrontier developed qCART™, a non-viral platform that enables rapid, scalable, and multiplex genetic engineering while preserving favorable T-cell characteristics. GF-CART01, the first qCART-derived clinical candidate, is an autologous CD19/CD20 dual-targeting CAR T-cell therapy armored with a T-cell homeostatic modulator and enriched for T_{SCM} cells, designed for enhanced persistence, antitumor activity, and durable clinical responses in patients with B-cell malignancies.

Methods: A first-in-human, phase 1, open-label, dose-escalation study (NCT06703892) was initiated in Taiwan to evaluate the safety, persistence, and preliminary clinical activity of GF-CART01 in subjects with relapsed or refractory (R/R) B-cell hematological malignancies. The study follows a traditional 3+3 dose-escalation design to determine the maximum tolerated dose and recommended phase 2 dose (RP2D). Following leukapheresis and manufacturing of GF-CART01, patients receive lymphodepleting chemotherapy with fludarabine and cyclophosphamide before a single GF-CART01 infusion. Safety assessments include dose-limiting toxicities (DLTs), treatment-emergent adverse events, CRS, and ICANS. CAR T-cell expansion and persistence are evaluated by droplet digital PCR, while serum cytokines are monitored as pharmacodynamic biomarkers. Clinical responses are assessed according to Lugano 2014 criteria and include overall response rate and duration of response.

Results: Three patients have been treated with dose level 1 (DL1; 8×10^6 CAR-positive cells). Notably, DL1 was less than one-tenth of the CAR T cell dosage used for currently approved CD19-directed CAR T therapies. For all treated patients, GF-CART01 consistently exhibited favorable product characteristics, including high proportions of T_{SCM} cells (range, 62.2-90.4% among $CD8^+$ CAR T cells), balanced CD8/CD4 ratios (range, 1.21-3.63), and low expression of exhaustion and senescence markers. There were no occurrences of DLTs, ICANS of any grade, severe infection, or other unexpected safety signals. Only one patient experienced any grade CRS (grade 2). All patients experienced grade ≥3 neutropenia following

lymphodepleting chemotherapy, which resolved with standard supportive care. Robust in vivo expansion of GF-CART01 and clinical activity was observed in all three patients. All three patients receiving DL1 achieved complete metabolic response by PET imaging at one month after infusion (100% CR).

Conclusions: Preliminary data from this ongoing study demonstrate that GF-CART01 can be reliably manufactured with favorable product quality, and it exhibits an encouraging safety profile at DL1. Early findings show robust expansion and durable complete responses at a substantially lower cell dose than conventional CAR T therapies. The study will continue with dose escalation to determine the RP2D and further follow-up to assess durability, persistence and clinical benefit.